UNIVERSIDADE ESTADUAL DE CAMPINAS
Faculdade de Engenharia Química

CARLA GIOMETTI FRANÇA

DESENVOLVIMENTO, CARACTERIZAÇÃO E DESEMPENHO DE HIDROGÉIS DE ÁCIDO HIALURÔNICO OXIDADO E RETICULADO COM DIHIDRAZIDA ADÍPICA NA PROLIFERAÇÃO DE CÉLULAS MESENQUIMAIS DO TECIDO ADIPOSO HUMANO

CAMPINAS
2020

CARLA GIOMETTI FRANÇA

DESENVOLVIMENTO, CARACTERIZAÇÃO E DESEMPENHO DE HIDROGÉIS DE ÁCIDO HIALURÔNICO OXIDADO E RETICULADO COM DIHIDRAZIDA ADÍPICA NA PROLIFERAÇÃO DE CÉLULAS MESENQUIMAIS DO TECIDO ADIPOSO HUMANO

Tese apresentada à Faculdade de Engenharia Química da Universidade Estadual de Campinas como parte dos requisitos exigidos para obtenção do título de Doutora em Engenharia Química.

Orientadora: Dra. Maria Helena Andrade Santana

ESTE TRABALHO CORRESPONDE À VERSÃO FINAL DA TESE DEFENDIDA PELA ALUNA CARLA GIOMETTI FRANÇA, E ORIENTADA PELA PROF. DRA. MARIA HELENA ANDRADE SANTANA

CAMPINAS

2020

Ficha catalográfica
Universidade Estadual de Campinas
Biblioteca da Área de Engenharia e Arquitetura
Rose Meire da Silva - CRB 8/5974

França, Carla Giometti, 1989-
F844d Desenvolvimento, caracterização e desempenho de hidrogéis de ácido hialurônico oxidado e reticulado com dihidrazida adípica na proliferação de células mesenquimais do tecido adiposo humano
/ Carla Giometti França. – Campinas, SP : [s.n.], 2020.

Orientador: Maria Helena Andrade Santana.
Tese (doutorado) – Universidade Estadual de Campinas, Faculdade de Engenharia Química.

1. Ácido hialurônico. 2. Microestrutura. 3. Engenharia tecidual. 4. Medicina regenerativa. I. Santana, Maria Helena Andrade, 1951-. II. Universidade Estadual de Campinas. Faculdade de Engenharia Química. III. Título.

Informações para Biblioteca Digital

Título em outro idioma: Development and characterization of oxidized hyaluronic acid hydrogels and crosslinked with dihydrazide and their perfomance in the proliferation of mesenchymal cells in human adipose tissue
Palavras-chave em inglês:
Hyaluronic acid
Microstructures
Tissue engineering
Regenerative medicine
Área de concentração: Engenharia Química
Titulação: Doutora em Engenharia Química
Banca examinadora:
Maria Helena Andrade Santana [Orientador]
Patrícia Severino
Ângela Cristina Malheiros Luzo
Amanda Gomes Marcelino Perez
Marcos Akira d'Ávila
Data de defesa: 16-12-2020
Programa de Pós-Graduação: Engenharia Química

Identificação e informações acadêmicas do(a) aluno(a)
- ORCID do autor: https://orcid.org/0000-0003-3527-7563
- Currículo Lattes do autor: http://lattes.cnpq.br/9403890201385862

Folha de Aprovação da Defesa de Tese de Doutorado defendida por Carla Giometti França em 16 de dezembro de 2020 pela banca examinadora constituída pelos doutores.

Profa. Dra. Maria Helena Andrade Santana – Presidente e Orientadora

FEQ / UNICAMP

Videoconferência

Dra. Patricia Severino

Instituto de Tecnologia e Pesquisa- UNIT

Videoconferência

Dra. Ângela Cristina Malheiros Luzo

Hemocentro - UNICAMP

Videoconferência

Dra. Amanda Gomes Marcelino Perez

Faculdade de Jaguariúna

Videoconferência

Dr. Marcos Akira D'Ávila

Faculdade de Engenharia Mecânica - UNICAMP

Videoconferência

A Ata da defesa com as respectivas assinaturas dos membros encontra-se no SIGA/Sistema de Fluxo de Dissertação/Tese e na Secretaria do Programa da Unidade.

AGRADECIMENTOS

Agradeço inicialmente à Prof. Dra. Maria Helena Andrade Santana por ter me acolhido em seu laboratório e me dado a oportunidade de realizar esse trabalho com tanto carinho e dedicação. Também agradeço pelos ensinamentos científicos.

Agradeço à Dra. Carolina Calinari e a Dra. Ângela Luzo pela colaboração e fornecimento das células mesenquimais de tecido adiposo humano. Também agradeço a *In Situ*, em especial a Juliana Magro, pelos ensinamentos.

Ao Prof. Dr. Marcos Akira D'Ávila e aos seus alunos, pela ajuda com a realização dos experimentos.

Aos membros da banca avaliadora do doutorado, Dra. Amanda Perez, Dra. Ângela Luzo, Dr. Marcos Akira e Dra. Patrícia Severino, que dedicaram seu tempo para a leitura do texto, e pelos comentários valiosos que ajudaram a melhorar o trabalho. E também aos suplentes Dra. Andrea Shimojo, Dr. Reinaldo Bastos, Dra. Carolina Caliari e Dra. Denise Villalva.

Agradeço à minha família e meu namorado Gustavo Nardim, pelo companheirismo mesmo estando longe, pelo apoio, amor e amizade. Sou eternamente grata.

Aos colegas de laboratório do LDPB pelo companheirismo e ajuda: Bruna Melo, Andrea Shimojo, André Calvalcanti, Daniel Pereira e Gilson Maia. E aos amigos Krissia Leme, Denise Villalva e Jacobo Montelongo por toda ajuda e colaboração durante esses anos.

Aos colegas e amigos da Exxtend Biotecnologia, em especial ao Bruno Tavares, pelo apoio, amizade, companheirismo e ajuda nessa reta final de ansiedade.

À Unicamp por proporcionar o aprendizado ao longo dos 6 anos.

Agradeço por fim, ao Conselho Nacional de Desenvolvimento Científico e Tecnológico (CNPq), processo 14092/2017-5, por financiar o projeto, tornando a realização desse trabalho possível.

“A menos que modifiquemos a nossa maneira de pensar, não seremos capazes de resolver os problemas causados pela forma como nos acostumamos a ver o mundo.”

Albert Einstein

RESUMO

O ácido hialurônico (HA) é um polissacarídeo natural presente em vários tecidos animais presente na matriz extracelular. HA possui propriedades mecânicas que são responsáveis pela lubrificação, amortecimento de choques e preservação das juntas articulares. Apesar das excelentes propriedades, o HA é rapidamente degradado *in vivo*. A sua estabilidade e tempo de meia vida tem sido melhorada através de modificação química nos seus grupos funcionais e reticulação. Um exemplo de modificação química é a oxidação parcial dos grupos hidroxilas do HA (oxi-HA), que favorece a extensão e compactação das cadeias permitindo a reticulação com dihidrazida adípica (ADH), por meio de reação tipo click, espontânea e sem uso de catalisadores ou iniciadores químicos. Entretanto a literatura ainda é escassa nos estudos do oxi-HA/ADH como biomaterial visando aplicação na medicina regenerativa. Dentro deste contexto, este trabalho teve como objetivo estudar as propriedades físico-químicas do oxi-HA/ADH e o seu desempenho como biomaterial para carreamento, proliferação de células mesenquimais do tecido adiposo humano (h-AdMSCs) e diferenciação condrogênica em associação com PRP. Os resultados obtidos mostraram que pela modulação do grau de oxidação e de reticulação com ADH é possível obter biomateriais com diferentes propriedades, assim como micro e nanoestruturas. As microestruturas particularmente, demostraram mais eficientes para a proliferação de AdMSCs, sendo uma estratégia promissora para a formação de microtecidos em estratégia do tipo b*ottom-up*. Além disso, as microestruturas com 2 e 5 mg não suprimiram a expansão da rede de fibrina do plasma rico em leucócitos e plaquetas (L-PRP) e melhoraram a proliferação celular. Os resultados de modulação e microestruturação do oxi-HA/ADH são inovadores e contribuem para uma o desenvolvimento de novos biomateriais baseados em oxi-HA/ADH para aplicações em engenharia de tecidos e medicina regenerativa.

Palavras chave: ácido hialurônico oxidado, dihidrazida adípica, microestruturas, engenharia tecidual, medicina regenerativa.

ABSTRACT

Tissue engineering and regenerative medicine work to develop new and effective treatments for a range of diseases. Hyaluronic acid (HA) is a natural polysaccharide present in the extracellular matrix and its exogenous product obtained from fermentation is widely used as a biomaterial. Despite its mechanical and biological properties, HA is rapidly degraded *in vivo*. Its stability can be improved through chemical modification in their functional groups and crosslinking. The HA association with platelet-rich-plasma (PRP) has shown benefits in regenerative medicine applications. The partial oxidation reaction of hydroxyl groups in HA (oxi-HA) favors extension and compacting of the chains allowing crosslinking with adipic dihydrazide acid (ADH), through a click-type reaction, spontaneous and without the use of chemical catalysts or initiators. However, the literature is still scarce on studies of oxi-HA/ADH as a biomaterial. Therefore, this work aimed to study the physical-chemical properties of the partial oxidation and crosslinking process (oxi-HA/ADH) and its performance as a biomaterial for carrying and proliferation of human- adipose mesenchymal cells (h-AdMSCs) and their chondrogenic differentiation in association with PRP. The results obtained showed that by modulating the degree of oxidation and crosslinking of HA it is possible to obtain biomaterials with different properties as well as micro and nanostructures. The microstructures, in particular, proved to be more efficient for the proliferation of AdMSCs, being a promising strategy for the formation of microtissues in a bottom-up strategy. In addition, microstructures with 2 and 5 mg did not suppress the expansion of the leukocyte- and platelet rich plasma (L-PRP) fibrin network and improved cell proliferation. The results of modulation and microstructuring of oxi-HA/ADH are innovative and contribute to the development of new biomaterials based on oxi-HA/ADH for applications in tissue engineering and regenerative medicine.

Keywords: oxidized hyaluronic acid, adipic dihydrazide acid, microstructures, tissue engineering, regenerative medicine.

LISTA DE ABREVIATURAS E SIGLAS

3D – Tridimensional

ADH – ácido dihidrazida adípica

FC – Fator de crescimento

HA – ácido hialurônico

h-AdMSC – célula mesenquimal do tecido adiposo

HMW – alto peso molecular

-IO_4 – periodato

IPN – *interpenetrating polymer network*

ISCT – Sociedade Internacional de Terapia Celular

LMW – baixo peso molecular

L-PRP – Plasma rico em plaquetas e leucócitos

MEC – matriz extracelular

MSC – célula mesenquimal

MW – peso molecular

$NaIO_4$ – periodato de sódio

OA – osteoartrite

oxi-HA – ácido hialurônico oxidado

oxi-HA/ADH – ácido hialurônico oxidado e reticulado com dihidrazida adípica

PRP – plasma rico em plaquetas

RBC – glóbulo vermelho

RM – medicina regenerativa

TE – engenharia tecidual

WB – sangue total

SUMÁRIO

CAPÍTULO 1:
INTRODUÇÃO GERAL

1. INTRODUÇÃO GERAL

O ácido hialurônico (HA) é um heteropolissacarídeo que existe naturalmente em vários tecidos animais. No corpo humano, as maiores concentrações de HA são encontradas na matriz extracelular dos tecidos conjuntivos moles (FRASER; LAURENT; LAURENT, 1997). Isolado primeiramente em 1934 do humor vítreo bovino por Karl Meyer e John Palmer (MEYER; PALMER, 1934), e posteriormente da crista de galo (BOAS, 1949; SWANN; CAULFIELD, 1975), atualmente a maior parte do HA é produzido por fermentação microbiana usando bactérias do gênero *Streptococci* (CHONG; BLANK; MCLAUGHLIN; NIELSEN, 2005). O HA exógeno de fonte microbiana possui propriedades iguais ao endógeno, e por isso vem sendo usado em várias aplicações médicas, principalmente no tratamento de doenças musculoesqueléticas (NICHOLLS; FIERLINGER; NIAZI; BHANDARI, 2017).

1.1. HA: estrutura, propriedades e funções

HA é composto de unidades alternadas de ácido D-glucurônico e N-acetilglicosamina unidas por ligações glicosídicas ß-1,4 e ß-1,3. Apesar da sua alta hidrofilicidade (domínios poli-hidroxílicos), o HA é um anfifílico, com domínios hidrofóbicos nas suas unidades CH. Em meio aquoso, esses domínios se agregam formando uma estrutura secundária do tipo fita retorcida, que se enovela aleatoriamente produzindo estruturas terciárias do tipo "*random coil*", estabilizadas por ligações físicas (HASCALL; LAURENT, 1997). Em solução fisiológica a estrutura terciária se expande, formando hidrogéis porosos que ocupam um grande volume (SCOTT, 1998)

HA possui propriedades mecânicas, viscosidade e viscoelasticidade, que são responsáveis pela lubrificação, amortecimento de choques e preservação das juntas articulares (COWMAN; SCHMIDT; RAGHAVAN; STECCO, 2015; TEMPLE-WONG; REN; QUACH; HANSEN *et al.*, 2016). Além de manter a arquitetura da matriz extracelular, o HA possui a capacidade de sinalização celular, que é a sua principal propriedade biológica. A sinalização resulta da ligação a receptores específicos expressos em muitas células tais como CD44, à molécula de adesão intracelular ICAM-1 e ao receptor mediador de motilidade RHAMM. Essas interações regulam as atividades funcionais das células tais como migração e proliferação, nos estados fisiológico e patológico (KNUDSON; KNUDSON, 1999; TURLEY; NOBLE; BOURGUIGNON, 2002).

1.2. Modificações químicas e físicas do HA

Várias modificações químicas podem ser feitas no HA nativo para torná-lo um material robusto e resistente à degradação. Os grupos carboxila e hidroxila são os sítios mais comuns para ativação e posterior ligação química covalente ou *crosslinking*. As modificações químicas dos grupos carboxílicos são amidação ou esterificação, enquanto reações de formação de éter, éster, hemiacetal e oxidação, ativam os grupos hidroxila com os agentes de acoplamento butanedioldiglicidil éter, divinil sulfone, glutaraldeído, brometo de cianogênio, succínico anidrido e periodato de sódio. O HA resultante, quimicamente modificado, tem propriedades físico-químicas diferentes do HA nativo, porém a maioria retém a sua biocompatibilidade e biodegradabilidade (BURDICK; PRESTWICH, 2011; PRESTWICH, 2001).

1.3. HA no tratamento de doenças musculoesqueléticas

Os distúrbios musculoesqueléticos são lesões que afetam ossos, músculos, articulações, ligamentos, tendões ou cartilagem, e causam dores, fraquezas, ruídos articulares e redução da amplitude de movimento (GOMEZ-GALAN; PEREZ-ALONSO; CALLEJON-FERRE; LOPEZ-MARTINEZ, 2017; VALERO; SIVANATHAN; BOSCHE; ABDEL-WAHAB, 2016). Atualmente, com o aumento da expectativa de longevidade devido à melhoria nas condições de vida (IBGE, 2008), os distúrbios musculoesqueléticos vem afetando significativamente a qualidade de vida da população idosa (GOMEZ-GALAN; PEREZ-ALONSO; CALLEJON-FERRE; LOPEZ-MARTINEZ, 2017; VALERO; SIVANATHAN; BOSCHE; ABDEL-WAHAB, 2016).

A osteoartrite (OA) é uma doença musculoesquelética que afeta principalmente as articulações, do quadril e joelhos. No mundo, OA é a quarta enfermidade que mais reduz a qualidade de vida, segundo a Organização Mundial de Saúde (OMS) (BRASIL, 2017; SUS, 2015). No Brasil, a osteoartrite acomete mais de 10 milhões de casos em adultos registrados, atingindo principalmente pessoas acima dos 41 anos de idade. Entretanto, adultos na faixa dos 30 anos de idade também sofrem com a doença (BRASIL, 2017).

A OA de joelho é a de maior incidência, sendo uma das principais causas de incapacidade de movimento da população adulta (BHOSALE; RICHARDSON, 2008; HE; LI; ALEXANDER; OCASIO-NIEVES *et al.*, 2020). OA de joelho é caracterizada por dor articular, degeneração da cartilagem e redução progressiva da função do joelho, afetando a capacidade do indivíduo para realizar atividades diárias (BADLEY; WILFONG; YIP; MILLSTONE *et al.*, 2020; CHENG; SOUZDALNITSKI;

VROOMAN; CHENG, 2012). Portanto, impacta negativamente fatores socioeconômicos, pois a deficiência associada muitas vezes leva a um desempenho prejudicado no trabalho e aposentadoria precoce. Estima-se que na faixa etária de 85 anos, 1 de cada 2 pessoas desenvolverá osteoartrite de joelho sintomática (LOESER, 2017).

HA tem sido extensamente usado no tratamento da OA de joelho. Injeções intra-articulares de HA produzem benefícios clínicos além da lubrificação e absorção de choque, por meio de vários mecanismos, tais como: proteção de condrócitos, mediante sinalização por meio do receptor CD44, estímulo da síntese de proteoglicanos e glicosaminoglicanos, efeitos anti-inflamatórios e alívio da dor. As evidências mostram que HA produz efeitos modificadores da doença, na preservação e restauração da matriz extracelular (ALTMAN; MANJOO; FIERLINGER; NIAZI *et al.*, 2015; NICHOLLS; FIERLINGER; NIAZI; BHANDARI, 2017).

Resultados mais favoráveis são obtidos com o tratamento intra-articular com HA de alta massa molar, e HA de fonte microbiana possui perfil bioquímico mais seguro. Comparativamente o tratamento com HA intra-articular proporciona maior alívio da dor, comparado aos corticoides, NSAID (n*onsteroidal anti-inflammatory drugs*) e fisioterapia. Além disso, o tratamento com ciclos repetidos parece adiar as intervenções cirúrgicas na osteoartrite do joelho e quadril, conforme mostrado por vários estudos. Portanto, HA intra-articular tem proporcionado tratamentos eficientes e muito menos invasivos, restringindo assim as intervenções cirúrgicas a casos especiais, além de evitar seus efeitos adversos e custos elevados.

1.4. HA no tratamento regenerativo

A engenharia de tecidos (TE) e a medicina regenerativa (RM) buscam atender à necessidade clínicas de reparo de tecidos danificados. Enquanto na TE o tecido é desenvolvido fora do corpo, a RM usa a capacidade regenerativa do próprio corpo para recrutar suas células-tronco, ativar células residentes no tecido ou implantar células previamente cultivadas, para recuperar a homeostase (KEENEY; LAI; YANG, 2011; VEGA; KWON; BURDICK, 2017). Ambas as estratégias empregam combinações únicas de materiais, células e sinais bioquímicos e mecânicos, que resultam no desenvolvimento crescente de tratamentos mais efetivos, eficazes e menos invasivos.

As células-troncos mesenquimais (MSCs) vêm despertando grande interesse, pela sua relevância clínica como um tipo de célula que pode ser facilmente colhida e expandida, e por não expressarem HLA (*human leukocyte antigen*), e por isso pode ser

obtido de banco de células, ou seja, ainda é de forma autóloga. Na engenharia de tecidos da cartilagem, as MSCs aparecem como uma alternativa aos condrócitos autólogos. As MSCs mais usadas são provenientes da medula óssea gordura e sinóvio. Em termos de sinais bioquímicos, destacam-se os fatores de crescimento TGF-β, IGF, BMPs, IGD, FGF e as proteínas morfogênicas BMP. (TIRUVANNAMALAI-ANNAMALAI; ARMANT; MATTHEW, 2014).

Apesar dos vários avanços, uma das principais limitações das MSCs é a qualidade da matriz extracelular gerada, e o desenvolvimento de *scaffolds* eficazes ainda é um desafio. Em geral o uso de biomateriais indutivos, como hidrogéis, é favorável, comparado aos materiais inertes. Nessa abordagem, HA emerge como um dos biomateriais indutivos mais estudados. Dentre os processos de fabricação de scaffolds tridimensionais duas abordagens são estudadas: *top-down* e *bottom-up,* Na abordagem convencional *top-down,* a estrutura porosa dos hidrogéis é previamente formada e a suspensão de células posteriormente dispersa na estrutura porosa. As limitações dessa estratégia são a vascularização lenta, gradientes de nutrientes devido à resistência difusiva, baixa densidade celular e distribuição não uniforme, que se refletem na qualidade do tecido formado (TIRUVANNAMALAI-ANNAMALAI; ARMANT; MATTHEW, 2014). Visando contornar as limitações difusivas, a abordagem (*bottom-up*) envolve microcarregadores com as células adsorvidas na superfície externa, cuja proliferação em multicamadas dará origem a microtecidos e posteriormente a um macro tecido (DECLERCQ; DE CALUWE; KRYSKO; BACHERT *et al.*, 2013). Os microcarreadores podem encapsular estimulantes dos sinais bioquímicos e ser dispostos em unidades repetitivas mimetizando a cartilagem nativa (MALDA; FRONDOZA, 2006). Atualmente os processos de produção de *scaffolds* estão evoluindo nas áreas de bioimpressão 3D, inclusive envolvendo HA (WEIS; SHAN; KUHLMANN; JUNGST *et al.*, 2018).

1.5. Associação do HA e o plasma rico em plaquetas (PRP)

O plasma-rico em plaquetas (PRP) é um produto autólogo derivado do sangue, rico em fatores de crescimento e proteínas. Adicionalmente, o PRP possui propriedades anti-inflamatórias e antimicrobianas e contém fibrinogênio, que mediante ativação química ou física decompõe-se em fibrina que polimeriza formando uma rede de fibras finas, que constitui o *scaffold* natural da regeneração tecidual. A rede de fibrina é importante por permitir a liberação gradual dos fatores de crescimento, proliferação de

células residentes ou recrutadas para o local da injúria, propriedades reológicas dos seus hidrogéis (LANA; SANTANA; BELANGERO; LUZO, 2014).

A associação do PRP com HA com tem trazido benefícios *in vitro* e *in vivo* (DE MELO; FRANCA; DAVILA; BATISTA *et al.*, 2020; LANA; WEGLEIN; SAMPSON; VICENTE *et al.*, 2016).

1.6. Evolução dos estudos no LDPB

O grupo de estudos do laboratório LDPB trabalha, desde 2009, na produção e caracterização de HA por fermentação, com estudos focados nas variáveis de processo, fonte de nitrogênio, meio de cultura e purificação (CAVALCANTI; MELO; OLIVEIRA; SANTANA, 2019; CAVALCANTI; SANTANA, 2019).

Como sequencia, iniciaram-se estudos do processo de produção do HA como biomaterial para aplicações na engenharia tecidual e medicina regenerativa. Nesses estudos, o HA foi estudado utilizando diferentes reticulações químicas e estruturas. No segmento o grupo começou a associar o HA com o plasma rico em plaquetas (PRP), avaliando as vantagens desta composição (BICUDO; SANTANA, 2012a; b; BICUDO; SANTANA, 2014; DE MELO; FRANCA; DAVILA; BATISTA *et al.*, 2020; DE MELO; SHIMOJO; PEREZ; LANA *et al.*, 2018; SHIMOJO; BRISSAC; PINA; LAMBERT *et al.*, 2015; SHIMOJO; DUARTE; LANA; LUZO *et al.*, 2019; SHIMOJO; GALDAMES; DUARTE; PINA *et al.*, 2014; SHIMOJO; GALDAMES; PEREZ; ITO *et al.*, 2016; SHIMOJO; PEREZ; GALDAMES; BRISSAC *et al.*, 2016; SHIMOJO; PIRES; DE LA TORRE; SANTANA, 2013; SHIMOJO; PIRES; LICHY; RODRIGUES *et al.*, 2015; SHIMOJO; PIRES; LICHY; SANTANA, 2015).

A Figura 1 mostra a evolução dos trabalhos do LDPB envolvendo HAs.

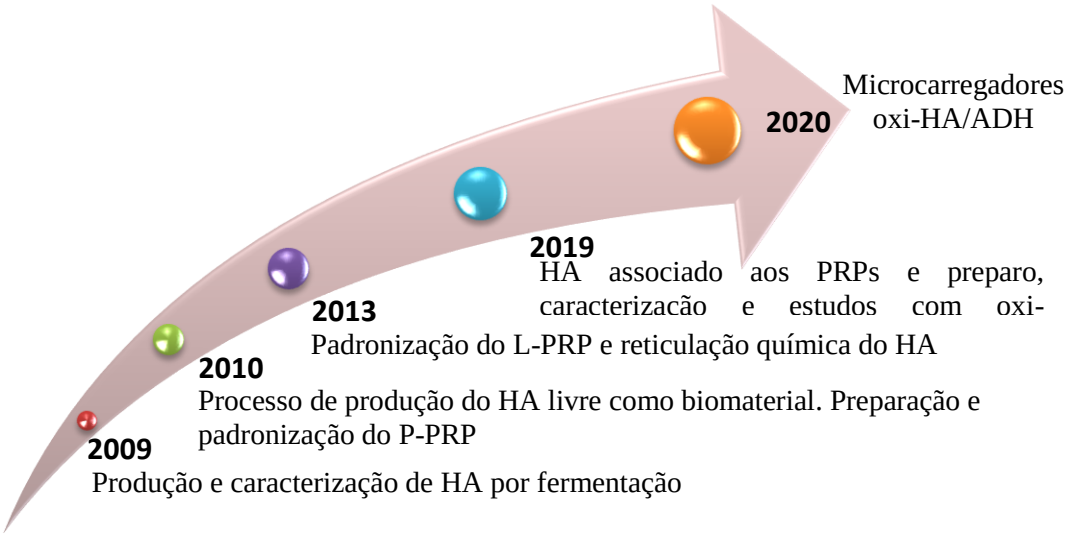

Figura 1. Linha do tempo da pesquisa de ácido hialurônico do grupo LDPB.

No LDPB os estudos com oxi-HA/ADH foram iniciados em 2017. A reação de reticulação do oxi-HA com o ADH é vantajosa para aplicações *in vivo* por ser uma reação tipo click que ocorre espontaneamente sem a necessidade de catalisadores ou iniciadores químicos, além do ADH ser facilmente metabolizada pelo corpo humano (FRANÇA; SACOMANI; VILLALVA; NASCIMENTO *et al.*, 2019; JIA; COLOMBO; PADERA; LANGER *et al.*, 2004; SU; CHEN; CHEN; LEE *et al.*, 2011; YEO; HIGHLEY; BELLAS; ITO *et al.*, 2006). Adicionalmente o sistema oxi-HA/ADH forma hidrogéis termossensíveis que são importantes para aplicações injetáveis. Enquanto injeções articulares de HA têm sido amplamente usadas nos tratamentos de osteoartrite de joelho, quadril, tornozelo e ombro, elas não são recomendadas para tratamentos de coluna cervical e lombar. Nesse último segmento, estudos com o oxi-HA/ADH têm apresentado resultados promissores na regeneração do núcleo pulposo (SU; CHEN; LIN, 2010).

A importância desses fatores, e adicionalmente a carência de estudos físico-químicos, estruturais e de engenharia, do sistema oxi-HA/ADH, motivaram o desenvolvimento do presente trabalho.

1.7. Objetivo e metas

O objetivo desse trabalho foi estudar as propriedades físico-químicas do ácido hialurônico oxidado e reticulado com dihidrazida adípica (oxi-HA/ADH), o desenvolvimento microestruturas carreadoras de células e os efeitos da sua associação com plasma rico em plaquetas (PRP) no crescimento e diferenciação condrogênica das

células mesenquimais do tecido adiposo humano (h-AdMSCs), visando aplicações em engenharia tecidual e medicina regenerativa.

O projeto seguiu as seguintes metas:

- Preparação e caracterização do acido hialurônico oxidado (oxi-HA) e reticulado com dihidrazida adípica (ADH), para a formação do hidrogel oxi-HA/ADH;
- Estudo da modulação das propriedades físico-químicas do oxi-HA/ADH;
- Desenvolvimento e caracterização de nano e microestruturas de oxi-HA/ADH;
- Caracterização dos efeitos da associação das microestruturas de oxi-HA/ADH com HA livre nas propriedades reológicas e injetabilidade;
- Caracterização do comportamento de adesão e crescimento das h-AdMSCs cultivadas nas microestruturas.

CAPÍTULO 2:
REVISÃO DA LITERATURA

2. REVISÃO DA LITERATURA

Esta seção esta apresentada em forma de artigo de revisão.

O artigo *Oxi-HA/ADH hydrogels: a novel approach in tissue engineering and regenerative medicine*, submetido ao periódico científico *Acs Biomaterials Science & Engineering*, trata-se de uma revisão abrangente sobre o hidrogel de ácido hialurônico, enfatizando os mecanismos de oxidação e reticulação, bem como sua aplicação.

Oxi-HA/ADH hydrogels: a novel approach in tissue engineering and regenerative medicine

Carla Giometti França[1], *Denise Gradella Villalva*[1], *and. Maria Helena Andrade Santana*[*,1]

[1]Department of Engineering of Materials and Bioprocesses, School of Chemical Engineering, University of Campinas (UNICAMP), 13083-852 Campinas, SP, Brazil

[*]Correspondence should be addressed to andrade@unicamp.br

Abstract

Hyaluronic acid (HA) is a natural polyelectrolyte abundant in mammalian connective tissues, such as cartilage and skin. The similar physicochemical, rheological, and biological properties of exogenous HA produced by fermentation have generated medical and dermo-cosmetic products. Chemical modifications such as crosslinking or conjugation in target groups of the HA molecule improve its properties and *in vivo* stability, expanding its applications. Currently, HA-based scaffolds and matrices are of great interest in tissue engineering and regenerative medicine. The partial oxidation of the proximal hydroxyl groups in HA to electrophilic aldehydes mediated by periodate has been rarely investigated. The introduced aldehyde groups in the HA backbone allow spontaneous crosslinking with adipic dihydrazide (ADH) without initiators or catalyzers. Furthermore, the oxi-HA/ADH system allows the customization of noncytotoxic and thermosensitive hydrogels that are useful for medical applications. This review provides an overview of the physicochemical properties of HA and its usual chemical modifications to better understand oxi-HA/ADH hydrogels, the modulation of oxi-HA/ADH properties by the oxidation degree and ADH concentration, their functional properties and the current clinical research. Finally, the review discusses the

development of biomaterials based on oxi-HA/ADH as a novel approach in tissue engineering and regenerative medicine.

Keywords: hydrogel, hyaluronic acid, crosslinking, tissue engineering, and medicine regenerative.

Graphical abstract. Oxi-HA/ADH hydrogels for tissue engineering and regenerative medicine.

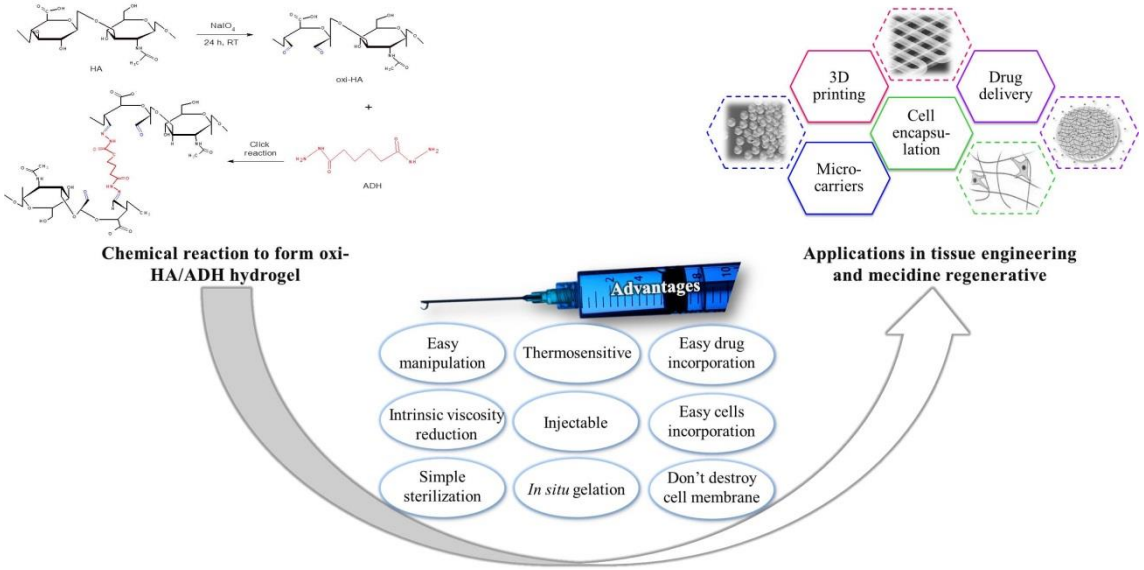

1. INTRODUCTION

Hyaluronic acid (HA) is a glycosaminoglycan comprising repeating disaccharide units of glucuronic acid and N-acetylglucosamine. HA is widely distributed in the extracellular matrix (ECM) and plays an important role in vertebrate tissue morphogenesis[1].

Isolated first in 1934 by Meyer and Palmer(MEYER; PALMER, 1934), HA has its evolutionary history supported by deep structural, physicochemical, and biological studies, resulted in an extensive network of clinical applications in the late 20th century. Laurent[3] summarized the history of HA research in the form of a tree, in which the great stages of development mark the trunk. The basic structural knowledge and evolution of

analysis techniques continued with research on the macromolecular and physiological properties, followed by molecular recognition, cell biology, and HA metabolism. These stages have extensive ramifications and were crowned with the development of HA as a product for clinical applications from Balazs' study[4].

In the last 40 years, with the support of studies on cell receptors, and technological development, tissue engineering has emerged as a science. Regenerative medicine is more recent, appearing during the 1990s. Until 2006, the focus of regenerative medicine was the research and production of knowledge about stem cells. Since 2006, the focus has shifted to the development of new products and therapies. Regenerative medicine is now much more than stem cell technology, covering basic biology to clinical applications[5].

Although exogenous avian HA was first explored, HA from fermentation, bio-HA, is currently the most used in clinical applications.

HA was first approved by regulatory authorities for use in human patients mainly as a viscoelastic fluid for pain in osteoarthritis and as sheet formulations for preventing surgical adhesions. Presently, HA hydrogels have been extensively studied for applications in tissue engineering and regenerative medicine[6, 7], diagnostics[8], cell immobilization[9], the separation of biomolecules or cells[10] and the regulation of biological adhesions as a barrier material[11] because of their desirable properties, such as adaptive chemistry, biodegradability, biocompatibility, viscoelasticity, biological activities, and chondrogenic potential[12].

Although versatile as a biomaterial, HA requires chemical functionalization and/or crosslinking reactions to improve stability and ensure the fidelity of the shape of the hydrogel constructs[13]. Generally, these chemical or physical modifications of HA can be controlled to maintain the biological functions of the polymer and are important

to overcome degradation. *In vivo*, the resilience of HA hydrogels depends on their rate of degradation by hyaluronidases and reactive oxygen and nitrogen species that can limit their effective use[14-18]. However, most of the usual crosslinkers are medium or large molecules that are not metabolized by the human body after HA degradation. Moreover, the crosslinking reactions require initiators or catalyzers, in addition to further purification to remove excess reagents.

The partial oxidation of HA catalyzed by a periodate ($NaIO_4$) is used to introduce aldehyde groups in HA glucuronic acid, providing opportunities for crosslinking with small metabolizable molecules such as adipic dihydrazide (ADH) by click reactions[19-23]. The HA/ADH hydrogel was initially studied for nucleus pulposus regeneration[24-26]. The improved injectability and *in situ* gelation motivated physicochemical studies aimed at novel applications[21, 27]. Our recent studies characterized the structural changes modulated by the oxidation degree and ADH concentration and the thermosensitivity of the HA/ADH hydrogels with different packings[28].

This review focuses on the preparation and characterization of the oxi-HA and oxi-HA/ADH and compares their properties and benefits regarding HA and HA/ADH prepared by typical chemical crosslink chemistry. Additionally, it presents the clinical studies and discusses the potential of oxi-HA/ADH-based biomaterials for applications in tissue engineering and regenerative medicine.

2. HYALURONIC ACID HYDROGELS

2.1. Molecular and structural domains

Hyaluronic acid (HA) is a nonsulfated glycosaminoglycan (GAG) comprising alternating units of D-glucuronic acid and N-acetyl-D-glucosamine, connected by β-1,3- and β-1,4-glycosidic bonds (Figure 1A). HA is negatively charged in neutral aqueous

solution because of its pKa value, approximately 3-4, referring to the carboxyl groups. Additionally, it forms a second structure because of hydrophobic interactions and intermolecular hydrogen bonds, enabling the aggregation of polymeric chains and formation of an extended meshwork (Figure B)[29]. The porous structure formed among the chains allows the diffusion of small and large molecules such as proteins (Figure C).

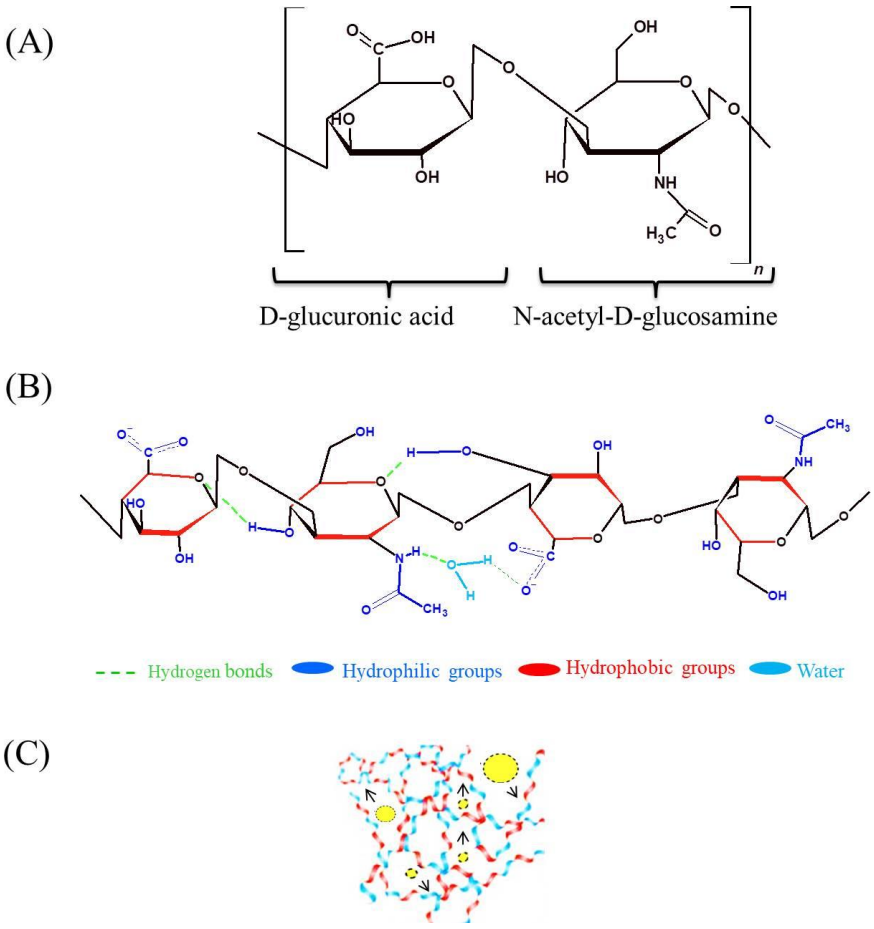

Figure 1. (A) Chemical structure of hyaluronic acid. (B) HA tetrasaccharide unit with the hydrophilic functional groups (in blue), hydrophobic moieties (in red) and hydrogen bonds (dashed lines in green). (C) Random coil structure of HA (blue: hydrophilic; red: hydrophobic) with the effects diffusion (free molecules with arrows).

2.2. HA hydrogels

The HA networks form three-dimensional (3D) hydrogels due to electrostatic or hydrophobic interactions between chain groups, maintaining a large amount of water in their swollen state[30].

However, the physically crosslinked hydrogels exhibit faster degradation behavior *in vivo*[12, 27, 31]. To overcome degradation and maintain the integrity of native HA, chemical or physical modification in functional groups of the native HA (carboxyl, hydroxyl, and amide) is exploited. Various chemical conjugations and covalent bonds improve mechanical strength and control stiffness, viscosity, solubility, degradation, and biological properties[14-18, 27, 32-34], maintaining their biocompatibility and biodegradability[15, 27].

HA, in the salt form of hyaluronate, is preferably functionalized at the carboxyl and hydroxyl groups of D-glucuronic and in the amino group of N-acetyl-glucosamine. Using carbodiimides or carbonyl diimidazole, the carboxyl group is covalently modified to form amide bonds, while the hydroxyl group can be modified to ether formation, ester formation, hemiacetal formation, and oxidation, and $–NHCOCH_3$ is modified by deacetylation, amidation, hemiacetylation, and hemiacetal formation[16].

2.3. HA hydrogels in tissue engineering and regenerative medicine

HA hydrogels are 3D carriers for growth factors and cells, resulting in the successful regeneration of different tissues, including bone and cartilage, as well as in the stimulation of angiogenesis[31, 35, 36]. Additional biological functionality may be incorporated by coupling proteins, amino acids, or therapeutic drugs[24, 37].

Presently, HA is an appealing starting material for hydrogel design due to its biocompatibility, native biofunctionality, biodegradability, high viscoelasticity, chondroprotective, nonimmunogenicity and versatility[12, 38, 39]. HA is widely studied in biomedical applications, including tissue engineering and regenerative medicine[6, 7],

diagnostics[8], cell immobilization[9], the separation of biomolecules or cells[10], and the regulation of biological adhesions as a barrier material[11]. Table 1 illustrates some HA-crosslinked biomaterials and their current applications.

Table 1. HA-crosslinked biomaterials and their applications in the biomedical field.

Biomaterial	Application	Reference
HA-Collagen matrix	Cartilage tissue repair and neural regeneration	40, 41
HA-Gelatin hydrogels	Bone regeneration and chondrogenic differentiation	42-45
HA-CHI composite	Cartilage tissue engineering	36, 46, 47
Oxidized HA-resveratrol hydrogel	Cell carrier for chondrocytes	48, 49
PGS-PCL-Me-HA	Heart valve tissue engineering	50
Thiolated-HA hydrogels	Tissue-engineered adipose substitutes	51-53
Collagen-PEG-grafted-HA	Intradermal drug delivery	54
Oxidized HA-gelatin microspheres	Drug delivery	55
HA-*g*-poly-(HEMA)	Lung tissue engineering	56
HA-ADH-EDCI	Drug delivery	57, 58
HA-DVS	Viscosupplements	59, 60
HA-BDDE	Viscosupplements	61-63
HA-PRP	Regenerative medicine	64-66

ADH – adipic dihydrazide

BDDE – 1,4-butanediol diglycidyl ether

CHI – chitosan

DVS – divinyl sulfone

HA – hyaluronic acid

Me – methacrylate

PCL – poly(ε-caprolactone)

PEG – polyethylene glycol

PGS – poly(glycerol sebacate)

poly(HEMA) – poly(2-hydroxyethyl methacrylate)

PRP- platelet-rich plasma

2.4. HA/ADH hydrogels

The most common methods described in the literature to crosslink high-molar-mass HA with ADH use N-(3-dimethylaminopropyl)-N′-ethylcarbodiimide hydrochloride (EDCI) or 1-ethyl-3-(3-dimethylaminopropyl) carbodiimide (EDC) as catalyzers. The reactions mediated by EDC/EDCI occur in aqueous acid solution (pH 4.0-4.75) only in the presence of the catalyzers.

ADH acts as a crosslinking agent in the phase where only one of the two hydrazide groups is intended to be coupled to the HA carboxylate. To avoid concomitant crosslinking during hydrazide functionalization, a large excess of ADH is applied[67, 68]. The reaction is stopped by an increase in the pH to 7.0. Both catalyzers are cytotoxic, with their elimination necessary by dialysis against alternating solutions of alcohol/water mixture and pure water.

Pouyani et al. (1994) described the methodology for the chemical modification of high-molar-mass HA (1.5×10^6 Da) using ADH in excess and EDC (1-ethyl-3-(3-dimethylaminopropyl carbodiimide as a catalyzer. The hydrogel obtained showed the potential of using three-dimensional matrices in the incorporation and controlled release of active compounds[69].

Lou et al. (2000) used the methodology of Pouyani et al. (1994) with modifications. They initially derivatized HA with ADH, followed by crosslinking with a macromolecular homobifunctional reagent; the poly(ethylene glycol)–propionaldehyde (PEG-diald) that resulted formed a polymer network under neutral aqueous conditions, suitable for *in situ* administration. The authors obtained a useful film for hydrophobic steroidal anti-inflammatory or drug delivery at wound sites. The film does not require purification and can be used directly after gelling39.

Wang et al. (2006) crosslinked the carboxyl groups of HA with the amine groups of glycol chitosan to form amide bonds. The carboxyl group of HA was initially activated in an aqueous solution by EDC at neutral pH and added to a glycol chitosan solution. The hydrogels had a soft and viscoelastic structure with adjustable biostability[70].

Zhang et al. (2010) studied the crosslinking of collagen (Col) with HA and Col with HA-ADH using genipin as a crosslinker. Genipin spontaneously reacts with the amine groups of Col, and Col/HA or Col/HA-ADH can be obtained directly by immersing the HA and HA/ADH hydrogels in a genipin solution. Regarding HA-ADH, the amine groups of Co and pendant hydrazide amino group from HA-ADH promoted a nucleophilic attack at the C-3 of the genipin opening dihydropyran ring, forming a nitrogen-iridoid. The results suggested that HA-ADH improved the crosslinking efficiency of genipin, producing hydrogels with enhanced mechanical resistance, and the water absorption and degradation rate were reduced[71]. Despite the satisfactory results, the use of EDC in HA-ADH derivatization required steps for purification that increase the production time and cost.

Homobifunctional ADH is a small, nontoxic, and nucleophilic dihydrazide that is easily metabolized by humans[72]. ADH forms spontaneous covalent bonds with HA, resulting in a 3D matrix in a few minutes. The hydrogels are stable, biocompatible, and thermoresistant biomaterials. *In vivo*, the HA/ADH hydrogels are gradually degraded by hyaluronidases, maintaining the gel state for up to 5 weeks after injection[24, 31]. Despite these advantages, *in vivo* applications still face challenges because foreign or inflammatory reactions can be induced[73].

3. PARTIAL OXIDATION OF HYALURONIC ACID (Oxi-HA)

Compounds with hydroxyl groups on adjacent atoms, such as HA, undergo oxidative cleavage when treated with periodically aqueous periodate (-IO_4). This is a simple and effective method to introduce reactive groups into polysaccharide structures[22, 23, 74]. Periodate treatment oxidizes the proximal hydroxyl groups (at the C2 and C3- carbons of glucuronic acid) to electrophilic aldehydes, thereby opening the sugar ring during oxidation and leaving them available for crosslinking (Figure 2) [24, 27].

The partial oxidation leads to the introduction of highly flexible links in otherwise rather stiff and extended structures. The aldehyde groups along the backbone serve as reactive chemical anchors for further reactions with nucleophilic molecules, allowing the immobilization and stabilization of compounds (drugs, biomolecules, cells)[75, 76] and hydrogel formation[77, 78].

HA partially oxidized with $NaIO_4$ requires a prolonged reaction time due to extensive intermolecular and intramolecular hydrogen bonding between the hydroxyl and carboxylate HA groups. This long time causes HA degradation and molecular weight reduction by at least an order of magnitude[21, 79]. Furthermore, after the reaction, dialysis must be performed to remove byproducts from the reaction. The presence of byproducts can lead to a decrease in cell viability and increased cytotoxicity[48].

Although $NaIO_4$ oxidation reduces the HA molar mass[79], the intrinsic viscosity of the solution, at a constant HA molar-mass , facilitates sterilization, which can be performed by passing through a 0.22-μm filter, the simplest method of sterilization[24]. Additionally, oxi-HA, as a liquid solution, can easily incorporate therapeutic agents and cells[24, 37].

Figure 2 describes the partial reaction between HA and $NaIO_4$.

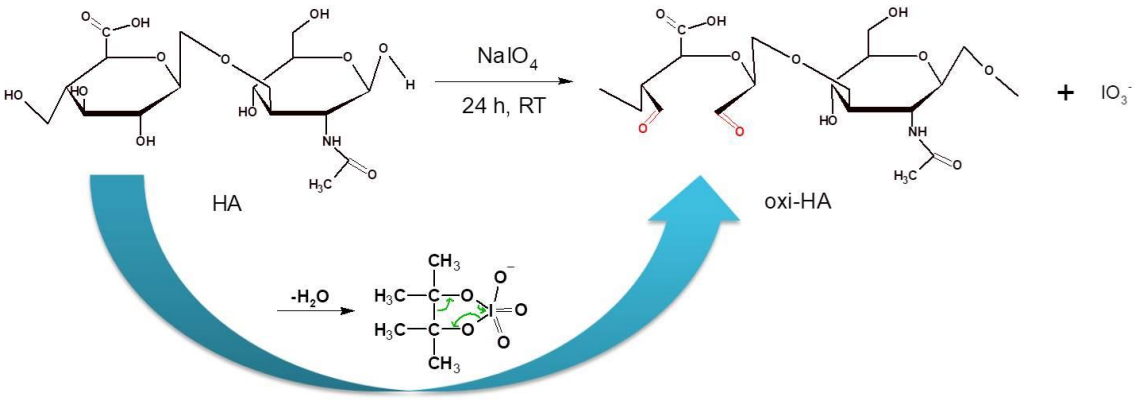

Figure 2. Partial oxidation of hyaluronic acid (HA) with sodium periodate ($NaIO_4$) to form oxidized hyaluronic acid (oxi-HA). In red, aldehyde groups are formed; in green, the bond breaks during oxidative cleavage.

The extent of oxidization in most chains is governed by electrostatic repulsion between carboxyl groups, implying a high sensitivity of chain extension or compaction in relation to ionic strength (Figure 3A). This approximation of the chains allows long-range intermolecular associations to occur, benefiting crosslinking with small molecules, such as ADH[21].

Partial oxidation allows HA stabilization. The N-acetyl-D-glucosamine units, in approximation to each other, provides a protective configuration to the entire HA molecule, decreasing the amount of crosslinker required and favoring molecular stabilization (Figure 3B)[80, 81].

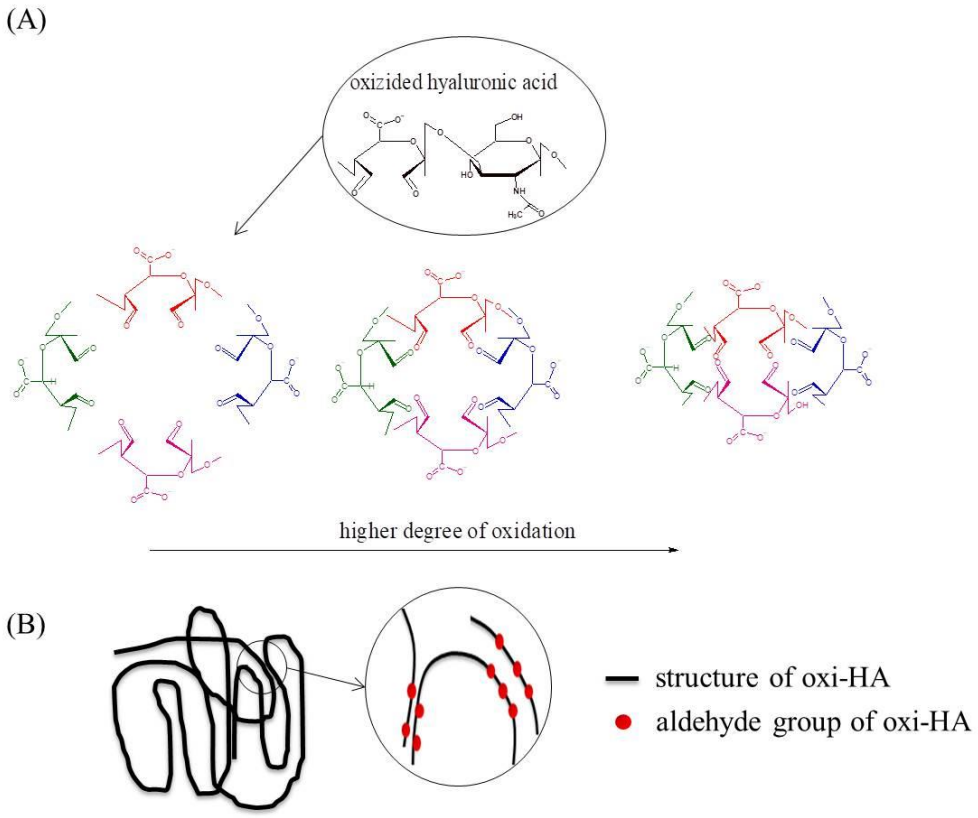

Figure 3. (A) Approximation of the aldehyde groups of oxi-HA with increasing degree of oxidation and (B) natural crosslinks (entanglements).

4. OXI-HA CROSSLINKING AND CONJUGATION

Different strategies for the crosslinking of oxi-HA hydrogels are found in the literature, providing the possibility to generate multifunctional materials.

Sheu et al. (2013) developed an injection therapy by applying an oxi-HA hydrogel crosslinked with resveratrol (Res), a suitable chondrocyte carrier. In that study, the hydrogel of oxi-HA/Res demonstrated suitable performance for treating cartilage defects, cartilage restoration, and tissue cartilage replacement because of its potential to lead to synthesis[48]. Despite the advantages of this finding, the matrix involves several principal steps of chemical reactions that use a toxic and carcinogenic solvent, such as tetrahydrofuran. Additionally, the cost of resveratrol could make the final cost of this material unfavorable compared with other methods using oxi-HA.

Deng et al. (2017) had a similar strategy to that of Tan's group (2009) concerning a crosslinking chitosan-HA-based hydrogel. Gelation was obtained via a Schiff base reaction between the amine group of chitosan and aldehyde of oxi-HA. They proposed an injectable hydrogel matrix for abdominal tissue regeneration. In a rat model with simulated open abdomen and a large abdominal wall defect, the application of the hydrogel matrix produced a rapid cellular response, suitable ECM deposition, and expressive neovascularization compared to the control and the fibrin hydrogel group[31].

Kim et al. (2017) mixed partially oxi-HA and glycol chitosan (GS) solutions to form hydrogels via a Schiff base reaction. The viscoelastic properties of hydrogels depended on the degree of oxidation of HA, oxi-HA/GC ratio, and polymer concentration. ATDC5 cells (chondrocytes) showed good viability within these hydrogels *in vitro,* and adequate stability under physiological conditions. The mechanical stiffness increased as the GC content increased because of higher crosslinks in the gels[82]. The results were consistent with Sun's group (2013) [83].

Tan et al. (2009) synthesized a new composite hydrogel reacting N-succinyl-chitosan (more water-soluble than chitosan) and the aldehyde groups of oxi-HA. The results showed that the time of gelling, structure, equilibrium swelling, compression modulus, and degradation *in vitro* was dependent on the two-component ratio. The composite hydrogels with increasing amounts of N-succinyl-chitosan in their composition showed a slower degradation rate and an improvement in the compression modulus compared with other hydrogel formulations[36].

Differently from the described examples, Martínez-Sanz et al. (2011) initially modified the carboxylic groups of HA, adding 3-amino-1,2-propanediol in a reaction involving hydroxyl benzotriazole. They used sodium periodate to quickly (5 minutes) transform the diol-modified HA into aldehyde-modified HA. The excess sodium

periodate was quenched by adding ethylene glycol, and EDC was used for controlling the degree of aldehyde functionality on HA. Aldehyde-modified HA undergoes modifications by the inclusion of a hydrazide in the aldehyde groups. To obtain the specificity necessary for the aimed application, they added an appropriate amount of rhBMP-2 solution to the hydrazide derivative-modified HA solution before the mixture of both solutions in two syringes were joined through a connector. This hydrogel was developed for *in vivo* bone augmentation healing and filling bone defects as a substitute to autologous bone grafting commonly present in clinical intervention[84]. The material is suitable for injection and gelation *in situ* because both components involved in this process are biocompatible and of the proper viscosity. Additionally, it is an adequate alternative for protein delivery. However, to obtain the final gel, four steps of reaction and at least two purification steps were involved.

In another example, Nimmo et al. (2011) developed a cytocompatible material with great potential for soft tissue engineering and regenerative medicine that also presented an elastic modulus similar to that of central nervous system tissue. They used a clean and one-step click reaction (Diels-Alder type) to crosslink the HA. They synthesized furan-modified HA derivatives and crosslinked them with dimaleimide-PEG. The furan/dimaleimide-PEG molar ratio could be controlled to offer different mechanical and degradation properties to the crosslinked hydrogels[85]. Furan is responsible for the binding between HA and PEG. It is flammable, toxic, and carcinogenic for some species, indicating that, during the methodology, there is a need for care and extreme attention.

Sun et al. (2012) used the same mechanism developed by Tan et al. (2009) to include dexamethasone (Dex) grafted onto the N-succinyl-chitosan before being crosslinked to the aldehyde groups of oxi-HA. Dex is used to treat inflammation and

autoimmune diseases and is an important factor in adipogenesis. The number of adipose-derived stem cells (ADSCs) on the surface of the hydrogel containing Dex was greater than that without it. Additionally, the inclusion of Dex in hydrogel slightly lowered the gelation time with a significantly higher swelling ratio[83]. Another research group crosslinked HA to Dex, producing good results in the attenuation of osteoarthritis[86].

Fu et al. (2017) studied the crosslinking of oxi-HA with azide-modified polyethylene glycol (PEG). First, they produced cyclooctyne-modified HA and quadruply azide-terminated PEG. The components gelated in few minutes when combined and formed a strong HA-PEG hydrogel. The hydrogel had a fast gelation time, good strength, slow degradation rate, high crosslinking density, good stability, excellent cell-compatibility, good mechanical properties, and biocompatibility. Based on these properties, the hydrogel would be useful in a wide range of applications, such as injection filling materials for plastic surgery[87]. Despite the low toxicity of PEG, the synthesis of this material is complex and involves four steps, making the final product more expensive and the cost/benefit ratio unfavorable.

5. Oxi-HA/ADH HYDROGELS

5.1. Partial oxidation and crosslinking reactions

The partial oxidation of HA is an alternative to avoid the use of EDC in HA-ADH hydrogels. Additionally, the crosslinking of oxi-HA with ADH presents benefits in terms of the process because it is a spontaneous reaction. The oxidation degree is controlled by the sodium periodate concentration and time of reaction, while the crosslinking degree can be modulated by the ADH concentration and temperature, purity, and initial molar mass of HA. The versatility of the oxi-HA/ADH hydrogels opens possibilities for applications in tissue engineering[88] and regenerative medicine.

The crosslinking reaction of oxi-HA with ADH to form oxi-HA/ADH hydrogels is described in Figure 4.

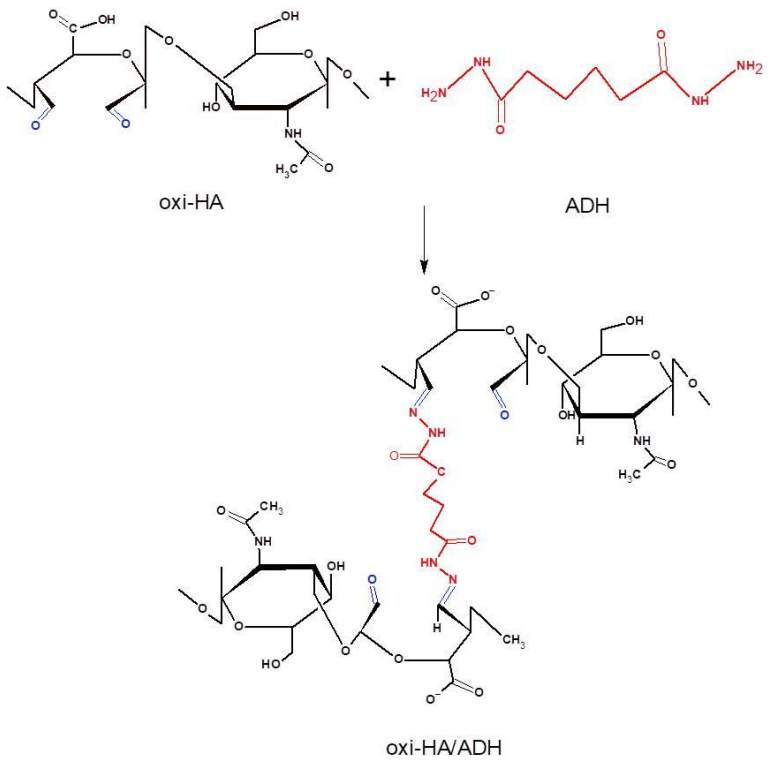

Figure 4. Chemical crosslinking mechanism of oxidized hyaluronic acid (oxi-HA in black with aldehyde groups in blue) crosslinking with adipic dihydrazide (ADH in red) to form the oxi-HA/ADH hydrogel.

Figure 5 summarizes the main properties of oxi-HA/ADH hydrogels, which are detailed below.

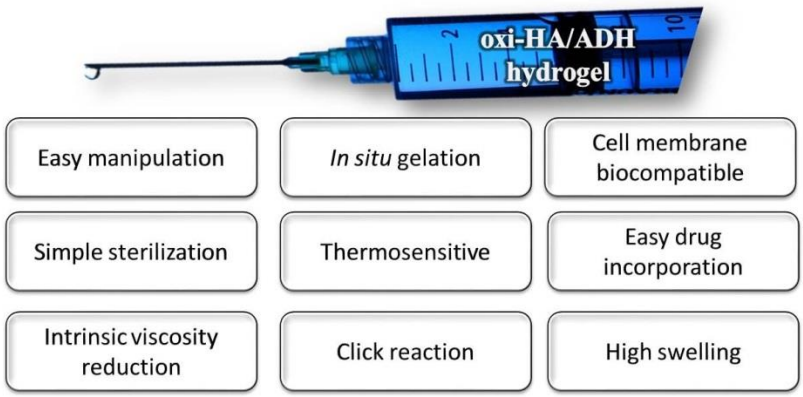

Figure 5. Properties of oxi-HA/ADH hydrogel

5.2. Structural and physicochemical characterizations of oxi-HA/ADH

The structural and physicochemical changes provided by the partial oxidation of HA and the ADH concentration were well characterized in recent studies by our group[28]. The partial oxidation of HA with $NaIO_4$ introduces dialdehyde groups into HA that form highly flexible domains, leading to the compaction of chains and an increase in the oxidation degree (Figure 3B). In contrast, at physiologic pH, the polymeric chains of nonoxidized HA overlap, forming a random coil structure with rigid domains and physical crosslinking. The approximation of the chains by compaction allows the formation of long-range intermolecular interactions and crosslinking with small molecules such as ADH.

The molar mass of oxi-HAs does not change substantially because the molecular modifications occur only in the D-glucuronate residues. The N-acetyl glucosamine groups remain intact and protect against total oxidation and the scission of the chains. Additionally, the flexibility of the aldehyde groups reflects the increasing zeta potential, and the compaction of the structures causes decreasing hydrodynamic volumes and a reduction in the viscosity.

For a high degree of oxidation, steric hindrances induce diffusion limitations and incomplete crosslinking despite the high number of aldehyde groups available in oxi-HA. Therefore, an optimum oxidation degree and an optimum ADH concentration are needed to achieve optimal crosslinking.

The structural changes and ADH crosslinking modulate functional properties, such as the gelation time, swelling, and stability of the oxi-HA/ADH hydrogels: the gelation time increases with increasing oxidation degree and ADH concentration, the highest stability and least amount of swelling were achieved at a moderate 65% oxidation degree and 4% ADH concentration.

Oxi-HA/ADH hydrogels are thermosensitive, an advantageous property due to the time available to handle the hydrogel before injection, fluidity of the hydrogel during injection and *in situ* gelation. Additionally, the hydrogel morphology with interconnected pores is essential for cell nutrition, proliferation, and migration related to cell growth. The degradation of oxi-HA 65%/ADH4 in PBS was slow, lasting 25 days. Oxi-HA/ADH hydrogels have a high-water swelling capacity, which is essential for cell growth.

This set of properties makes oxi-HA/ADH hydrogels promising for applications in tissue engineering and regenerative medicine.

5.2.1. Click reactions

The introduced aldehyde groups in the HA backbone from partial oxidation allow spontaneous crosslinking by the click reaction with ADH.

In chemical synthesis, the click reactions comprise compatible small molecules used in conjugation. They are driven quickly and irreversibly to produce a high yield of a single reaction product, with high reaction specificity. They generate minimal byproducts, allows bioorthogonality and are not disturbed by water. These qualities make click reactions particularly suitable for complex biological environments[12, 89].

The concept of click synthesis has been used in pharmacology and has emerged as an innovative and versatile strategy to construct novel functional hydrogels. HA and other biopolymers have the potential for a wide range of click reactions due to their reactive functional groups and are advantageous over traditional crosslinking because of their high yield, rapid reactivity under mild conditions, superior chemo-selectivity, and specificity with nontoxic byproducts[12].

The click reactions have also been referred to as Schiff-base reactions.This type of reaction is one of the most widely accepted strategies to preparation of hydrogels,

particularly because of the mild reaction conditions and high reaction rates. Schiff bases in hyaluronic acid are typically obtained by the condensation of an aldehyde with primary amines, forming imine linkages. This reaction occurs in the absence of crosslinking agents that could be cytotoxic[27, 31, 36, 90].

Figure 6 shows the main classes of biomedical applications of click hydrogels[91].

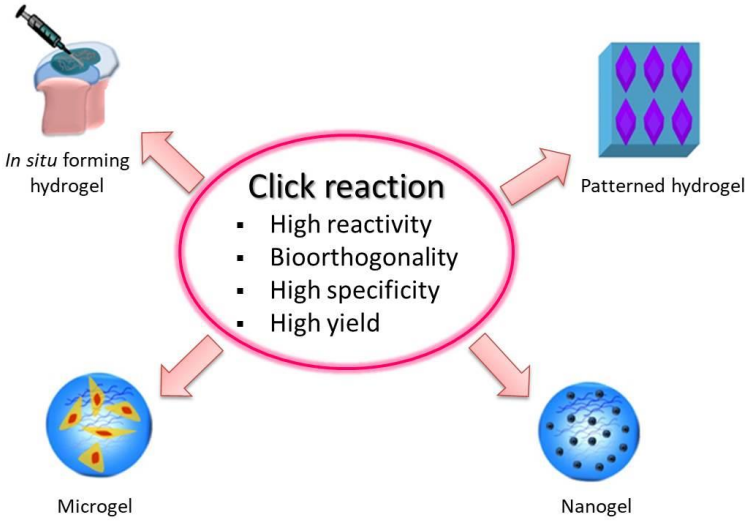

Figure 6. Classes of biomedical applications of click hydrogels: in situ forming hydrogel, patterned hydrogel (scaffolds), microgels, and nanogels.

The most innovative application of click reactions is *in situ* gelation with the perspectives of being minimally invasive *in vivo* applications. The mixture of the two components, in a liquid state, could be injected to become a gel inside the body at the desired site in a few minutes. The hydrogels can entrap growth factors or cells in the physiological environment or in *vitro* cell culture as a functional provisional ECM in tissue engineering. In general, these hydrogels reduce cell death or loss of bioactivity of the encapsulated drugs or growth factors[89] because of the absence of toxicity and side effects. The *in situ* click hydrogels also have demonstrated great potential for injectable systems for long-term sustained drug and protein release[91]. Importantly, the imine

linkages undergo hydrolysis under acid conditions, limit their use as an injectable hydrogel in pH slightly acidic[27, 31, 36, 90].

The click reactions are also used to crosslink micro and nanogels, as well as to form patterned hydrogels to guide cell growth and tissue regeneration[92-94].

5.2.2. Thermosensitivity

Thermosensitive hydrogels have been extensively studied for various applications, such as drug delivery[95, 96], cell culture[97, 98], bioreactors[99, 100], and diagnostics[101].

Thermosensitive hydrogels comprise exclusively of an interpenetrating network of polymeric chains that can undergo phase transitions to the gel-sol state because of temperature manipulation. The biopolymer contains hydrophobic and hydrophilic components in the structures, and the phenomenon of the thermal response is derived from the delicate balance, interaction, and arrangements between the hydrophobic and hydrophilic portions of the polymer monomer[102, 103]. The variation in the temperature affects the interactions between the segments of the polymer (hydrophilic and hydrophobic) and water molecules. This new packing of the segments changes the solubility of the reticulated network, causing the transition to the sol-gel phase, the phenomenon of the transition from a solution to a gel[104].

These hydrogels can be divided into two categories: thermosensitive negative or positive hydrogels[105]. For thermosensitive negative hydrogels, decreasing the temperature—*i.e.*, a lower critical solution temperature (LCST)—causes an increase in the water solubility of the hydrogel. In this case, the hydrogen bond between the hydrophilic segments of the polymer and molecules is dominant. However, as the temperature increases—that is, above the LCST, the hydrophobic interactions between hydrophobic groups become stronger and the hydrogen bond becomes weaker, making

them increasingly hydrophobic and insoluble and causing gelation. However, thermosensitive positive hydrogels are formed after cooling a polymer solution with an upper critical solution temperature (UCST). Thus, the water solubility of the hydrogel increases as the temperature increases and gelation occurs with the decrease in temperature[106].

The most significant factor in polymeric systems is the level of solubility that is reached above the LCST due to the entanglement and collapse of the polymeric chains in the network. Factors such as the polymer concentration, chemical structure, and molecular weight also affect the gelation process. Examples of polymers implemented as thermosensitive hydrogels include poloxamers or pluronics[107, 108], chitosan[109, 110], gelatin[111], as well as cellulose derivatives[112], and the synthetic poly(N-isopropylacrylamide) (PNIPAAm) and its derivatives[107] that have been identified largely in the field of drug administration and the engineering of bone tissues[113].

Injectable hydrogels using hyaluronic acid have been explored as cell and biomolecule delivery systems because they can be readily integrated into the gelling matrix[114-117]. This hydrogel allows formation *in situ* and an easy and homogeneous cell distribution within any size or shape of the defect before gelation, in addition to allowing good physical integration to the defect, avoiding an open surgery procedure, and facilitating the use of minimally invasive approaches for material delivery[118, 119]. Hydrogel formation for many systems occurs almost instantly when the gelation temperature is reached[120]. Each system has its advantages and disadvantages, and the choice of hydrogel depends on its intrinsic properties and application[121].

5.2.2.1. Thermogelling mechanisms

Several mechanisms underlying thermogelling in aqueous solutions are much debated in the literature. This phenomenon of sol-gel phase separation is governed by

the balance of hydrophilic and hydrophobic portions in the polymer chain and by the free energy of the mixture. The free energy of association varies with enthalpy, entropy, and temperature (eq.1)[120, 122].

$$\Delta G = \Delta H - T\Delta S \qquad \text{(eq. 1)}$$

A polymer, when dissolved in water, undergoes three types of interactions: interactions between polymer molecules, between polymer and water, and between water molecules. For polymers that exhibit an LCST, the increase in temperature results in negative free energy of the system, making the water-polymer association unfavorable and facilitating the other two types of interactions. This negative free energy (ΔG) is attributed to the higher entropy term (ΔS) in relation to the increase in the enthalpy term (ΔH) in the thermodynamic relationship (eq. 1). Entropy increases because of water-water associations, which are the interactions that govern the system. This phenomenon is called the hydrophobic effect. Alternatively, some amphiphilic polymers, which self-assemble in solution, show gel formation due to polymer-polymer interactions when the temperature is increased[123-125].

For oxi-HA/ADH hydrogels at temperatures above 37°C, the polymer shrinks and becomes hydrophobic; at temperatures below 37°C, the hydrogels swell and become hydrophilic (Figure 7). This responsive behavior by segregating water molecules from chains at temperatures above the phase temperature occurs due to the entropic gain of the system, wherein an aqueous environment, it is superior to the enthalpic gain of the connections between the water molecules and chains in this phase transition[28, 126, 127.]

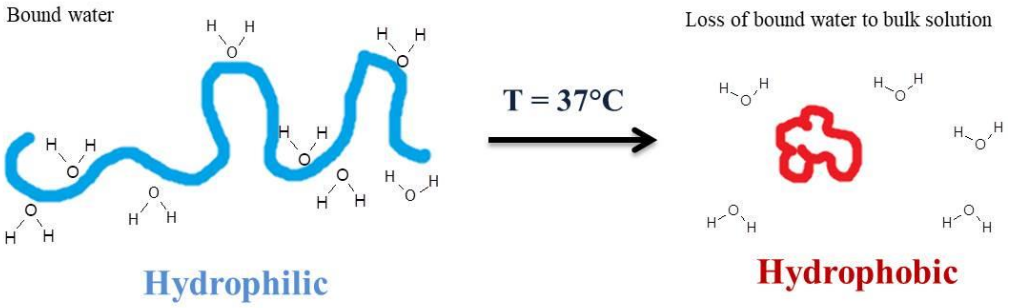

Figure 7. Schematic of the thermoresponsive behavior of the oxi-HA/ADH hydrogel.

5.2.3. Injectable thermosensitive hydrogels

The implantation of premolded hydrogels in the body requires an invasive surgical procedure that can cause pain and discomfort to the patient, in addition to cost and time, causing a limitation in clinical use. In contrast, injectable hydrogels not only have the typical advantages of conventional hydrogels but can be injected with minimal invasiveness at the destination sites and used for irregularly shaped locations, providing more comfort (less pain) and a faster recovery period for patients, as well as lower costs and fewer complications and side effects[128, 129].

Three main mechanisms are proposed for the injectability of a material[129]: 1) *In situ* gelling liquids: these materials are normally a flowable solution or liquid before and during injection and form a gel after injection into the body. The hydrogel of chitosan with glycerol phosphate disodium salt is an example of growth factor delivery and chondrocyte encapsulation for cartilage tissue engineering[109]; 2) injectable gels: these materials are found in the gel form before injection, can flow during injection because of shear forces and revert to a gel after injection. The hydrogel of hyaluronic acid with methylcellulose is an example of the delivery of therapeutic agents for the repair of spinal cord injuries[130]; 3) injectable particles: these particles, which can be nano, micro, or macroscale, depending on the desired outcomes, are immersed in a liquid phase before and during the injection. They can be self-assembled or aggregate to form a gel

after injection. The hydrogel is composed of FITC-conjugated mesoporous silica nanoparticles and a shell formed by a layer of hyaluronic acid for drug delivery to target tumors (anticancer)[131].

Injectable hydrogels have been developed as promising and successful biomaterials for several applications, including the administration of therapeutic agents, cells, and bioactive molecules, the treatment of inflammatory and infectious diseases and cancers and tissue repair and regeneration[113, 132, 133]. HA is the most commonly used biomaterial in tissue engineering and regenerative medicine[134, 135].

6. OXI-HA/ADH HYDROGELS IN TISSUE ENGINEERING AND REGENERATIVE MEDICINE

The aldehyde-hydrazide reaction has currently attracted interest in hydrogel design because of its high efficiency, cytocompatibility, simplicity, reversibility, and mild reaction conditions. In particular, these hydrogels seem to be a promising approach for tissue engineering[39].

Jia et al. (2004) obtained the material HA-ADH and crosslinked it with a previously prepared oxi-HA (by sodium periodate). They aimed to obtain an ideal material for bupivacaine release to be injected or gelled *in situ* during surgeries. These hydrogels are considered a safe and effective means of prolonging the duration of the block of local anesthetics, making them useful in clinical applications[79].

Su et al. (2010) studied the oxi-HA with ADH as an injectable hydrogel for cell culture. The hydrogel was biocompatible with nucleus pulposus cells and allowed the development of aggrecan and type II collagen, which are the main components in the ECM of this cell type, indicating that the hydrogel could be maintained in phosphate-buffered saline for at least 35 days. These results suggest an injectable hydrogel can play a role in nucleus pulposus replacement and can synthesize new tissue through a

minimally invasive therapy, overcoming the problems of traditional implants (preformed scaffolds *in vitro),* such as the migration of the scaffolds, requirement of surgery for the implant, and irregular surgical defects that are difficult to fill[24].

Hu et al. (2017) evaluated the *in vitro* and *in vivo* cytocompatibility and the anti-adherent effect of oxi-HA/ADH hydrogels with different cell types present in the vertebral column to prevent postoperative epidural fibrosis. The injectable hydrogel filled an irregular surgical defect, became a gel only *in situ* and was delivered using a minimally invasive method. These properties indicated that the material could prevent epidural fibrosis, inhibit the adherence of fibroblasts and reduce scar tissue formation of scar tissue. Thus, the hydrogel presented reasonable biocompatibility for neural cells, Schwann cells, fibroblasts, and myoblasts. *In vivo* studies showed that the gelification was suitable to cover the exposed neural structure at the laminectomy site[37].

Liang et al. (2018) investigated the viability and effect of radiotherapy treatment using the combination of the oxi-HA/ADH hydrogel with carboplatin (platinum-based antineoplastic agent) commonly applied in the clinical treatment of cancer. The technique aimed to improve the control of tumor growth and treatment of malignant glioma. The gelation time of the material was 17 s. For the subcutaneous tumor model of mice, this gelation time was suitable for intratumoral injection and hydrogel stabilization. For human brain tumor applications, the gelation time had to be increased to approximately 3 minutes. Their results demonstrated an effective, convenient, and safe treatment in a mouse model that simplifies drug administration and avoids an excess of radiation for the treatment of glioma[136].

The versatility of the oxi-HA/ADH hydrogels enables improvements or combinations with other substances to obtain novel properties. Ma et al. (2017) crosslinked oxi-HA in the presence of ADH and poly-ethylene glycol (PEG) to improve

the toughness of oxi-HA/ADH hydrogels. The preparation was the same as that for oxi-HA/ADH with only the addition of PEG in the oxi-HA solution. The *in situ* formation of the hydrogel containing PEG occurred in approximately 20 s. They observed that increasing the PEG content prolonged the gelation time, likely because the PEG molecules disturb the movement of ADH molecules and, consequently, the reaction time. Oxi-HA/ADH hydrogels are pseudoplastic fluids, but part of the network structure was lost following the addition of PEG. PEG fills the internal pore of the porous 3D structure, shrinking the hydrogel and decreasing its crosslinking density to improve the compression resistance[137]. The new PEGylated hydrogel material promoted better adhesion to the CD44 receptor when gelled *in situ*[138]. This higher stability is useful for bottom-up methods of cell culture, inhibiting biopolymer chain breaks. According to the cell type, the incorporation of movement and pressure (hydrostatic pressure and shear stress) inside the bioreactor is essential; thus, a material with higher toughness is advised[139].

More recently, Weis et al. (2018) evaluated hydrogels based on oxidized hyaluronic acid crosslinked with ADH for their suitability as bioinks for 3D bioprinting[140]. Liao et al. (2020) studied the oxi-HA/ADH hydrogel loaded with vancomycin and evaluated its biocompatibility, drug release, *in vitro* antimicrobial activity, and effectiveness in a biofilm model[141].

Despite their innumerable advantages, oxi-HA/ADH hydrogels remain to be explored in micro or nanoparticles. Oxi-HA/ADH hydrogels in the form of particles is a potential technology that offers promising and wide applications in the fields of biomaterials, regenerative medicine incorporating cells, and modular tissue engineering[142].

7. CONCLUSIONS

Oxi-HA/ADH hydrogels have unique properties and potentialize various approaches for developing novel biomaterials for tissue engineering and regenerative medicine that can improve existing therapies or motivate the development of novel therapies. Further research must be conducted to explore these hydrogel properties in nano and microparticles and the growth of cells in scaffolds, as well as the growth and differentiation of stem cells for clinical applications.

Funding This study was supported by the National Council for Scientific and Technological Development (CNPq), grant number 140924/2017-5, and the São Paulo Research Foundation (FAPESP), grant numbers 2019/12665-3 and 2016/10132-0.

Compliance with ethical standards

Conflict of Interest The authors declare no conflicts of interest.

References

1. Spicer, A. P.; Tien, J. Y., Hyaluronan and morphogenesis. Birth Defects Research Part C: Embryo Today 2004, 72 (1), 89-108.

2. Meyer, K.; Palmer, J. W., The polysaccharide of the vitreous humor. Journal of Biological Chemistry 1934, 107 (3), 629-634.

3. Laurent, T. G. "The tree": Hyaluronan research in the 20th century. http://www.glycoforum.gr.ip/science/hyaluronan/HA23E.html) (accessed A1).

4. Balazs, E. A.; Leschiner, A.; Leschiner, A.; Band, P. Chemically modified hyaluronic acid preparation and method of recovery thereof from animal tissues. 1987.

5. Berthiaume, F.; Maguire, T. J.; Yarmush, M. L., Tissue Engineering and Regenerative Medicine: History, Progress, and Challenges. Annual Review of Chemical and Biomolecular Engineering, Vol 2 2011, 2, 403-430.

6. Lee, K. Y.; Mooney, D. J., Hydrogels for tissue engineering. Chemical Reviews 2001, 101 (7), 1869-1879.

7. Spiller, K. L.; Maher, S. A.; Lowman, A. M., Hydrogels for the Repair of Articular Cartilage Defects. Tissue Engineering Part B-Reviews 2011, 17 (4), 281-299.

8. van der Linden, H. J.; Herber, S.; Olthuis, W.; Bergveld, P., Stimulus-sensitive hydrogels and their applications in chemical (micro)analysis. Analyst 2003, 128 (4), 325-331.

9. Jen, A. C.; Wake, M. C.; Mikos, A. G., Review: Hydrogels for cell immobilization. Biotechnology and Bioengineering 1996, 50 (4), 357-364.

10. Wang, K. L.; Burban, J. H.; Cussler, E. L., HYDROGELS AS SEPARATION AGENTS. Advances in Polymer Science 1993, 110, 67-79.

11. Bennett, S. L.; Melanson, D. A.; Torchiana, D. F.; Wiseman, D. M.; Sawhney, A. S., Next-generation HydroGel films as tissue sealants and adhesion barriers. Journal of Cardiac Surgery 2003, 18 (6), 494-499.

12. Radhakrishnan, J.; Subramanian, A.; Krishnan, U. M.; Sethuraman, S., Injectable and 3D Bioprinted Polysaccharide Hydrogels: From Cartilage to Osteochondral Tissue Engineering. Biomacromolecules 2017, 18 (1), 1-26.

13. Zhu, W. B.; Mow, V. C.; Rosenberg, L. C.; Tang, L. H., DETERMINATION OF KINETIC CHANGES OF AGGRECAN-HYALURONAN INTERACTIONS IN

SOLUTION FROM ITS RHEOLOGICAL PROPERTIES. Journal of Biomechanics 1994, 27 (5), 571-579.

14. Walimbe, T.; Panitch, A.; Sivasankar, P. M., A Review of Hyaluronic Acid and Hyaluronic Acid-based Hydrogels for Vocal Fold Tissue Engineering. Journal of Voice 2017, 31 (4), 416-423.

15. Burdick, J. A.; Prestwich, G. D., Hyaluronic Acid Hydrogels for Biomedical Applications. Advanced Materials 2011, 23 (12), H41-H56.

16. Ahadian, S.; Savoji, H.; Khademhosseini, A., Recent Advances in Hydrogels for Tissue Engineering. Chemical Engineering Progress 2018, 114 (5), 56-63.

17. Hoare, T. R.; Kohane, D. S., Hydrogels in drug delivery: Progress and challenges. Polymer 2008, 49 (8), 1993-2007.

18. Schante, C. E.; Zuber, G.; Herlin, C.; Vandamme, T. F., Chemical modifications of hyaluronic acid for the synthesis of derivatives for a broad range of biomedical applications. Carbohydrate Polymers 2011, 85 (3), 469-489.

19. Painter, T.; Larsen, B., FURTHER ILLUSTRATION OF NEAREST-NEIGHBOR AUTOINHIBITORY EFFECTS IN OXIDATION OF ALGINATE BY PERIODATE ION. Acta Chemica Scandinavica 1973, 27 (6), 1957-1962.

20. Jeanloz, R. W.; Forchielli, E., STUDIES ON HYALURONIC ACID AND RELATED SUBSTANCES .4. PERIODATE OXIDATION. Journal of Biological Chemistry 1951, 190 (2), 537-546.

21. Kristiansen, K. A.; Dalheim, M. O.; Christensen, B. E., Periodate oxidation and macromolecular compaction of hyaluronan. Pure and Applied Chemistry 2013, 85 (9), 1893-1900.

22. Wong, S. S., Chemistry of protein conjugation and cross-linking. 1991; p 340.

23. Solomons, G.; Fryhle, C., Organic chemistry. 7 ed.; John Wiley & Sons: 1999; p 1344.

24. Su, W. Y.; Chen, Y. C.; Lin, F. H., Injectable oxidized hyaluronic acid/adipic acid dihydrazide hydrogel for nucleus pulposus regeneration. Acta Biomaterialia 2010, 6 (8), 3044-3055.

25. Chen, Y. C.; Su, W. Y.; Yang, S. H.; Gefen, A.; Lin, F. H., In situ forming hydrogels composed of oxidized high molecular weight hyaluronic acid and gelatin for nucleus pulposus regeneration. Acta Biomaterialia 2013, 9 (2), 5181-5193.

26. Collin, E. C.; Grad, S.; Zeugolis, D. I.; Vinatier, C. S.; Clouet, J. R.; Guicheux, J. J.; Weiss, P.; Alini, M.; Pandit, A. S., An injectable vehicle for nucleus pulposus cell-based therapy. Biomaterials 2011, 32 (11), 2862-2870.

27. Khunmanee, S.; Jeong, Y.; Park, H., Crosslinking method of hyaluronic-based hydrogel for biomedical applications. Journal of Tissue Engineering 2017, 8.

28. França, C. G.; Sacomani, D. P.; Villalva, D. G.; Nascimento, V. F.; Dávila, J. L.; Santana, M. H. A., Structural changes and crosslinking modulated functional properties of oxi-HA/ADH hydrogels useful for regenerative purposes. European Polymer Journal 2019, 121 (109288).

29. Fallacara, A.; Baldini, E.; Manfredini, S.; Vertuani, S., Hyaluronic acid in the third millennium. Polymers 2018, 10, 701.

30. Buwalda, S. J.; Boere, K. W. M.; Dijkstra, P. J.; Feijen, J.; Vermonden, T.; Hennink, W. E., Hydrogels in a historical perspective: From simple networks to smart materials. Journal of Controlled Release 2014, 190, 254-273.

31. Deng, Y. M.; Ren, J. N.; Chen, G. P.; Li, G. E.; Wu, X. W.; Wang, G. F.; Gu, G. S.; Li, J. S., Injectable in situ cross-linking chitosan-hyaluronic acid based hydrogels for abdominal tissue regeneration. Scientific Reports 2017, 7.

32. Bulpitt, P.; Aeschlimann, D., New strategy for chemical modification of hyaluronic acid: Preparation of functionalized derivatives and their use in the formation of novel biocompatible hydrogels. Journal of Biomedical Materials Research 1999, 47 (2), 152-169.

33. Kolb, H. C.; Finn, M. G.; Sharpless, K. B., Click chemistry: Diverse chemical function from a few good reactions. Angewandte Chemie-International Edition 2001, 40 (11), 2004-+.

34. Crescenzi, V.; Cornelio, L.; Di Meo, C.; Nardecchia, S.; Lamanna, R., Novel hydrogels via click chemistry: Synthesis and potential biomedical applications. Biomacromolecules 2007, 8 (6), 1844-1850.

35. Kim, J.; Kim, I. S.; Cho, T. H.; Lee, K. B.; Hwang, S. J.; Tae, G.; Noh, I.; Lee, S. H.; Park, Y.; Sun, K., Bone regeneration using hyaluronic acid-based hydrogel with bone morphogenic protein-2 and human mesenchymal stem cells. Biomaterials 2007, 28 (10), 1830-1837.

36. Tan, H. P.; Chu, C. R.; Payne, K. A.; Marra, K. G., Injectable in situ forming biodegradable chitosan-hyaluronic acid based hydrogels for cartilage tissue engineering. Biomaterials 2009, 30 (13), 2499-2506.

37. Hu, M. H.; Yang, K. C.; Sun, Y. H.; Chen, Y. C.; Yang, S. H.; Lin, F. H., IN SITU FORMING OXIDISED HYALURONIC ACID/ADIPIC ACID DIHYDRAZIDE HYDROGEL FOR PREVENTION OF EPIDURAL FIBROSIS AFTER LAMINECTOMY. European Cells & Materials 2017, 34, 307-320.

38. Schiraldi, C.; La Gatta, A.; De Rosa, M., Biotechnological production and application of hyaluronan. In Biopolymers, London, UK: IntechOpen, 2010.

39. Trombino, S.; Servidio, C.; Curcio, F.; Cassano, R., Strategies for Hyaluronic Acid-Based Hydrogel Design in Drug Delivery. Pharmaceutics 2019, 11 (8).

40. Matsiko, A.; Levingstone, T. J.; O'Brien, F. J.; Gleeson, J. P., Addition of hyaluronic acid improves cellular infiltration and promotes early-stage chondrogenesis in a collagen-based scaffold for cartilage tissue engineering. Journal of the Mechanical Behavior of Biomedical Materials 2012, 11, 41-52.

41. Park, S. N.; Lee, H. J.; Lee, K. H.; Suh, H., Biological characterization of EDC-crosslinked collagen-hyaluronic acid matrix in dermal tissue restoration. Biomaterials 2003, 24 (9), 1631-1641.

42. Vaca-González, J. J.; Clara-Trujillo, S.; Guillot-Ferriols, M.; Ródenas-Rochina, J.; Sanchis, M. J.; Ribelles, L. G.; Garzón-Alvarado, D. A.; Ferrer, G. G., Effect of electrical stimulation on chondrogenic differentiation of mesenchymal stem cells cultured in hyaluronic acid – Gelatin injectable hydrogels. Bioelectrochemistry 2020, 134 (107536).

43. Park, S. N.; Kim, J. K.; Suh, H., Evaluation of antibiotic-loaded collagen-hyaluronic acid matrix as a skin substitute. Biomaterials 2004, 25 (17), 3689-3698.

44. Hou, K. T.; Liu, T. Y.; Chiang, M. Y.; Chen, C. Y.; Chang, S. J.; Chen, S. Y., Cartilage Tissue-Mimetic Pellets with Multifunctional Magnetic Hyaluronic Acid-Graft-Amphiphilic Gelatin Microcapsules for Chondrogenic Stimulation. Polymers 2020, 12 (4).

45. Thi, P. L.; Son, J. Y.; Lee, Y.; Ryu, S. B.; Park, K. M.; Park, K. D., Enzymatically Crosslinkable Hyaluronic Acid-Gelatin Hybrid Hydrogels as Potential Bioinks for Tissue Regeneration. Macromolecular Research 2020, 28 (4), 400-406.

46. Lu, K. Y.; Lin, Y. C.; Lu, H. T.; Ho, Y. C.; Weng, S. C.; Tsai, M. L.; Mi, F. L., A novel injectable in situ forming gel based on carboxymethyl hexanoyl chitosan/hyaluronic acid polymer blending for sustained release of berberine. Carbohydrate Polymers 2019, 206, 664-673.

47. Park, H.; Choi, B.; Hu, J. L.; Lee, M., Injectable chitosan hyaluronic acid hydrogels for cartilage tissue engineering. Acta Biomaterialia 2013, 9 (1), 4779-4786.

48. Sheu, S. Y.; Chen, W. S.; Sun, J. S.; Lin, F. H.; Wu, T., Biological characterization of oxidized hyaluronic acid/resveratrol hydrogel for cartilage tissue engineering. Journal of Biomedical Materials Research Part A 2013, 101 (12), 3457-3466.

49. Li, H. R.; Qi, Z. P.; Zheng, S.; Chang, Y. X.; Kong, W. J.; Fu, C.; Yu, Z. Y.; Yang, X. Y.; Pan, S., The Application of Hyaluronic Acid-Based Hydrogels in Bone and Cartilage Tissue Engineering. Advances in Materials Science and Engineering 2019, 2019.

50. Eslami, M.; Vrana, N. E.; Zorlutuna, P.; Sant, S.; Jung, S.; Masoumi, N.; Khavari-Nejad, R. A.; Javadi, G.; Khademhosseini, A., Fiber-reinforced hydrogel scaffolds for heart valve tissue engineering. Journal of Biomaterials Applications 2014, 29 (3), 399-410.

51. Young, J. L.; Tuler, J.; Braden, R.; Schup-Magoffin, P.; Schaefer, J.; Kretchmer, K.; Christman, K. L.; Engler, A. J., In vivo response to dynamic hyaluronic acid hydrogels. Acta Biomaterialia 2013, 9 (7), 7151-7157.

52. Asim, M. H.; Silberhumer, S.; Shahzadi, I.; Jalil, A.; Matuszczak, B.; Bernkop-Schnurch, A., S-protected thiolated hyaluronic acid: In-situ crosslinking hydrogels for 3D cell culture scaffold. Carbohydrate Polymers 2020, 237.

53. Xu, Z. X.; Li, W. Y.; Yang, L.; Tang, S.; Hu, Q. L.; Wang, Y. X., Construction of Biomimetic Cross-linking Polyplexes with Thiolated-HA Shielding. Chemical Journal of Chinese Universities-Chinese 2012, 33 (2), 404-408.

54. Surini, S.; Akiyama, H.; Morishita, M.; Takayama, K.; Nagai, T., Polyion complex of chitosan and sodium hyaluronate as an implant device for insulin delivery. Stp Pharma Sciences 2003, 13 (4), 265-268.

55. Weng, L.; Ivanova, N. D.; Zakhaleva, J.; Chen, W. L., In vitro and in vivo suppression of cellular activity by guanidinoethyl disulfide released from hydrogel microspheres composed of partially oxidized hyaluronan and gelatin. Biomaterials 2008, 29 (31), 4149-4156.

56. Radhakumary, C.; Nandkumar, A. M.; Nair, P. D., Hyaluronic acid-g-poly(HEMA) copolymer with potential implications for lung tissue engineering. Carbohydrate Polymers 2011, 85 (2), 439-445.

57. Bicudo, R. C. S.; Santana, M. H. A., Production of hyaluronic acid (HA) nanoparticles by a continuous process inside microchannels: Effects of non-solvents, organic phase flow rate, and HA concentration. Chemical Engineering Science 2012, 84, 134-141.

58. Schramm, C.; Spitzer, M. S.; Henke-Fahle, S.; Steinmetz, G.; Januschowski, K.; Heiduschka, P.; Geis-Gerstorfer, J.; Biedermann, T.; Bartz-Schmidt, K. U.; Szurman, P., The Cross-linked Biopolymer Hyaluronic Acid as an Artificial Vitreous Substitute. Investigative Ophthalmology & Visual Science 2012, 53 (2), 613-621.

59. Shimojo, A. A. M.; Pires, A. M. B.; Lichy, R.; Santana, M. H. A., The Performance of Crosslinking with Divinyl Sulfone as Controlled by the Interplay Between the Chemical Modification and Conformation of Hyaluronic Acid. Journal of the Brazilian Chemical Society 2015, 26 (3), 506-512.

60. Borzacchiello, A.; Russo, L.; Malle, B. M.; Schwach-Abdellaoui, K.; Ambrosio, L., Hyaluronic Acid Based Hydrogels for Regenerative Medicine Applications. Biomed Research International 2015, 2015.

61. Shimojo, A. A. M.; Pires, A. M. B.; Lichy, R.; Rodrigues, A. A.; Santana, M. H. A., The crosslinking degree controls the mechanical, rheological, and swelling properties of hyaluronic acid microparticles. Journal of Biomedical Materials Research Part A 2015, 103 (2), 730-737.

62. Lee, D. Y.; Cheon, C.; Son, S.; Kim, Y. Z.; Kim, J. T.; Jang, J. W.; Kim, S. S., Influence of Molecular Weight on Swelling and Elastic Modulus of Hyaluronic Acid Dermal Fillers. Polymer-Korea 2015, 39 (6), 976-980.

63. Xue, Y.; Chen, H. Y.; Xu, C.; Yu, D. H.; Xu, H. J.; Hu, Y., Synthesis of hyaluronic acid hydrogels by crosslinking the mixture of high-molecular-weight hyaluronic acid and low-molecular-weight hyaluronic acid with 1,4-butanediol diglycidyl ether. Rsc Advances 2020, 10 (12), 7206-7213.

64. de Melo, B. A. G.; Franca, C. G.; Davila, J. L.; Batista, N. A.; Caliari-Oliveira, C.; d'Avila, M. A.; Luzo, A. C. M.; Lana, J.; Santana, M. H. A., Hyaluronic acid and fibrin from L-PRP form semi-IPNs with tunable properties suitable for use in regenerative medicine. Materials Science & Engineering C-Materials for Biological Applications 2020, 109.

65. De Angelis, B.; D'Autilio, M.; Orlandi, F.; Pepe, G.; Garcovich, S.; Scioli, M. G.; Orlandi, A.; Cervelli, V.; Gentile, P., Wound Healing: In Vitro and In Vivo Evaluation of a Bio-Functionalized Scaffold Based on Hyaluronic Acid and Platelet-Rich Plasma in Chronic Ulcers. Journal of Clinical Medicine 2019, 8 (9).

66. Gilat, R.; Haunschild, E. D.; Knapik, D. M.; Evuarherhe Jr, A.; Parvaresh, K. C.; Cole, B. J., Hyaluronic acid and platelet-rich plasma for the management of knee osteoarthritis. International Orthopaedics 2020.

67. Yun, Y. H.; Goetz, D. J.; Yellen, P.; Chen, W. L., Hyaluronan microspheres for sustained gene delivery and site-specific targeting. Biomaterials 2004, 25 (1), 147-157.

68. Prestwich, G. D.; Marecak, D. M.; Marecek, J. F.; Vercruysse, K. P.; Ziebell, M. R., Controlled chemical modification of hyaluronic acid: synthesis, applications, and biodegradation of hydrazide derivatives. Journal of Controlled Release 1998, 53 (1-3), 93-103.

69. Pouyani, T.; Harbison, G. S.; Prestwich, G. D., NOVEL HYDROGELS OF HYALURONIC-ACID - SYNTHESIS, SURFACE-MORPHOLOGY, AND SOLID-STATE NMR. Journal of the American Chemical Society 1994, 116 (17), 7515-7522.

70. Wang, W., A novel hydrogel crosslinked hyaluronan with glycol chitosan. Journal of Materials Science-Materials in Medicine 2006, 17 (12), 1259-1265.

71. Zhang, L.; Xiao, Y. M.; Jiang, B.; Fan, H. S.; Zhang, X. D., Effect of Adipic Dihydrazide Modification on the Performance of Collagen/Hyaluronic Acid Scaffold. Journal of Biomedical Materials Research Part B-Applied Biomaterials 2010, 92B (2), 307-316.

72. Jia, X. Q.; Yeo, Y.; Clifton, R. J.; Jiao, T.; Kohane, D. S.; Kobler, J. B.; Zeitels, S. M.; Langer, R., Hyaluronic acid-based microgels and microgel networks for vocal fold regeneration. Biomacromolecules 2006, 7 (12), 3336-3344.

73. Hemshekhar, M.; Thushara, R. M.; Chandranayaka, S.; Sherman, L. S.; Kemparaju, K.; Girish, K. S., Emerging roles of hyaluronic acid bioscaffolds in tissue engineering and regenerative medicine. International Journal of Biological Macromolecules 2016, 86, 917-928.

74. Pereira, I.; Simoes, J.; Evtyugin, D. V.; Rouif, S.; Coimbra, M. A.; Domingues, M. R. M.; Gama, M., Effects of gamma irradiation and periodate oxidation on the structure of dextrin assessed by mass spectrometry. European Polymer Journal 2018, 103, 158-169.

75. Takei, T.; Sato, M.; Ijima, H.; Kawakami, K., In Situ Gellable Oxidized Citrus Pectin for Localized Delivery of Anticancer Drugs and Prevention of Homotypic Cancer Cell Aggregation. Biomacromolecules 2010, 11 (12), 3525-3530.

76. Ragothaman, M.; Palanisamy, T.; Kalirajan, C., Collagen-poly(dialdehyde) guar gum based porous 3D scaffolds immobilized with growth factor for tissue engineering applications. Carbohydrate Polymers 2014, 114, 399-406.

77. Su, W. Y.; Chen, K. H.; Chen, Y. C.; Lee, Y. H.; Tseng, C. L.; Lin, F. H., An Injectable Oxidated Hyaluronic Acid/Adipic Acid Dihydrazide Hydrogel as a Vitreous Substitute. Journal of Biomaterials Science-Polymer Edition 2011, 22 (13), 1777-1797.

78. Gomez, C. G.; Rinaudo, M.; Villar, M. A., Oxidation of sodium alginate and characterization of the oxidized derivatives. Carbohydrate Polymers 2007, 67 (3), 296-304.

79. Jia, X. Q.; Colombo, G.; Padera, R.; Langer, R.; Kohane, D. S., Prolongation of sciatic nerve blockade by in situ cross-linked hyaluronic acid. Biomaterials 2004, 25 (19), 4797-4804.

80. Ågerup, B.; Wik, O., NASHA™ – the MONOGRAPH. Q-Med AB: Sweden 2008; p 28.

81. Scott, J. E. Secondary and tertiary structures of hyaluronan in aqueous solution. Some biological consequences. http://glycoforum.gr.jp/science/hyaluronan/HA02/HA02E.html.

82. Kim, D. Y.; Park, H.; Kim, S. W.; Lee, J. W.; Lee, K. Y., Injectable hydrogels prepared from partially oxidized hyaluronate and glycol chitosan for chondrocyte encapsulation. Carbohydrate Polymers 2017, 157, 1281-1287.

83. Sun, J. C.; Xiao, C.; Tan, H. P.; Hu, X. H., Covalently crosslinked hyaluronic acid-chitosan hydrogel containing dexamethasone as an injectable scaffold for soft tissue engineering. Journal of Applied Polymer Science 2013, 129 (2), 682-688.

84. Martinez-Sanz, E.; Ossipov, D. A.; Hilborn, J.; Larsson, S.; Jonsson, K. B.; Varghese, O. P., Bone reservoir: Injectable hyaluronic acid hydrogel for minimal invasive bone augmentation. Journal of Controlled Release 2011, 152 (2), 232-240.

85. Nimmo, C. M.; Owen, S. C.; Shoichet, M. S., Diels-Alder Click Cross-Linked Hyaluronic Acid Hydrogels for Tissue Engineering. Biomacromolecules 2011, 12 (3), 824-830.

86. Zhang, Z. W.; Wei, X. C.; Gao, J. Z.; Zhao, Y.; Zhao, Y. M.; Guo, L.; Chen, C. W.; Duan, Z. Q.; Li, P. C.; Wei, L., Intra-Articular Injection of Cross-Linked Hyaluronic Acid-Dexamethasone Hydrogel Attenuates Osteoarthritis: An Experimental Study in a Rat Model of Osteoarthritis. International Journal of Molecular Sciences 2016, 17 (4).

87. Fu, S. L.; Dong, H.; Deng, X. Y.; Zhuo, R. X.; Zhong, Z. L., Injectable hyaluronic acid/poly(ethylene glycol) hydrogels crosslinked via strain-promoted azide-alkyne cycloaddition click reaction. Carbohydrate Polymers 2017, 169, 332-340.

88. Boehler, R. M.; Graham, J. G.; Shea, L. D., Tissue engineering tools for modulation of the immune response. Biotechniques 2011, 51 (4), 239-+.

89. Ossipov, D. A.; Piskounova, S.; Varghese, O. P.; Hilborn, J., Functionalization of Hyaluronic Acid with Chemoselective Groups via a Disulfide-Based Protection Strategy for In Situ Formation of Mechanically Stable Hydrogels. Biomacromolecules 2010, 11 (9), 2247-2254.

90. Liu, H. N.; Guo, N. N.; Wang, T. T.; Guo, W. W.; Lin, M. T.; Huang-Fu, M. Y.; Vakili, M. R.; Xu, W. H.; Chen, J. J.; Wei, Q. C.; Han, M.; Lavasanifar, A.; Gao, J. Q., Mitochondrial Targeted Doxorubicin-Triphenylphosphonium Delivered by Hyaluronic Acid Modified and pH Responsive Nanocarriers to Breast Tumor: in Vitro and in Vivo Studies. Molecular Pharmaceutics 2018, 15 (3), 882-891.

91. Jiang, Y. J.; Chen, J.; Deng, C.; Suuronen, E. J.; Zhong, Z. Y., Click hydrogels, microgels and nanogels: Emerging platforms for drug delivery and tissue engineering. Biomaterials 2014, 35 (18), 4969-4985.

92. DeForest, C. A.; Polizzotti, B. D.; Anseth, K. S., Sequential click reactions for synthesizing and patterning three-dimensional cell microenvironments. Nature Materials 2009, 8 (8), 659-664.

93. van Dijk, M.; Rijkers, D. T. S.; Liskamp, R. M. J.; van Nostrum, C. F.; Hennink, W. E., Synthesis and Applications of Biomedical and Pharmaceutical Polymers via Click Chemistry Methodologies. Bioconjugate Chemistry 2009, 20 (11), 2001-2016.

94. Heller, D. A.; Levi, Y.; Pelet, J. M.; Doloff, J. C.; Wallas, J.; Pratt, G. W.; Jiang, S.; Sahay, G.; Schroeder, A.; Schroeder, J. E.; Chyan, Y.; Zurenko, C.; Querbes, W.; Manzano, M.; Kohane, D. S.; Langer, R.; Anderson, D. G., Modular 'Click-in-Emulsion' Bone-Targeted Nanogels. Advanced Materials 2013, 25 (10), 1449-1454.

95. Bae, Y. H.; Okano, T.; Hsu, R.; Kim, S. W., THERMOSENSITIVE POLYMERS AS ON-OFF SWITCHES FOR DRUG RELEASE. Makromolekulare Chemie-Rapid Communications 1987, 8 (10), 481-485.

96. Dunshee, L. C.; Sullivan, M. O.; Kiick, K. L., Manipulation of the dually thermoresponsive behavior of peptide-based vesicles through modification of collagen-like peptide domains. Bioengineering & Translational Medicine 2020, 5 (1).

97. von Recum, H. A.; Kim, S. W.; Kikuchi, A.; Okuhara, M.; Sakurai, Y.; Okano, T., Novel thermally reversible hydrogel as detachable cell culture substrate. Journal of Biomedical Materials Research 1998, 40 (4), 631-639.

98. Utrata-Wesolek, A.; Oleszko-Torbus, N.; Bochenek, M.; Kosowski, D.; Kowalczuk, A.; Trzebicka, B.; Dworak, A., Thermoresponsive polymer surfaces and their application in tissue engineering. Polimery 2018, 63 (5), 327-338.

99. Park, T. G.; Hoffman, A. S., THERMAL CYCLING EFFECTS ON THE BIOREACTOR PERFORMANCES OF IMMOBILIZED BETA-GALACTOSIDASE IN TEMPERATURE-SENSITIVE HYDROGEL BEADS. Enzyme and Microbial Technology 1993, 15 (6), 476-482.

100. Shakya, A. K.; Nandakumar, K. S., An update on smart biocatalysts for industrial and biomedical applications. Journal of the Royal Society Interface 2018, 15 (139).

101. Bulmus, V.; Ding, Z. L.; Long, C. J.; Stayton, P. S.; Hoffman, A. S., Site-specific polymer-streptavidin bioconjugate for pH-controlled binding and triggered release of biotin. Bioconjugate Chemistry 2000, 11 (1), 78-83.

102. Xue, W.; Hamley, I. W.; Huglin, M. B., Rapid swelling and deswelling of thermoreversible hydrophobically modified poly(N-isopropylacrylamide) hydrogels prepared by freezing polymerisation. Polymer 2002, 43 (19), 5181-5186.

103. Qiu, Y.; Park, K., Environment-sensitive hydrogels for drug delivery. Advanced Drug Delivery Reviews 2012, 64, 49-60.

104. Bajpai, A. K.; Shukla, S. K.; Bhanu, S.; Kankane, S., Responsive polymers in controlled drug delivery. Progress in Polymer Science 2008, 33 (11), 1088-1118.

105. Jeong, B.; Kim, S. W.; Bae, Y. H., Thermosensitive sol-gel reversible hydrogels. Advanced Drug Delivery Reviews 2012, 64, 154-162.

106. Peppas, N. A.; Bures, P.; Leobandung, W.; Ichikawa, H., Hydrogels in pharmaceutical formulations. European Journal of Pharmaceutics and Biopharmaceutics 2000, 50 (1), 27-46.

107. Gil, E. S.; Hudson, S. M., Stimuli-reponsive polymers and their bioconjugates. Progress in Polymer Science 2004, 29 (12), 1173-1222.

108. Niu, G. G.; Du, F. Y.; Song, L.; Zhang, H. B.; Yang, J.; Cao, H.; Zheng, Y. D.; Yang, Z.; Wang, G. J.; Yang, H.; Zhu, S. Q., Synthesis and characterization of reactive poloxamer 407s for biomedical applications. Journal of Controlled Release 2009, 138 (1), 49-56.

109. Chenite, A.; Chaput, C.; Wang, D.; Combes, C.; Buschmann, M. D.; Hoemann, C. D.; Leroux, J. C.; Atkinson, B. L.; Binette, F.; Selmani, A., Novel injectable neutral solutions of chitosan form biodegradable gels in situ. Biomaterials 2000, 21 (21), 2155-2161.

110. Ruel-Gariepy, E.; Leclair, G.; Hildgen, P.; Gupta, A.; Leroux, J. C., Thermosensitive chitosan-based hydrogel containing liposomes for the delivery of hydrophilic molecules. Journal of Controlled Release 2002, 82 (2-3), 373-383.

111. Mishra, D.; Bhunia, B.; Banerjee, I.; Datta, P.; Dhara, S.; Maiti, T. K., Enzymatically crosslinked carboxymethyl-chitosan/gelatin/nano-hydroxyapatite injectable gels for in situ bone tissue engineering application. Materials Science & Engineering C-Materials for Biological Applications 2011, 31 (7), 1295-1304.

112. Lee, S. C.; Cho, Y. W.; Park, K., Control of thermogelation properties of hydrophobically-modified methylcellulose. Journal of Bioactive and Compatible Polymers 2005, 20 (1), 5-13.

113. Kondiah, P. J.; Choonara, Y. E.; Kondiah, P. P. D.; Marimuthu, T.; Kumar, P.; du Toit, L. C.; Pillay, V., A Review of Injectable Polymeric Hydrogel Systems for Application in Bone Tissue Engineering. Molecules 2016, 21 (11).

114. Huang, H. Q.; Qi, X. L.; Chen, Y. H.; Wu, Z. H., Thermo-sensitive hydrogels for delivering biotherapeutic molecules: A review. Saudi Pharmaceutical Journal 2019, 27 (7), 990-999.

115. Ohya, S.; Nakayama, Y.; Matsuda, T., Thermoresponsive artificial extracellular matrix for tissue engineering: Hyaluronic acid bioconjugated with poly(N-isopropylacrylamide) grafts. Biomacromolecules 2001, 2 (3), 856-863.

116. Mayo, L.; Quaglia, F.; Borzacchiello, A.; Ambrosio, L.; La Rotonda, M. I., A novel poloxamers/hyaluronic acid in situ forming hydrogel for drug delivery: Rheological, mucoadhesive and in vitro release properties. European Journal of Pharmaceutics and Biopharmaceutics 2008, 70 (1), 199-206.

117. Babo, P. S.; Santo, V. E.; Gomes, M. E.; Reis, R. L., Development of an Injectable Calcium Phosphate/Hyaluronic Acid Microparticles System for Platelet

Lysate Sustained Delivery Aiming Bone Regeneration. Macromolecular Bioscience 2016, 16 (11), 1662-1677.

118. Hou, Q. P.; De Bank, P. A.; Shakesheff, K. M., Injectable scaffolds for tissue regeneration. Journal of Materials Chemistry 2004, 14 (13), 1915-1923.

119. Nuttelman, C. R.; Rice, M. A.; Rydholm, A. E.; Salinas, C. N.; Shah, D. N.; Anseth, K. S., Macromolecular monomers for the synthesis of hydrogel niches and their application in cell encapsulation and tissue engineering. Progress in Polymer Science 2008, 33 (2), 167-179.

120. Klouda, L., Thermoresponsive hydrogels in biomedical applications A seven-year update. European Journal of Pharmaceutics and Biopharmaceutics 2015, 97, 338-349.

121. Vashi, A. V.; Keramidaris, E.; Abberton, K. M.; Morrison, W. A.; Wilson, J. L.; O'Connor, A. J.; Cooper-White, J. J.; Thompson, E. W., Adipose differentiation of bone marrow-derived mesenchymal stem cells using Pluronic F-127 hydrogel in vitro. Biomaterials 2008, 29 (5), 573-579.

122. Klouda, L.; Mikos, A. G., Thermoresponsive hydrogels in biomedical applications. European Journal of Pharmaceutics and Biopharmaceutics 2008, 68 (1), 34-45.

123. Southall, N. T.; Dill, K. A.; Haymet, A. D. J., A view of the hydrophobic effect. Journal of Physical Chemistry B 2002, 106 (3), 521-533.

124. Hoffman, A. S., INTELLIGENT POLYMERS IN MEDICINE AND BIOTECHNOLOGY. Artificial Organs 1995, 19 (5), 458-467.

125. Ruel-Gariepy, E.; Leroux, J. C., In situ-forming hydrogels - review of temperature-sensitive systems. European Journal of Pharmaceutics and Biopharmaceutics 2004, 58 (2), 409-426.

126. Alarcon, C. D. H.; Pennadam, S.; Alexander, C., Stimuli responsive polymers for biomedical applications. Chemical Society Reviews 2005, 34 (3), 276-285.

127. Tekin, H.; Sanchez, J. G.; Tsinman, T.; Langer, R.; Khademhosseini, A., Thermoresponsive Platforms for Tissue Engineering and Regenerative Medicine. Aiche Journal 2011, 57 (12), 3249-3258.

128. Lee, J. H., Injectable hydrogels delivering therapeutic agents for disease treatment and tissue engineering. Biomaterials Research 2018, 22.

129. Mellati, A.; Akhtari, J., Injectable hydrogels: a review of injectability mechanisms and biomedical applications. Research in Molecular Medicine 2018, 6 (4).

130. Gupta, D.; Tator, C. H.; Shoichet, M. S., Fast-gelling injectable blend of hyaluronan and methylcellulose for intrathecal, localized delivery to the injured spinal cord. Biomaterials 2006, 27 (11), 2370-2379.

131. Chen, X.; Liu, Z. N., A pH-Responsive Hydrogel Based on a Tumor-Targeting Mesoporous Silica Nanocomposite for Sustained Cancer Labeling and Therapy. Macromolecular Rapid Communications 2016, 37 (18), 1533-1539.

132. Baumann, M. D.; Kang, C. E.; Stanwick, J. C.; Wang, Y. F.; Kim, H.; Lapitsky, Y.; Shoichet, M. S., An injectable drug delivery platform for sustained combination therapy. Journal of Controlled Release 2009, 138 (3), 205-213.

133. Davoodi, P.; Ng, W. C.; Yan, W. C.; Srinivasan, M. P.; Wang, C. H., Double-Walled Microparticles-Embedded Self-Cross-Linked, Injectable, and Antibacterial Hydrogel for Controlled and Sustained Release of Chemotherapeutic Agents. Acs Applied Materials & Interfaces 2016, 8 (35), 22785-22800.

134. Allemann, I. B.; Baumann, L., Hyaluronic acid gel (Juvederm (TM)) preparations in the treatment of facial wrinkles and folds. Clinical Interventions in Aging 2008, 3 (4), 629-634.

135. Falcone, S. J.; Berg, R. A., Crosslinked hyaluronic acid dermal fillers: a comparison of rheological properties. Journal of Biomedical Materials Research Part A 2008, 87A (1), 264-271.

136. Liang, H. K. T.; Lai, X. S.; Wei, M. F.; Lu, S. H.; Wen, W. F.; Kuo, S. H.; Chen, C. M.; Tseng, W. Y. I.; Lin, F. H., Intratumoral injection of thermogelling and sustained-release carboplatin-loaded hydrogel simplifies the administration and remains the synergistic effect with radiotherapy for mice gliomas. Biomaterials 2018, 151, 38-52.

137. Ma, X. B.; Xu, T. T.; Chen, W.; Wang, R.; Xu, Z.; Ye, Z. W.; Chi, B., Improvement of Toughness for the Hyaluronic Acid and Adipic Acid Dihydrazide Hydrogel by PEG. Fibers and Polymers 2017, 18 (5), 817-824.

138. Sargazi, A.; Kamali, N.; Shiri, F.; Majd, M. H., Hyaluronic acid/polyethylene glycol nanoparticles for controlled delivery of mitoxantrone. Artificial Cells Nanomedicine and Biotechnology 2018, 46 (3), 500-509.

139. Portner, R.; Nagel-Heyer, S.; Goepfert, C.; Adamietz, P.; Meenen, N. M., Bioreactor design for tissue engineering. Journal of Bioscience and Bioengineering 2005, 100 (3), 235-245.

140. Weis, M.; Shan, J. W.; Kuhlmann, M.; Jungst, T.; Tessmar, J.; Groll, J., Evaluation of Hydrogels Based on Oxidized Hyaluronic Acid for Bioprinting. Gels 2018, 4 (4).

141. Liao, C. H.; Chen, C. S.; Chen, Y. C.; Jiang, N. E.; Farn, C. J.; Shen, Y. S.; Hsu, M. L.; Chang, C. H., Vancomycin-loaded oxidized hyaluronic acid and adipic acid dihydrazide hydrogel: Bio-compatibility, drug release, antimicrobial and biofilm model. Journal of Microbiology Immunology and Infection 2020, 53 (4), 525-531.

142. Sideris, E.; Griffin, D. R.; Ding, Y. C.; Li, S. R.; Weaver, W. M.; Di Carlo, D.; Hsiai, T.; Segura, T., Particle Hydrogels Based on Hyaluronic Acid Building Blocks. Acs Biomaterials Science & Engineering 2016, 2 (11), 2034-2041.

CAPÍTULO 3:
RESULTADOS E DISCUSSÃO

3. RESULTADOS E DISCUSSÃO

Este capítulo é apresentado na forma de artigos, contendo a metodologia empregada, resultados obtidos e discussão.

No primeiro artigo, *Structural changes and crosslinking modulated functional properties of oxi-HA/ADH hydrogels useful for regenerative purposes*, publicado no periódico científico *European Polymer Journal* em outubro 2019 (doi: 10.1016/j.eurpolymj.2019.109288), trata da caracterização dos efeitos do grau de oxidação e de reticulação com ADH na modulação das propriedades estruturais e físico-químicas do hidrogel, além de validar protocolos de preparo dos hidrogéis de oxi-HA/ADH.

No segundo artigo, *Particulate oxi-HA/ADH hydrogels for tissue engineering and regenerative medicine applications*, artigo a ser submetido ao periódico científico *Materials Science & Engineering C*, trata da influência dos parâmetros de processo na produção de nano e microestruturas, caracterização físico-química, e desempenho na proliferação de h-MSCs, para aplicação como blocos de construção de módulos para a formação de microtecidos em abordagem b*ottom-up*.

No terceiro artigo, *The association of L-PRP and oxi-HA/ADH microparticles forms suitable structures for regenerative purposes*, artigo a ser submetido ao periódico científico *Journal of Materials Science: Materials in Medicine*, trata do desenvolvimento de uma nova estrutura matricial composta por microtransportadores oxi-HA/ADH e L-PRP e avaliando a influência dessa associação, bem como a distribuição dos fatores de crescimento e proliferação celular *in vitro* de células mesenquimais do tecido adiposo (h-AdMSCs).

3.1. Structural changes and crosslinking modulated functional properties of oxi-HA/ADH hydrogels useful for regenerative purposes

Artigo publicado no periódico científico *European Polymer Journal* (doi: 10.1016/j.eurpolymj.2019.109288).

Structural changes and crosslinking modulated functional properties of oxi-HA/ADH hydrogels useful for regenerative purposes

Carla Giometti França[1]; Daniel Pereira Sacomani[1]; Denise Gradella Villalva[1]; Vicente Franco Nascimento[2]; José Luis Dávila[2] and Maria Helena Andrade Santana[*,1]

[1]Department of Materials and Bioprocess Engineering, School of Chemical Engineering, University of Campinas, 13083-852, Campinas, São Paulo, Brazil.
[2]Department of Manufacturing and Materials Engineering, School of Mechanical Engineering, University of Campinas, 13083-852, Campinas, São Paulo, Brazil.

*Correspondence should be addressed to mariahelena.santana@gmail.com

Abstract

Partially oxidized hyaluronic acid (oxi-HA) crosslinked with adipic acid dihydrazide (ADH) has been explored as a promising injectable biomaterial for cell-based therapy and regenerative purposes. However, there is a lack of basic scientific studies and medical applications to support the technological approaches and optimizations of these biomaterials. Thus, we provided a relationship connecting the structural changes to the functional properties, which are modulated by the oxi-HA oxidation degree and ADH crosslinking. Oxi-HA was obtained from the reaction with sodium periodate ($NaIO_4$), which oxidizes the proximal hydroxyl in aldehydes groups by opening the sugar ring and promoting macromolecular compaction. The results showed that the oxi-HA oxidation degree caused the structural changes that increased the zeta potential and decreased the hydrodynamic volume and viscosity. Therefore, the extrusion force, injectability, and ADH crosslinking were benefited by the click chemistry. Additionally, the ADH concentration modulated the functional properties such as the swelling, stability, gelation time, and thermosensitivity of the oxi-HA/ADH hydrogels. These results are relevant for supporting the design and optimization of novel hyaluronic acid-based formulations for applications in the broad field of tissue regeneration.

Keywords: oxidized hyaluronic acid, adipic acid dihydrazide, structure changes, functional properties, injectable applications.

1. Introduction

In the last 10 years, research interest in tissue repair has shifted from hydrogel implants to injectable formulations capable of in situ gelling. Several advantages of using injectable hydrogels over conventional implants include improved patient comfort, cost reduction, the ability to repair irregular tissue defects, and a decrease in the risk of implant migration. Further benefits are the homogeneous incorporation of cells, molecules or bioactive drugs and the secure delivery to the target site [1-4]. Polysaccharides such as chitosan, alginate, and others are often used to prepare hydrogels for a broad range of medical and pharmaceutical applications [5, 6].

Thermosensitive hydrogels are especially attractive due to their spontaneous gelling at body temperature, which eliminates the need for a chemical reaction or external heating to achieve polymerization [7].

Hyaluronic acid (HA) is a natural polysaccharide that is biodegradable, biocompatible, and nonimmunogenic and is composed of N-acetyl-D-glucosamine and D-glucuronic acid linked by β-1,4-glycosidic bonds [8]. HA occurs in a wide range of sizes and has been classified in high (> 10^6 Da), intermediate (10^4 to 10^5 Da), and low HA (< 10^4 Da) molar masses [9]. Due to its various functions and physicochemical properties, HA has been widely used for osteoarthritis treatments [10], drug delivery [11, 12], and tissue engineering [4, 13-15]. To overcome the rapid degradation behavior *in vivo*, chemical or physical modifications of the functional groups of HA, such as its carboxyl, hydroxyl, and $–NHCOCH_3$ groups, have been explored for chemical crosslinking [16-20].

HA is preferably functionalized at its carboxyl group sites [14]. Partial oxidation of the hydroxyl groups of HA, which is catalyzed by periodate ($NaIO_4$), is used for the introduction of highly flexible links in the otherwise rather stiff and extended structures [2, 21]. The electrostatic repulsion of the oxidized chains governs the chain extension or compaction that allows long-range intermolecular associations to occur, allowing for crosslink with small molecules, such as adipic acid dihydrazide (ADH) [22]. The oxidized HA (oxi-HA) can also be connected to other molecules, such as resveratrol, forming an injectable and biocompatible hydrogel (oxi-HA/Res) suitable for chondrocyte cells, which can be used to treat cartilage defects [23].

As studies on these materials have progressed, reacting oxi-HA with ADH by click chemistry has attracted attention due to the advantages of applying the resulting

oxi-HA/ADH hydrogels to *in vivo* applications. Bifunctional ADH is a small, nontoxic, nucleophilic molecule that is quickly metabolized by the human body. The bonding between oxi-HA and ADH is covalent and occurs rapidly without the need for any chemical catalysts or initiators [2, 4, 23-27].

Technological developments have supported applications of injectable oxi-HA/ADH hydrogels as drug delivery systems: Jia et al. (2004) studied the use of an oxi-HA/ADH hydrogel as a vehicle for the anesthetic bupivacaine to prolong the duration of the pain block [26]. Yeo et al. (2007) studied the barrier effects of oxi-HA-ADH hydrogels combined with poly(lactic-co-glycolic acid) (PLGA) nanoparticles for drug delivery to prevent postoperative peritoneal adhesions from forming [28]. Ma et al. (2017) added poly(ethylene glycol) (PEG) to oxi-HA/ADH hydrogels to improve the gelation time, hydrogel toughness, and compression resistance [4].

Oxi-HA/ADH has also been used for regenerative treatments; Su et al. (2010) fabricated an injectable hydrogel with suitable biocompatibility using oxi-HA (with a high oxidation degree) and ADH. The hydrogel could assist nucleus pulposus cells to synthesize type II collagen and facilitate aggrecan mRNA gene expression, which is essential for tissue regeneration [2]. Collin et al. (2011) investigated the potential of a stabilized type II collagen hydrogel using a PEG-ether tetra-succinimidyl glutarate (4S-StarPEG) crosslinker enriched with HA. The stabilized and functionalized type II collagen/HA hydrogel system showed promise for use as an injectable reservoir system for intervertebral disc regeneration [29].

Although there are basic scientific studies on and medical or pharmaceutical applications of oxi-HA, both are still scarce and isolated. In general, there is a lack of necessary connections between the structure and functional properties for supporting technological approaches of these materials for desired purposes.

In this study, we prepared and characterized oxi-HA/ADH hydrogels by varying the oxidation degree and ADH concentrations, thus providing a relationship between the structural changes and functional properties. Additionally, we discuss these findings for regenerative purposes.

2. Materials and methods

2.1. Materials and reagents

Hyaluronic acid (HA) with an average molecular weight of 8.54×10^5 Da was purchased from Tops Shandong Topscience Biotech Co. (Rizhao, CH). Sodium

periodate ($NaIO_4$), ethylene glycol, adipic acid dihydrazide (ADH), trichloroacetic acid, picrysulfonic acid solution (TNBS) and tert-butyl carbazate (t-BC) were purchased from Sigma-Aldrich Inc. (Saint Louis, Missouri, USA). Phosphate buffered saline (PBS) was supplied from Laborclin Ltda (Pinhais, Paraná, BR). Dialysis membranes with a nominal MWCO of 12,000 – 16,000 Da were sourced from Inlab (Diadema, São Paulo, BR).

2.2. Methods

2.2.1. Preparation of oxi-HA

Oxi-HA was synthesized according to the reported procedure [4, 30] with modifications. HA with a concentration of 1% (w/v) was dissolved in double-distilled water at room temperature, and then an aqueous periodate ($NaIO_4$) solution (10.67%) was added. The reaction occurred at room temperature for 24 hours in a dark environment. The $NaIO_4$:HA ratio was calculated as $NaIO_4$ mol per HA dimer mol. The reaction was stopped by the addition of ethylene glycol for a half hour. The molar ratio of ethylene glycol to $NaIO_4$ was 1:6. The resulting solution was dialyzed with double-distilled water for 3 days by using a semipermeable membrane (with a MWCO of 12,000 – 16,000 Da). Finally, the dialyzed solution was lyophilized, yielding a white fluffy product.

2.2.2. Preparation of the oxi-HA/ADH hydrogel

Oxi-HAs with three degrees of oxidation were separately dissolved overnight in a PBS (pH of 7.4, at 4°C) to obtain a final concentration of 6% (*w/v*). Then, 2, 4 and 8% (*w/v*) ADH solutions were also prepared in PBS at 4°C. The oxi-HA and ADH solutions were mixed in an Eppendorf tube at a volume ratio of 4:1 oxi-HA/ADH. The Eppendorf tubes were submerged in a bath containing water and ice (close to 0°C) to obtain the oxi-HA/ADH2, oxi-HA/ADH4, and oxi-HA/ADH8 hydrogels. The hydrogels were obtained by increasing the temperature from 4 to 37ºC.

2.2.3. Determination of the oxidation degree

The oxidation degree (OD) was quantified by measuring the number of aldehyde functional groups in oxi-HA using t-BC and TNBS according to the method described by Lin et al. (2011) [30]. t-BC can react with aldehydes, forming stable carbazone compounds similar to hydrazone. This method is indirect due to the difficulty of directly quantifying the aldehyde groups. Briefly, 25 µL of oxi-HA (0.6%) and 25 µL of t-BC (30 mM) in 1% aqueous trichloroacetic acid were well mixed and allowed to react in an

Eppendorf tube at room temperature for 24 hours. Afterward, 0.5 mL of aqueous TNBS (6 mM, 0.1 M borate buffer, and a pH of 8) was transferred into the Eppendorf tube and allowed to react with the excess t-BC for 60 minutes at room temperature. Then, the solution was diluted with hydrochloric acid (0.5 N) in a ratio of 1:40 (v/v). The absorbance of the solutions was measured with a Genesys 6 spectrophotometerTM (Thermo Fisher Scientific, Massachusetts, USA) at 330 nm. A standard calibration curve was obtained with t-BC solutions ranging from 5 mM up to 30 mM (Eq. 1) to determine the amount of unreacted t-BC, to convert the result into the dialdehyde content, and to calculate the OD (Eq. 2). All the experiments were done in triplicate.

$$y = 0.0145x - 0.0264 \quad R^2 = 0.9902 \qquad \text{Eq. 1}$$

where y is the absorbance, and x is the t-BC concentration (g/L).

$$OD(\%) = \left(\frac{n_{t-BC,i} - n_{t-BC,f}}{n_{oxi-HA\ dimer}}\right) \times 100 \qquad \text{Eq. 2}$$

where $n_{t\text{-}BC,i}$ and $n_{t\text{-}BC,f}$ are the initial and final number of moles of t-BC, respectively, and and $n_{oxi\text{-}HA\ dimer}$ is a number of moles of the HA dimer.

2.2.4. Yield of the oxidation process

The yield of the oxidation process was determined by the mass ratio according to Eq. 3.

$$Process\ yield\ (\%) = \left(\frac{m_f}{m_i}\right) \times 100 \qquad \text{Eq. 3}$$

where m_i and m_f are the initial mass of HA and final mass of oxi-HA, respectively.

2.2.5. Viscosity, molar mass distribution, and hydrodynamic diameter

The viscosity of the nonoxidized HA solution (6% w/v) was determined by using a rheometer (MCR-102, Anton Paar). The operating parameters of the equipment were as follows: the geometry was plate-plate (PP50-SN29897, d = 1 mm), the shear rate was 0.01 to 1000 1/s, and the temperature was set to 25ºC. The viscosity of the oxi-HA solutions (6% *w/v*) was determined by an SV-10 viscometer (A&D Company, Ltd, Tokyo, Japan) at room temperature (25ºC) because this viscosity was out of the precision range of the rheometer.

The distribution of the HA molar mass and the equivalent hydrodynamic volume of oxi-HA were determined by size-exclusion chromatography using a Shimadzu chromatography system (Shimadzu Corporation, Kyoto, Japan) equipped with a 7.8 mm x 35 mm Polysep-GFC-P column guard (Phenomenex, Torrance, CA, USA) and a gel filtration column (Polysep-GFC-P6000, 7.8 mm x 300 mm; Phenomenex, Torrance, CA, USA). The peak profile was monitored with a Shimadzu RID-6A refractive index detector (Shimadzu Corporation, Kyoto, Japan).

Initially, the samples were filtered through a 0.22-μm syringe. Afterward, 20 μL of each sample was injected, and NaNO3 (0.1 mol/L) was used as the mobile phase at 1.0 mL/min and 25°C. HA analytical standards (Hyalose, Oklahoma City, OK, USA) with molar masses ranging from 50 to 1000 kDa were used for the calibration curve. Due to the absence of standards, the molar mass of the oxi-HA samples was not determined. However, for oxi-HA, a hydrodynamic volume equivalent to the volume of the nonoxidized HA in a defined range of molar mass and eluted at the same time was considered.

The zeta potential was measured with a Zetasizer (Malvern, Nano - ZS) The solution concentrations were 0.1% (w/v), and the measurements were performed at 25ºC in a 1 cm optical path cuvette. The refractive and absorbance indices for oxi-HA were 1.33 and 0.001 u.a., respectively. The measurements were acquired in triplicate.

2.2.6. Functional groups

The functional groups of oxi-HA and oxi-HA/ADH with different degrees of oxidation were identified by Fourier transform infrared (FTIR) spectroscopy using a Nicolet 6700 (Thermo Scientific, Madison, USA) instrument equipped with an attenuated total reflectance (ATR) accessory and ZnSe crystal. The spectra were obtained in the range of 800 – 1800 cm^{-1} with a 4 cm^{-1} resolution, and 128 scans were collected. The samples were previously lyophilized for 24 hours and immediately analyzed.

2.2.7. Crystallinity

The X-ray diffractograms (XRD) were obtained using a X'PERT PW3050 (Philips) diffractometer, and CuKα radiation with a wavelength of 1.54 Å was used. The scanning speed was 0.6°/min, and the measurement range was 2θ = 5–50°. The XRD analysis was conducted to study the changes in the crystallinity of the hydrogels.

2.2.8. Gelation point

A rheometer (MCR-102, Anton Paar, Graz, Austria) with a cone and plate geometry (CP-50-1) was used to evaluate the gelation time of oxi-HA/ADH. The measurements were performed at two working temperatures: the preservation temperature at 4ºC and the body temperature at 37°C. The temperature of 4°C was chosen considering the operation time available for the mixture of the components, i.e., the oxi-HA and ADH solutions must be adequate for handling before gelation. In addition, 37°C was selected to evaluate the gelation time of the oxi-HA/ADH hydrogel while simulating normal body conditions. The oscillation time sweep mode was operated at 1 Hz and 10 Pa for the determination of the elastic modulus or storage modulus G' and the viscosity or loss modulus G". The crossover point of G' and G" was defined as the gel point and the corresponding time as the gelation time [31, 32].

2.2.9. Swelling

The swelling ratio (SR) or water absorption capacity was determined by swelling the dried and previously weighed oxi-HA/ADH in PBS (at a pH of 7.4) for 24 hours at 37°C. The swollen hydrogels were weighed after the removal of excess water by keeping the surfaces on a filter paper. The SR was calculated using Eq. 4.

$$SR = \frac{w_d - w_s}{w_d} \quad \text{Eq. 4}$$

where w_s and w_d are the weights of the hydrogels in the swollen state and dry state, respectively.

2.2.10. Degradation

The degradation profile of the oxi-HA/ADH hydrogels in PBS at 37ºC was determined according to the gravimetric method described by Tang and Spector (2007) [33]. The weight loss ratio (WL) of the hydrogels in PBS was calculated during the degradation using Eq. 5.

$$WL(\%) = \left(\frac{w_0 - w_t}{w_0}\right) \times 100 \quad \text{Eq. 5}$$

where w_0 and w_t are the weights of the hydrogels in the final dry state and initial dry state, respectively. The surface area/hydrogel mass ratio was 16 cm^2/g. The inverse of the degradation represents the stability of the hydrogels.

2.2.11. Images and morphology

The images of the oxi-HA hydrogels were obtained after 24 hours of gelation. After that, the samples were lyophilized and kept in a desiccator.

The morphology of the oxi-HA/ADH hydrogels was obtained by scanning electron microscopy (SEM) (LEO 440i, Cambridge, England) using a current and voltage of 50 pA and 10 kV, respectively. The average sizes of the pores were determined by measuring 100 individual pores from three different images using ImageJ software.

2.2.12. Extrusion force

Initially, oxi-HA/ADH was loaded in 1-mL plastic syringes (27 G¾ in). Subsequently, the force required to extrude was measured using a TA.XT.plus texture analyzer (Stable Micro Systems, Vienna Court, United Kingdom) (load Cell 50 kg) at 25°C and with a 5.0 mm/min extrusion rate.

2.3. Statistical analysis

Each experiment was carried out in triplicate unless otherwise specified. All the results are presented as the mean ± standard deviation (SD). The experimental data from all the studies were analyzed using analysis of variance (ANOVA). The statistical significance was set to p-value ≤ 0.05.

3. Results

3.1. Structural changes of oxi-HA

The HA oxidation performed by $NaIO_4$ occurs by cleaving the carbon-carbon connections, forming aldehyde groups [34, 35]. The molecular modification introduces flexible residues, causing decreases in the persistence length and compaction of the chains with an increasing degree of oxidation. Therefore, structural changes occur, which are controlled by the electrostatic repulsion of the carboxyl groups [22]. The partial oxidation of HA provides highly flexible dialdehydes only for the glucuronic acid residues, preventing the influence of the adjacent oxidized residues. Therefore, although the reaction is a first-order reaction with respect to $NaIO_4$, the reaction is time-consuming due to diffusive limitations [22, 36, 37]. Figure 1 shows the chemical reaction of HA oxidation by sodium periodate.

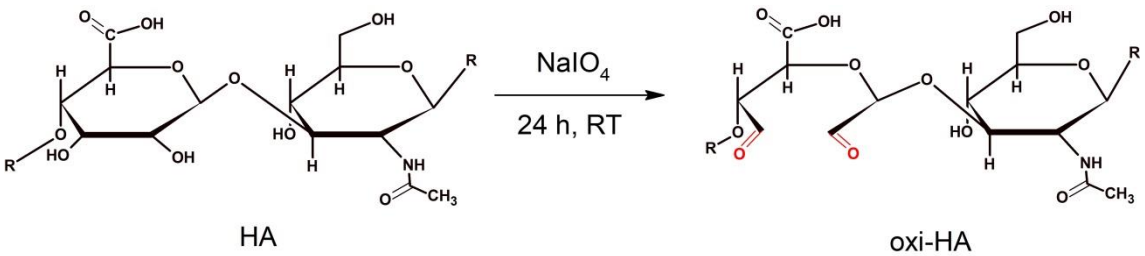

Figure 1. The chemical reaction of hyaluronic acid oxidation by sodium periodate. The cleavage of the carbon-carbon bond leads to the ring opening of the 4-linked D-glucuronate residues, forming aldehyde groups. HA: hyaluronic acid, oxi-HA: oxidized hyaluronic acid, $NaIO_4$: sodium periodate, and RT: room temperature.

Here, the oxidation was carried out with 1:1, 2:1 and 3:1 $NaIO_4$/HA molar ratios for 24 h. The reaction was characterized by determining the yield and OD of oxi-HA, as described in 2.2.3 and 2.2.4.

Table 1 shows that the $NaIO_4$/HA molar ratio controlled the OD. The OD changed from approximately 44 to 82%, characterizing the low, moderate and high ODs. The decrease in the yield for the sample prepared with the highest degree of oxidation was due to the diffusional limitations of the $NaIO_4$ interactions and as a result of the compaction of the modified HA chains during oxidation. The structural changes promoted the alignment of the flexible chains in the shear direction, thus allowing a rapid flow of fluid, unlike the response expected for the overlapping and rigid domains of the physical crosslinks in nonoxidized HA. Therefore, a reduction in the viscosity observed in oxi-Has in comparison to that observed in nonoxidized HA. To a lesser extent, the viscosity decreased as the oxidation degree increased.

The entangled structure of HA showed a zeta potential of -29 ±4 mV due to the internal and external distribution of the dissociated carboxyl groups. The zeta potential slightly decreased at low ODs, due to the low compaction of the partially oxidized polymer structure, even with 44% oxidation of the carboxyl groups. However, at moderate and high ODs, a substantial increase (absolute values) was observed (Table 1). Previous studies [22] have shown that, besides decreasing the intrinsic and persistence length provided by the partial oxidation, a similar behavior was also observed for the molar mass dependence of the radius of gyration. However, for increasing the ODs, a progressive shift to a lower gyration radius was observed, which the authors ascribed to the compaction.

It is known that the Debye length represents the length of the double electric layer provided by the ions around a particle, which affects the electrostatic potential. The zeta potential determines the electrostatic potential at the slipping plane, which includes the Debye length. Therefore, it could be inferred that the compaction of the structures due to the partial oxidation should affect the zeta potential. Considering the influence of the OD on the structure compaction, although 44% of the HA groups (low

OD) were oxidized and the viscosity decreased, the compaction was not enough to modify the Debye cloud substantially, and a slight change in the zeta potential was observed. In contrast, at moderate and high ODs, the increase in the zeta potential (absolute values) was significant.

Table 1. Oxidation degree (OD), yield of the process, viscosity and zeta potential of hyaluronic acid oxidized by $NaIO_4$ for 24 h.

	HA	Low OD oxi-HA	Moderate OD oxi-HA	High OD oxi-HA
$NaIO_4$ /HA molar ratio	-	1:1	2:1	3:1
OD (%)	-	44 ±4[b]	65 ±4[c]	82 ±5[d]
Yield (%)	-	73 ±2[e,f]	77 ±2[f]	72 ±1[e]
Viscosity (mPa·s)	$3x10^6$ ±$1x10^5$[a]	5 ±0[g]	3 ±0[h]	3 ±0[i]
Zeta potential (mV)	-29 ±4[j]	-26 ±3[j]	-36 ±3[k]	-42 ±3[l]

*Mean±SD (n = 3). Mean values with the same letter indicate that there is no significant difference ($p < 0.05$) according to the Tukey test.

Figure 2 shows the molar mass distribution of nonoxidized HA and the equivalent hydrodynamic volume of oxi-HAs for the same elution time.

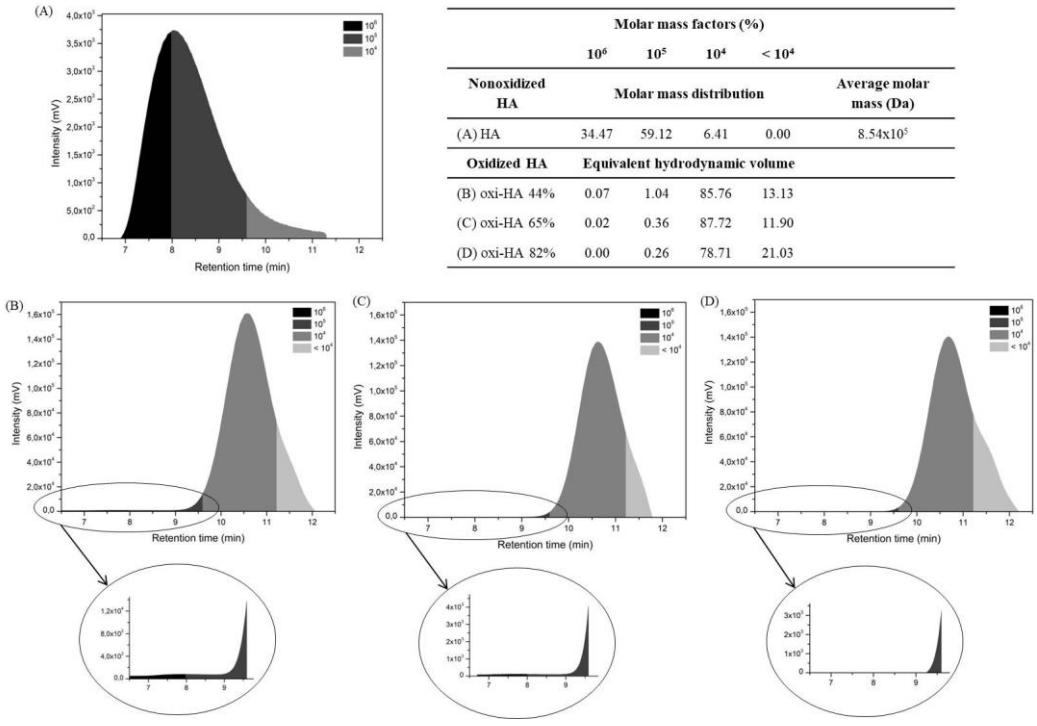

	Molar mass factors (%)			
	10^6	10^5	10^4	$< 10^4$
Nonoxidized HA	**Molar mass distribution**			**Average molar mass (Da)**
(A) HA	34.47	59.12	6.41	0.00	$8.54x10^5$
Oxidized HA	**Equivalent hydrodynamic volume**			
(B) oxi-HA 44%	0.07	1.04	85.76	13.13	
(C) oxi-HA 65%	0.02	0.36	87.72	11.90	
(D) oxi-HA 82%	0.00	0.26	78.71	21.03	

Figure 2. Molar mass distribution of (A) nonoxidized HA and the equivalent hydrodynamic volumes of (B) oxi-HA 43.53% (C), oxi-HA 64.71% and (D) oxi-HA 81.86%.

The gel exclusion profile of nonoxidized HA (Figure 2A) with respect to the retention time in the column shows the molar mass distribution of nonoxidized HA, which was obtained using a previous calibration curve prepared with HA standards. The higher fraction of 10^5 Da followed by the fractions of 10^6 and 10^4 corresponded to 59.12, 34.47 and 6.41%, respectively. Therefore, the nonoxidized HA average molar mass was $8.54x10^5$ Da.

The profiles of Figure 2 (B and D) show the patterns obtained for oxi-HA. It could be observed that when the oxidation degree increases, the fractions of the total area move to the right towards smaller hydrodynamic volumes. Due to the lack of oxi-HA standards, it was not possible to determine their molar masses accurately. However, the hydrodynamic values of oxi-HAs can be compared to the equivalent sizes of the nonoxidized HA structures with 10^5 to $< 10^4$ Da molar masses for the same elution time.

The reduction of the hydrodynamic volumes should also be attributed to the compaction of the partially oxidized structures since the molar mass did not substantially change by varying the OD, as previously reported. HA undergoes less degradation during oxidation than alginate because only the D-glucuronate residues are oxidized, and the periodate-resistant N-acetyl-D-glucosamine exerts a protective effect [22].

The behavior of the hydrodynamic volume also agrees with the observed zeta potentials. In addition, compaction could also be confirmed by the effective crosslinking with small molecules such ADH, as described in the subsequent sections.

3.2. Molecular changes

The FTIR spectrum (Figure 3a) was determined to confirm the presence of aldehyde groups in oxi-HAs. New peaks corresponding to aldehyde functional groups could be observed in the FTIR spectra in C and D at 1717 and 1723 cm^{-1}, respectively, and in B, C and D at approximately 840 cm^{-1}, which is associated with the C=O stretching of the oxi-HA structure. The intensity of these signals increased with increasing the oxidation degrees, as shown from B to D. The peaks at 1152 and 893 cm^{-1} in spectrum A of non-oxidized HA were related to C-O-C (ether bond) and C-H. These two peaks shifted to approximately 1116 and 874 cm^{-1} in spectra B, C and D, revealing the formation of aldehyde functional groups.

Figure 3b shows the formation of a new peak at 1584 cm^{-1}, which was associated with the N-H functional group of ADH. At the same time, the peak at 1717 cm^{-1} was

observed to become weaker due to the aldehyde consumption, which formed amine bonds between oxi-HA and ADH.

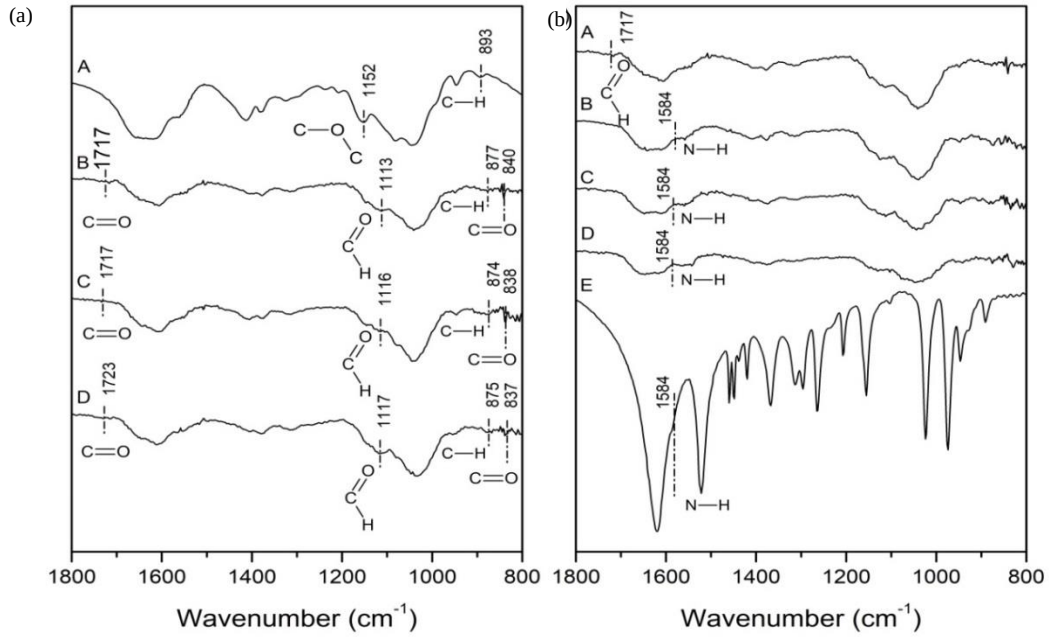

Figure 3. (a) ATR-FTIR spectra of (A) HA, (B) oxi-HA 44%, (C) oxi-HA 65%, and (D) oxi-HA 82%. (b) ATR-FTIR spectra of (A) oxi-HA 65%, (B) oxi-HA 65%/ADH2, (C) oxi-HA 65%/ADH4, (D) oxi-HA 65%/ADH8, and (E) ADH.

3.3. Crystallinity

Figure 4 shows the XRD pattern of the oxi-HA hydrogels.

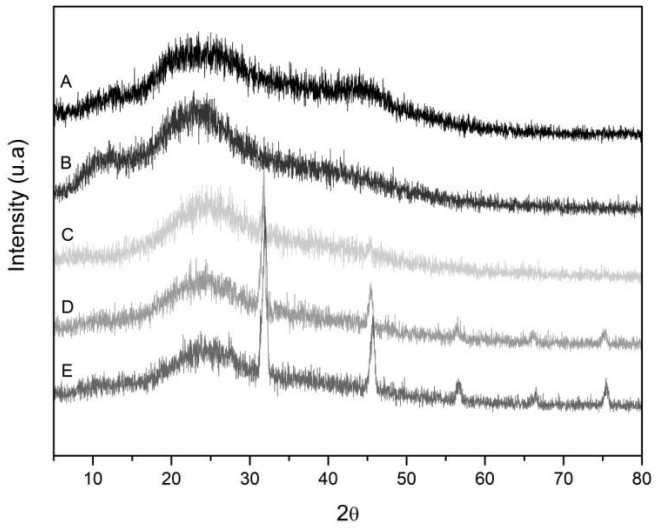

Figure 4. X-ray diffractograms of (A) HA, (B) oxi-HA 44%, (C) oxi-HA 44%/ADH2, (D) oxi-HA 44%/ADH4 and (E) oxi-HA 44%/ADH8.

The XRD patterns of HA and oxi-HA (Figure 4 A and B) showed a wide diffraction peak at 2θ = 24°, which was due to the amorphous nature of the sample. In the diffractograms (Figure 4 C to E), the amorphous domain was also observed. However, in the oxi-HA/ADH hydrogels, the characteristic peak intensity at 2θ = 45° is gradually strengthened after adding 2%, 4% and 8% contents of ADH into oxi-HA. This phenomenon suggests that the interaction between oxi-HA and ADH favors structural organization [38-40].

3.4. Gelation time

In general, gels have viscous and elastic properties, represented by the elastic or storage (G') and viscous or loss (G") moduli. To achieve a hydrogel with desirable behaviors, G' must be greater than G", the material is closer a solid.

Here, the evolution of the rheological parameters G' and G" were used for determination of the crossover point (G' > G"), which defined the gelation time of the hydrogels. Figure 5 shows the gelation time of the hydrogels as a function of ADH concentration for oxi-HA 65%. Furthermore, the effects of temperature on the gelation time are also shown. The table shown in Figure 5 summarizes the gelation time of the hydrogels based on their mechanical behaviors.

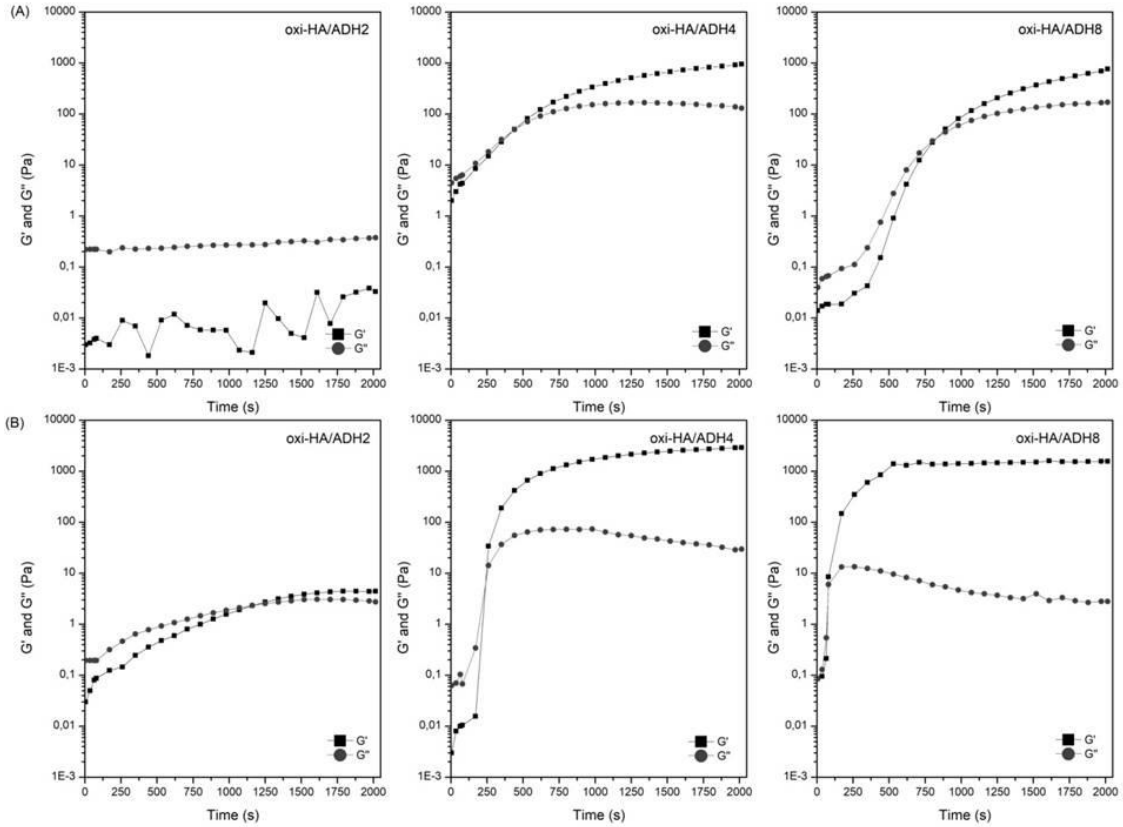

Hydrogel	Oxidation degree (%)	Gelation time (s)	
		4ºC	37ºC
oxi-HA/ADH2		> 2000	1153
oxi-HA/ADH4	65	440	231
oxi-HA/ADH8		821	71

Figure 5. Gelation behavior of crosslinked oxi-HA/ADH hydrogels formed at (A) 4ºC and (B) 37ºC in a 6% (w/v) oxi-HA 65% solution with various concentrations of ADH (2, 4 and 8% w/v). The gelation time was determined based on the crossover point when G' (elastic modulus) > G" (loss modulus). The table summarizes the gelation time of the hydrogels based on their mechanical behaviors.

Figure 5A shows the results of the oxi-HA/ADH hydrogels at 4°C. Although an incipient tendency, no gelation, or a long gelation time > 2000 s could be observed for the oxi-HA/ADH 2% hydrogel. Shorter gelation times were verified for oxi-HA/ADH 4% (440 s) and oxi-HA/ADH 8% (821 s). Note that the gelation time of hydrogels prepared with a higher ADH concentration at 4°C did not proportionally decreased as expected. The excess ADH and the reduction of the mobility of the oxi-HA chains do not favor the gelation time.

Figure 5B shows the rheological results of the oxi-HA/ADH hydrogels at 37°C. The gelation times of the hydrogels decreased substantially with the increased temperature, indicating faster gelation. These results are beneficial for injectable medical applications because of the thermosensitivity of hydrogels. This property allows for the adjusting of the time to handle the material before gelation. Additionally, it also allows for the injection of low viscosity materials and in situ gelation. Therefore, thermosensitivity is an essential feature for in situ applications of the hydrogels [7].
Although the gelation time is proportional to the ADH concentration, the values of G' were similar for ADH 4% and ADH 8%, indicating steric or diffusion limitations of ADH crosslinking. In accordance, the lower G" value of ADH 8% indicates the partial presence of the nonmodified aldehyde groups of oxi-HA due to incomplete ADH crosslinking.

3.5. Swelling

Although hydration is beneficial to the cells grown in tissue engineering applications, it can make the hydrogel matrix fragile, deformed or broken under the application of external forces [41].

Table 2 summarizes the swelling ratios of the oxi-HA/ADH hydrogels. The oxi-HA/ADH hydrogels had a high water swelling capacity, allowing for their rapid hydration after one-day of immersion in PBS. It is known that the higher the crosslinking degree, the less the water absorption is. Therefore, ADH 8% reduced the swelling ratio more than ADH 4%. However, the lowest swelling ratio was observed for oxi-HA 65%. These results agree with the rheological behavior shown in section 3.4, which indicates the structural limitations of ADH 8% crosslinking.

Table 2. Swelling ratio of the oxi-HA/ADH hydrogels after 24 h.

Oxidation degree (%)	ADH concentration (%)	Swelling ratio (-)
44	4	19.80 ±2.10[a]
	8	13.05 ±0.07[b]
65	4	13.58 ±0.31[b]
	8	9.78 ±0.40[c]
82	4	15.53 ±0.23[d]
	8	11.53 ±0.29[c]

*Mean±SD (n = 3). Mean values with the same letter indicate that there is no significant difference ($p < 0.05$) according to the Tukey test.

3.6. Degradation

Figure 6 shows the degradation kinetics of the oxi-HA hydrogels in a PBS solution. The degradation profiles, in terms of the remaining mass fraction, show the synergistic effects of the structural changes of the oxi-HA oxidation degree and the diffusion limitations on ADH crosslinking.

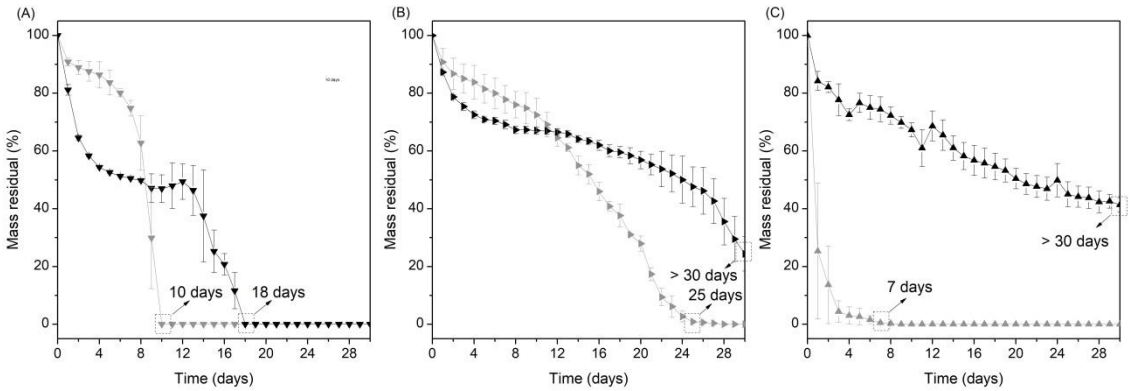

Figure 6. Degradation profile of the (A) oxi-HA 44%, (B) oxi-HA 65% and (C) oxi-HA 82% hydrogels in (light gray) 4% and (dark gray) 8% ADH solutions.

Based on the oxidation degree, the most stable hydrogel was oxi-HA 65% in both the ADH solutions. The presence of the non-crosslinked oxidized groups reduced the stability of the hydrogels in 4% ADH, thus decreasing its degradation time, as observed in Figure 6 A and C. The longest time of 20 days for the intermediate oxidation degree (oxi-HA 65%) indicated the highest performance of crosslinking in 4% ADH (Figure 6B). For 8% ADH, the crosslinking was benefited mainly in the presence of a higher number of oxidized groups (Figure 6 B and C). Although slight differences

were observed, the degradation time in Figure 6B was slower than that in Figure 6A, indicating that better crosslinking performance was achieved at the conditions shown in Figure 6B, according to the swelling results. The compaction of the HA chains in the more oxidized HA sample hindered the transport of 8% ADH, thus decreasing the degree of crosslinking and promoting progressive degradation.

3.7. Macroscopic and SEM images

Figure 7 (1) shows the macroscopic images obtained from the oxi-HA/ADH hydrogels, and Figure 7 (2 and 3) shows the micrographs obtained by SEM.

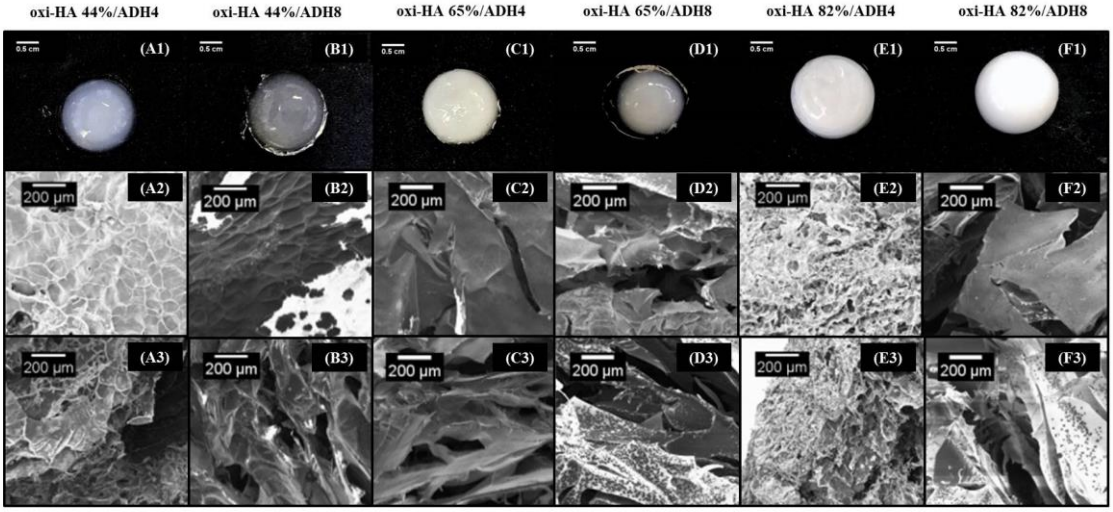

Hydrogel	(A3) oxi-HA44%/ADH4	(B3) oxi-HA44%/ADH8	(C3) oxi-HA65%/ADH4	(D3) oxi-HA65%/ADH4	(E3) oxi-HA82%/ADH4	(F3) oxi-HA82%/ADH8
Pores size (µm)	80 ±30[a]	228 ±134[b]	215 ±102[b]	354 ±121[b]	61 ± 28[a]	352 ±167[b]

*Mean±SD (n = 100). Mean values with the same letter indicate that there is no significant difference ($p < 0.05$) according to the Tukey test.

Figure 7. Oxi-HA hydrogel images: (A and B) oxi-HA 44% with 4% ADH and 8% ADH, respectively, (C and D) oxi-HA 65% with 4% ADH and 8% ADH, respectively, and (E and F) oxi-HA 82% with 4% ADH and 8% ADH, respectively. (A-F1) are the macroscopic images, (A-F2) are the surface scanning electron microscopic images, and (A-F3) is the fracture scanning electron microscopic images.

Although the N-H band (Figure 3b) appeared in the FTIR analysis, no extensive gelation was experimentally nor macroscopically observed with 2% ADH for the various oxi-HA oxidation degrees.

Regarding the oxidation degree (Figure 7 A1 to F1), the macroscopic view of the hydrogels shows a whitish gradient and varying sizes, which depend on the velocity and OD.

The micrographs of oxi-HA 44%/ADH4 and oxi-HA 82%/ADH8 (Figure 7 A3 and F3) show three-dimensional structures with interconnected and rounded pores. The other hydrogels (Figure 7 B3 to D3 and F3) had leaf shape morphologies, were more rigid, and had fewer and larger pores than the oxi-HA 44%/ADH4 and oxi-HA 82%/ADH8 hydrogels. The quantitative analysis shows the substantial differences in the average pore sizes of the structures as determined by measuring 100 individual pores from three different images using ImageJ software. The effects were more pronounced for the low and higher ODs, especially for 4% ADH, compared with the moderate OD. For the 82% OD, the oxi-HA chains are extremely compacted, and ADH diffusion limits the crosslinking. In contrast, for the 44% OD, some oxi-HA chains are not close enough for the crosslinking reaction to occur. For the last situation, the material was observed to be more fragile. For the 65% OD, the ADH crosslinking was benefited by producing large pores for in both 4% and 8% ADH (Figure 7 C3 and D3). These results are consistent with the oxidation yield shown in Table 1, evidencing that optimum oxidation occurred for the moderate oxi-HA.

Although the average pore size analysis was consistent, the unreliable determinations of the porosity were obtained by both gravimetric and nitrogen isotherms.

3.8. Extrusion force

The extrusion force characterizes the injectability of the hydrogels and is proportional to the resistance of the hydrogel to flow due to the crosslinking intensity and gelation time.

Herein, the extrusion forces of the hydrogels with different degrees of oxidation (low, moderate, and high) and ADH concentrations (4 and 8% *w/v*) were determined five minutes after preparing the oxi-HA and ADH mixture. The controls were the nonoxidized HA and oxi-HA samples that were both prepared without crosslinking. Figure 8 shows the substantial differences between the extrusion forces of these samples, in which the extrusion force for non-oxi HA was much higher than that for oxi-HAs at the same ADH concentration of 6% (*w/v*). Slight differences were observed

between the oxi-HAs. The differences reflect the substantial drop in the oxi-HA viscosity due to the oxidation with $NaIO_4$.

A suitable extrusion force for injections in clinical applications is up to 20 N to avoid side effects such as pain, discomfort, bruising, bleeding, and edema in the patient [42, 43]. Therefore, the oxi-HA/ADH hydrogels were suitable for injectable applications, due to their low extrusion forces (3 N). Furthermore, the oxi-HA/ADH hydrogels can be handled before injection without substantial gelation five minutes after mixing their components.

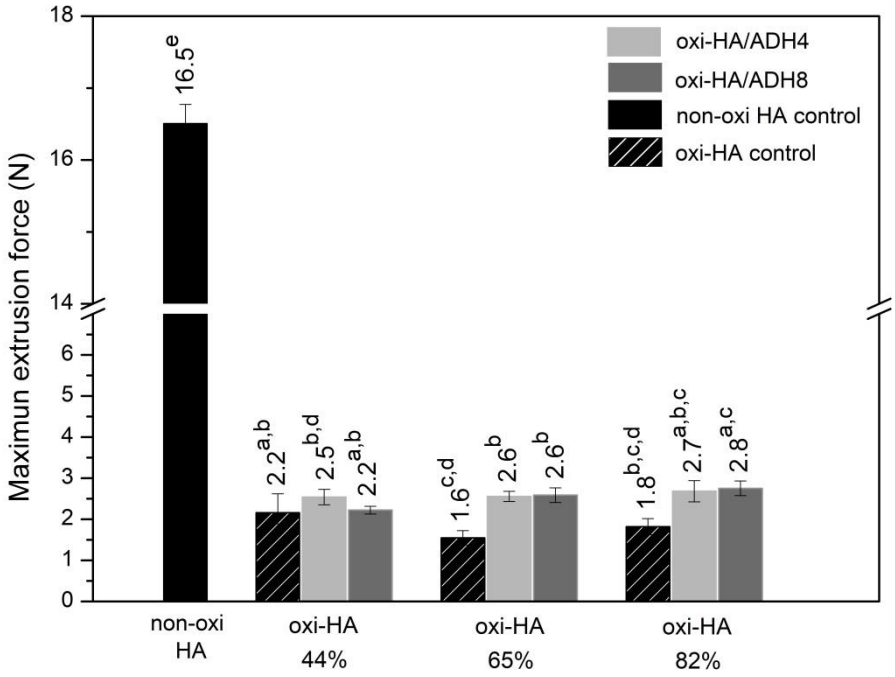

*Mean±SD (n = 3). Mean values with the same letter indicate that there is no significant difference ($p < 0.05$) according to the Tukey test.

Figure 8. Maximum extrusion force of the oxi-HA/ADH hydrogels (gray labels). All measurements were obtained 5 min after the mixture of the components. The controls nonoxidized HA (black label) and oxi-HA (cracked black label) prepared without crosslinking.

4. Structural changes and functional properties of oxi-HA/ADH

Figure 9 summarizes the relationship between the structural changes and the functional properties of oxi-HA/ADH mediated by the oxi-HA and ADH concentrations.

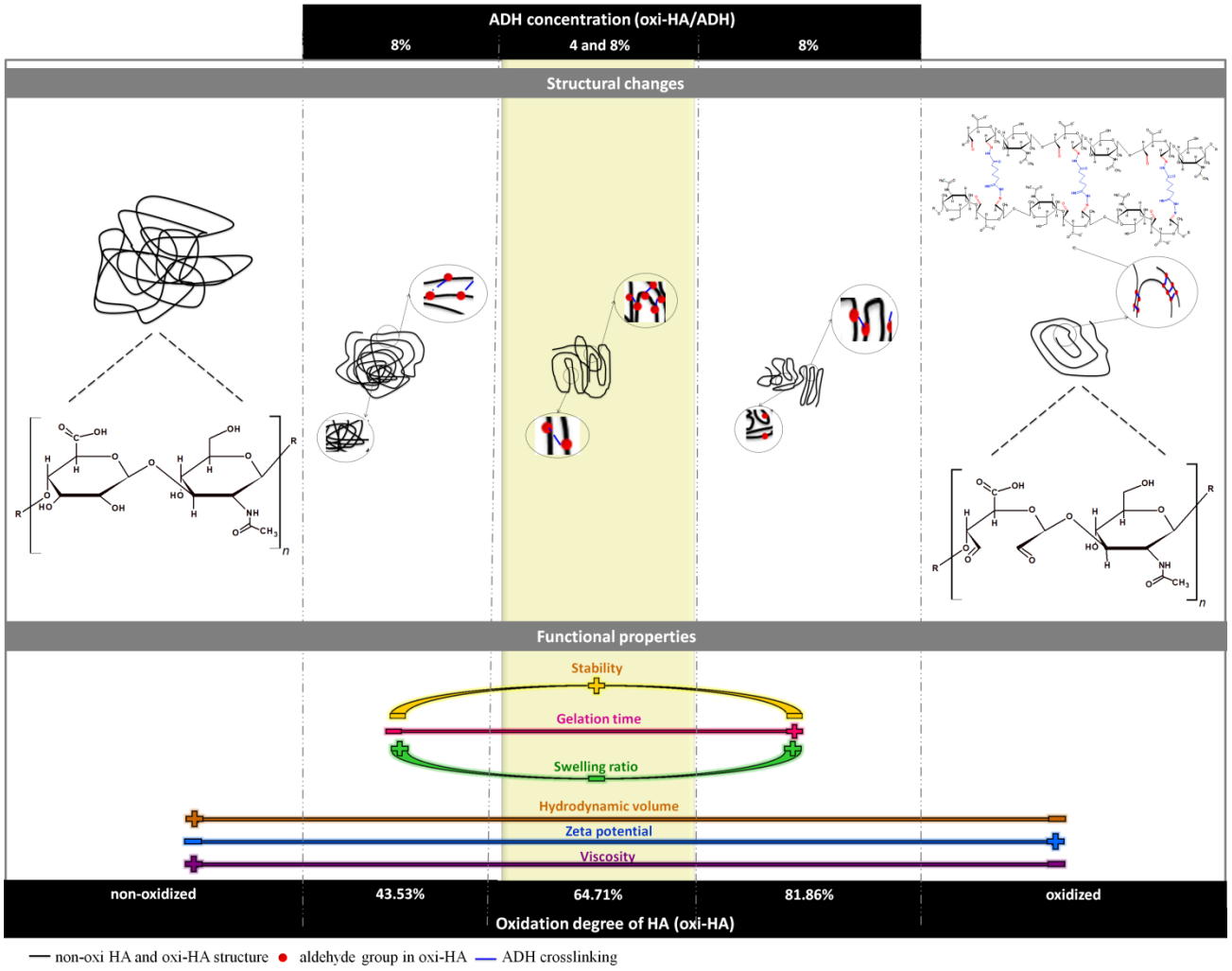

Figure 9. Structural changes and functional properties of the oxi-HA/ADH hydrogel. The colored arrows (bottom and middle of the figure) indicate the increase (+) or decrease (-) in the functional properties. The highlighted yellow region represents the optimum oxi-HA/ADH hydrogel.

The nonoxidized HA sample is composed of a monomeric unit of D-glucuronic acid and N-acetyl glucosamine. At a physiologic pH, the polymeric chains of nonoxidized HA are overlapping, forming a random coil structure with rigid domains and physical crosslinking. The partial oxidation of HA with $NaIO_4$ introduces aldehyde groups into HA via opening the glucuronic acid ring and oxidizing the nearby OH groups. The dialdehydes form highly flexible domains, leading to the compaction of chains with an increase in the oxidation degree. The molecular modifications occur only in the D-glucuronate residues, while the N-acetyl glucosamine groups remain intact and protect against total oxidation and the scission of the chains. Therefore, the molar mass of oxi-Has does not change substantially.

The flexibility of the aldehyde groups reflects the increasing zeta potential, and the compaction of the structures causes decreasing hydrodynamic volumes and reduction in viscosity.

The approximation of the chains by compaction allows for the formation of long-range intermolecular interactions and crosslinking with small molecules such as ADH, which is a bifunctional crosslinker agent that has the advantage of being metabolized by the human body. For a high degree of oxidation, steric hindrances induce diffusion limitations and incomplete crosslinking in spite of the high number of aldehyde groups available on oxi-HA. Therefore, there is an optimum degree of oxidation and ADH concentration to achieve optimal crosslinking.

Finally, the structural changes and ADH crosslinking modulate the functional properties such as the gelation time, swelling, and stability of the oxi-HA/ADH hydrogels. Except for the gelation time, which increased with increasing oxidation degree and ADH concentration, the highest stability and the least amount of swelling was achieved at a moderate 65% OD and 4% ADH concentration.

The oxi-HA/ADH hydrogels are suitable for injectable formulations for regenerative applications, and the thermosensitivity of these oxi-HA/ADH hydrogels is advantageous due to the time available to handle the hydrogel before injection, the fluidity of the hydrogel during injection and *in situ* gelation.

The hydrogel morphology with interconnected pores is essential for cell nutrition, proliferation, and migration to promote the vascularization and formation of new tissues. Furthermore, the stability of hydrogels is promising for cell cultivation *in vivo*. The degradation of oxi-HA 65%/ADH4 in PBS was slow, 25 days. The oxi-HA/ADH hydrogels have a high-water swelling capacity, which is essential for cell

growth. The oxi-HA/ADH hydrogels also have the potential for tissue engineering applications, according to cell viability experiments, which are not in the scope of this article.

An optimal consistency of hydrogels required for specific applications can be reached by adjusting the oxidation degree and ADH concentration.

Conclusions

Structural changes modulate the functional properties mediated by the oxi-HA oxidation degree and ADH concentrations. The properties of the oxi-HA hydrogels are amenable for regenerative purposes, allowing for the injectability, thermosensitivity and in situ gelation of the hydrogels. The relationship between the structural changes and the functional properties enabled the design and optimization of injectable formulations for the regeneration of specific tissues. Further research must be conducted to study the ability of the oxi-HA/ADH hydrogels to grow mesenchymal cells and differentiate in desired tissues.

Acknowledgments

The authors acknowledge Prof. Dr. Marcos Akira D'Ávila for the rheological measurements carried out in his laboratory.

Funding

This study was supported by the CNPq (Conselho Nacional de Desenvolvimento Científico e Tecnológico Brazil) (process 140924/2017-5 and 153611/2016-2) and FAPESP (Fundação de Amparo à Pesquisa do Estado de São Paulo) (process 2016/10132-0).

Conflicts of Interest

The authors declare no conflicts of interest.

Data availability

The raw/processed data required to reproduce these findings cannot be shared at this time, as the data also forms part of an ongoing study.

References

[1] S.R. Van Tomme, G. Storm, W.E. Hennink, In situ gelling hydrogels for pharmaceutical and biomedical applications, Int. J. Pharm. 355(1-2) (2008) 1-18. https://doi.org/10.1016/j.ijpharm.2008.01.057.

[2] W.Y. Su, Y.C. Chen, F.H. Lin, Injectable oxidized hyaluronic acid/adipic acid dihydrazide hydrogel for nucleus pulposus regeneration, Acta Biomater. 6(8) (2010) 3044-3055. https://doi: 10.1016/j.actbio.2010.02.037.

[3] T. Thambi, V.H.G. Phan, D.S. Lee, Stimuli-sensitive injectable hydrogels based on polysaccharides and their biomedical applications, Macromol. Rapid Commun. 37(23) (2016) 1881-1896. https://doi.org/10.1002/marc.201600371.

[4] X.B. Ma, T.T. Xu, W. Chen, R. Wang, Z. Xu, Z.W. Ye, B. Chi, Improvement of toughness for the hyaluronic acid and adipic acid dihydrazide hydrogel by PEG, Fibers Polym. 18(5) (2017) 817-824. https://doi.org/10.1007/s12221-017-6986-1.

[5] A. Singh, P.K. Sharma, V.K. Garg, G.G. Garg, Hydrogels: a review, Int. J. Pharm. Sci. Rev. Res. 4(2) (2010) 97 - 105. ISSN 0976-044X.

[6] V. Nascimento, C. França, J. Hernández-Montelongo, D. Machado, M. Lancellotti, M. Cotta, R. Landers, M. Beppu, Influence of pH and ionic strength on the antibacterial effect of hyaluronic acid/chitosan films assembled layer-by-layer, Europ. Polym. J. 109(2018) 109 - 205. https://doi.org/10.1016/j.eurpolymj.2018.09.038.

[7] L. Yu, G.T. Chang, H. Zhang, J.D. Ding, Injectable block copolymer hydrogels for sustained release of a PEGylated drug, Int. J. Pharm. 348(1-2) (2008) 95-106. https://doi.org/10.1016/j.ijpharm.2007.07.026.

[8] A.S. Maharjan, D. Pilling, R.H. Gomer, High and low molecular weight hyaluronic acid differentially regulate human fibrocyte differentiation, PLoS One 6(10) (2011). https://doi.org/10.1371/journal.pone.0026078.

[9] H.G. Garg, C.A. Hales, Chemistry and biology of hyaluronan, first ed., Elsevier Science, Amsterdam, 2004. ISBN: 9780080472225.

[10] E.A. Balazs, J.L. Denlinger, Viscosupplementation: a new concept in the treatment of osteoarthritis, J. Rheumatol. Suppli. 20(1993) 3-9. ISSN: 0315-162X.

[11] K.P. Vercruysse, G.D. Prestwich, Hyaluronate derivatives in drug delivery, Crit. Rev. Ther. Drug Carrier Syst. 15(5) (1998) 513-55. ISSN: 0743-4863.

[12] J.P. Quinones, J. Jokinen, S. Keinanen, C.P. Covas, O. Bruggemann, D. Ossipov, Self-assembled hyaluronic acid-testosterone nanocarriers for delivery of anticancer drugs, Europ. Polym. J. 99(2018) 384-393. https://doi.org/10.1016/j.eurpolymj.2017.12.043.

[13] X.Z. Shu, Y.C. Liu, F.S. Palumbo, Y. Lu, G.D. Prestwich, In situ crosslinkable hyaluronan hydrogels for tissue engineering, Biomaterials 25(7-8) (2004) 1339-1348. https://doi.org/10.1016/j.biomaterials.2003.08.014.

[14] R. Jin, L.S.M. Teixeira, A. Krouwels, P.J. Dijkstra, C.A. van Blitterswijk, M. Karperien, J. Feijen, Synthesis and characterization of hyaluronic acid-poly(ethylene glycol) hydrogels via Michael addition: An injectable biomaterial for cartilage repair, Acta Biomate. 6(6) (2010) 1968-1977. https://doi.org/10.1016/j.actbio.2009.12.024.

[15] J. Elisseeff, K. Anseth, D. Sims, W. McIntosh, M. Randolph, M. Yaremchuk, R. Langer, Transdermal photopolymerization of poly(ethylene oxide)-based injectable hydrogels for tissue-engineered cartilage, Plast. Reconstr. Surg. 104(4) (1999) 1014-1022. ISSN: 0032-1052. [16] T. Walimbe, A. Panitch, P.M. Sivasankar, A Review of hyaluronic acid and hyaluronic acid-based hydrogels for vocal fold tissue engineering, J. Voice 31(4) (2017) 416-423. https://doi.org/10.1016/j.jvoice.2016.11.014.

[17] J.A. Burdick, G.D. Prestwich, Hyaluronic acid hydrogels for biomedical applications, Adv. Mater. 23(12) (2011) H41-H56. https://doi.org/10.1002/adma.201003963.

[18] S. Ahadian, H. Savoji, A. Khademhosseini, Recent Advances in hydrogels for tissue engineering, Chemical Engineering Progress 114(5) (2018) 56-63. ISSN: 0360-7275.

[19] T.R. Hoare, D.S. Kohane, Hydrogels in drug delivery: progress and challenges, Polymer. 49(8) (2008) 1993-2007. https://doi.org/10.1016/j.polymer.2008.01.027.

[20] C.E. Schante, G. Zuber, C. Herlin, T.F. Vandamme, Chemical modifications of hyaluronic acid for the synthesis of derivatives for a broad range of biomedical applications, Carbohydr. Polym. 85(3) (2011) 469-489. https://doi.org/10.1016/j.carbpol.2011.03.019.

[21] S. Khunmanee, Y. Jeong, H. Park, Crosslinking method of hyaluronic-based hydrogel for biomedical applications, J. Tissue Eng. 8 (2017). https://doi.org/10.1177/2041731417726464. [22] K.A. Kristiansen, M.O. Dalheim, B.E. Christensen, Periodate oxidation and macromolecular compaction of hyaluronan, Pure Appl. Chem. 85(9) (2013) 1893-1900. https://doi.org/10.1351/PAC-CON-13-01-05.

[23] S.Y. Sheu, W.S. Chen, J.S. Sun, F.H. Lin, T. Wu, Biological characterization of oxidized hyaluronic acid/resveratrol hydrogel for cartilage tissue engineering, J. Biomed. Mater. Res. A. 101(12) (2013) 3457-3466. https://doi.org/10.1002/jbm.a.34653.

[24] X.Q. Jia, Y. Yeo, R.J. Clifton, T. Jiao, D.S. Kohane, J.B. Kobler, S.M. Zeitels, R. Langer, Hyaluronic acid-based microgels and microgel networks for vocal fold

regeneration, Biomacromolecules. 7(12) (2006) 3336-3344. https://doi.org/10.1021/bm0604956.

[25] H.P. Tan, C.M. Ramirez, N. Miljkovic, H. Li, J.P. Rubin, K.G. Marra, Thermosensitive injectable hyaluronic acid hydrogel for adipose tissue engineering, Biomaterials. 30(36) (2009) 6844-6853. https://doi.org/10.1016/j.biomaterials.2009.08.058.

[26] X.Q. Jia, G. Colombo, R. Padera, R. Langer, D.S. Kohane, Prolongation of sciatic nerve blockade by in situ cross-linked hyaluronic acid, Biomaterials. 25(19) (2004) 4797-4804. https://doi.org/10.1016/j.biomaterials.2003.12.012.

[27] W.Y. Su, K.H. Chen, Y.C. Chen, Y.H. Lee, C.L. Tseng, F.H. Lin, An injectable oxidated hyaluronic acid/adipic acid dihydrazide hydrogel as a vitreous substitute, J. Biomater. Sci. Polym. Ed. 22(13) (2011) 1777-1797. https://doi.org/10.1163/092050610X522729.

[28] Y. Yeo, C.B. Highley, E. Bellas, T. Ito, R. Marini, R. Langer, D.S. Kohane, In situ cross-linkable hyaluronic acid hydrogels prevent post-operative abdominal adhesions in a rabbit model, Biomaterials. 27(27) (2006) 4698-4705. https://doi.org/10.1016/j.biomaterials.2006.04.043.

[29] E.C. Collin, S. Grad, D.I. Zeugolis, C.S. Vinatier, J.R. Clouet, J.J. Guicheux, P. Weiss, M. Alini, A.S. Pandit, An injectable vehicle for nucleus pulposus cell-based therapy, Biomaterials 32(11) (2011) 2862-2870. https://doi.org/10.1016/j.biomaterials.2011.01.018.

[30] F.H. Lin, W.Y. Su, Y.C. Chen, K.H. Chen, Cross-linked oxidated hyaluronic acid for use as vitreous substitute, National Health Research Institutes, United States, 2011, p. 19. Application number: 12/871,923.

[31] W.B. Yoon, B.Y. Kim, J.W. Park, Rheological characteristics of fibrinogen-thrombin solution and its effects on surimi gels, J. Food Sci. 64(2) (1999) 291-294. https://doi.org/10.1111/j.1365-2621.1999.tb15885.x.

[32] S. Mortimer, A.J. Ryan, J.L. Stanford, Rheological behavior and gel-point determination for a model Lewis acid-initiated chain growth epoxy resin, Macromolecules. 34(9) (2001) 2973-2980. https://doi.org/10.1021/ma001835x.

[33] S.Q. Tang, M. Spector, Incorporation of hyaluronic acid into collagen scaffolds for the control of chondrocyte-mediated contraction and chondrogenesis, Biomed. Mater. 2(3) (2007) S135-S141. https://doi.org/ 10.1088/1748-6041/2/3/S10.

[34] G. Solomons, C. Fryhle, Organic chemistry, seventh ed., John Wiley & Sons Inc, New York, 1999. ISBN-13: 978-0471190950.

[35] S.S. Wong, Chemistry of protein conjugation and cross-linking, second ed., CRC Press, Florida, 1991.ISBN: 9780849374913.

[36] R.W. Jeanloz, E. Forchielli, Studies on hyaluronic acid and related substances .4. Periodate oxidation, J. Biol. Chem. 190(2) (1951) 537-546. ISNN: 0021-9258.

[37] T. Painter, B. Larsen, Further illustration of nearest-neighbor autoinhibitory effects in oxidation of alginate by periodate ion, Acta Chem. Scand. 27(6) (1973) 1957-1962. https://doi.org/10.3891/acta.chem.scand.27-1957.

[38] M.A. de Moraes, E. Paternotte, D. Mantovani, M.M. Beppu, Mechanical and biological performances of new scaffolds made of collagen hydrogels and fibroin microfibers for vascular tissue engineering, Macromol. Biosci. 12(9) (2012) 1253-1264. https://doi.org/10.1002/mabi.201200060.

[39] B.S. Gholizadeh, F. Buazar, S.M. Hosseini, S.M. Mousavi, Enhanced antibacterial activity, mechanical and physical properties of alginate/hydroxyapatite bionanocomposite film, Int. J. Biol. Macromol. 116 (2018) 786-792. https://doi.org/10.1016/j.ijbiomac.2018.05.104

[40] C.G. Franca, V.F. Nascimento, J. Hernandez-Montelongo, D. Machado, M. Lancellotti, M.M. Beppu, Synthesis and properties of silk fibroin/konjac glucomannan blend beads, Polymers. 10(8) (2018). https://doi:10.3390/polym10080923.

[41] J. Enrione, F. Osorio, D. Lopez, C. Weinstein-Oppenheimer, M.A. Fuentes, R. Ceriani, D.I. Brown, F. Albornoz, E. Sanchez, P. Villalobos, R.A. Somoza, M.E. Young, C.A. Acevedo, Characterization of a gelatin/chitosan/hyaluronan scaffold-polymer, Electron. J. Biotechn. 13(5) (2010). https://doi.org/10.2225/vol13-issue5-fulltext-15.

[42] J. Kablik, G.D. Monheit, L.P. Yu, G. Chang, J. Gershkovich, Comparative physical properties of hyaluronic acid dermal fillers, Dermatol. Surg. 35(1) (2009) 302-312. https://doi.org/10.1111/j.1524-4725.2008.01046.x.

[43] A.A.M. Shimojo, S.E.M. Galdames, A.G.M. Perez, T.H. Ito, A.C.M. Luzo, M.H.A. Santana, In vitro performance of injectable chitosan-tripolyphosphate scaffolds combined with platelet-rich plasma, Tissue Eng. and Regen. Med. 13(1) (2016) 21-30. https://doi.org/10.1007/s13770-015-9111-9.

3.2. Particulate oxi-HA/ADH hydrogels for tissue engineering and regenerative medicine applications

Artigo a ser submetido no periódico científico *Materials Science & Engineering C.*

Particulate oxi-HA/ADH hydrogels for tissue engineering and regenerative medicine applications

Carla Giometti França[1], Krissia Caroline Leme[2], Denise Gradella Villalva[1], Jéssica Heline Lopes da Fonseca[3], Ângela Cristina Malheiros Luzo[2], Carolina Caliari Oliveira[4] & Maria Helena Andrade Santana[*,1]

[1]Department of Materials and Bioprocess Engineering, School of Chemical Engineering, University of Campinas, 13083-852, Campinas, São Paulo, Brazil.
[2]Haematology & Hemotherapy Center, Umbilical Cord Blood Bank, University of Campinas, 13083-878, Campinas, São Paulo, Brazil.
[3]Department of Manufacturing and Materials Engineering, School of Mechanical Engineering, University of Campinas, 13083-852, Campinas, São Paulo, Brazil.
[4]*In situ* Cell Therapy, Supera Park, 14056-680, Ribeirão Preto, São Paulo, Brazil.

*Correspondence to: Maria Helena Andrade Santana (e-mail: andrade@unicamp.br)

Abstract

Due to introducing control on the cell scale, including adhesion, topography, and surface properties, particulate biomaterials have expanded the applications of monolithic bulk hydrogels as scaffolds. Hyaluronic acid (HA) is a natural biopolymer present in the extracellular matrix of various tissues. HA hydrogels mimic the stem-cell niche and have a broad range of applications in regenerative medicine. The hydrogels of partially oxidized HA (oxi-HA) provide various advantages in facilitated crosslinking with adipic dihydrazide (ADH) by click reaction, thermosensitivity, and *in situ* gelation. However, while the results of clinical studies support these bulk hydrogels' activity, the development of oxi-HA/ADH particles remains unexplored. In the present study, we aimed to determine technological parameters for the preparation of oxi-HA/ADH nano- and microparticles, characterize their physicochemical and mechanical properties, and evaluate their cell-laden capability for *in vitro* proliferation of human adipose-derived mesenchymal cells (h-AdMSCs). We also investigated cryoprotection and injectability of the particulate structures. The results showed that the crosslinked nano- and microparticles can be obtained without further purification. The operational variables controlled the yield, mean diameter, and zeta potential. Individually, the microparticles were found to be efficient for AdMSCs proliferation; however, at the same

concentration, the nanoparticles allowed for the cell survival only, and further adjustments would be necessary. The microparticles demonstrated gel-like behavior and allowed for a smooth injection alone or in association with bulk HA. Therefore, oxi-HA/ADH nano- and microparticles can be meaningfully used in tissue engineering and regenerative medicine.

Keywords: oxidized hyaluronic acid, nanoparticles, microparticles, tissue engineering, regenerative medicine

Graphical abstract. Oxi-HA/ADH bulk and particulate hydrogels for tissue engineering and regenerative medicine.

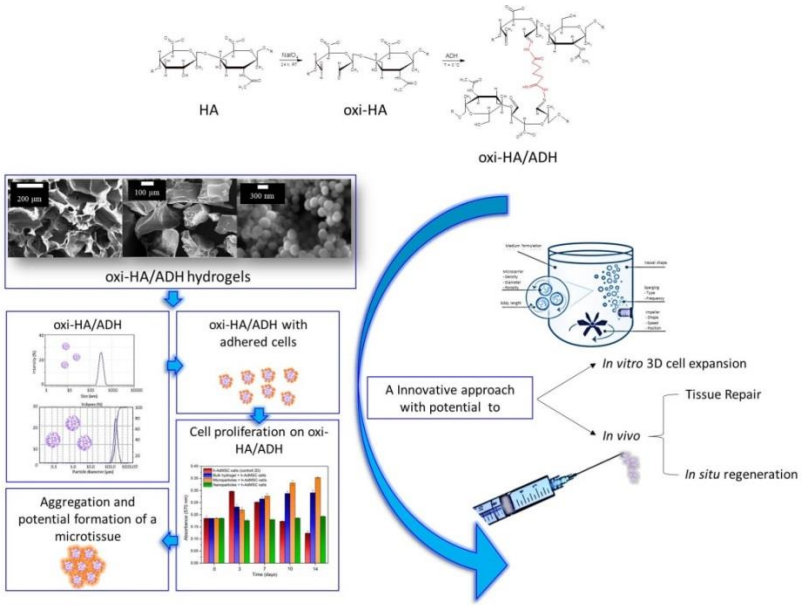

1. INTRODUCTION

Hyaluronic acid (HA) is a biopolymer abundantly present in various human tissues. Exogenous HA, obtained from microbial fermentation, exhibits the same properties as endogenous HA, including the highly hydrated structure, viscous and viscoelastic properties, signalization via cell receptors, anti-inflammatory effects, and cell protection [1-3]. The flexibility of molecular groups for chemical modifications, including crosslinking, increases HA stability *in vivo* and expands the range of biomedical applications of their hydrogels [4, 5].

Scaffolds are temporary structures that support desirable interactions with seeded cells, allowing for their proliferation and migration, as well as for the formation of a three-dimensional tissue. Hydrogels mimic the extracellular matrix and have been widely used as scaffolds in tissue engineering and regenerative medicine [6]. By

introducing control on the cell scale, including adhesion, topography, and surface properties, nano- and microparticles improve the scaffolding properties of monolithic bulk hydrogels [7].

The synthesis of HA nano- and microparticles involves various processes. For instance, Yun et al. [8] emulsified an aqueous phase containing HA in mineral oil with a surfactant and then crosslinked the formed particles with ADH in a reaction mediated by chloride carbodiimide (EDCl) as a catalyzer. The experimental results showed that the emulsifying technique produced polydisperse particles, with most sizes ranging from 2 to 23 μm. To overcome these limitations, the precipitation technique was considered. The nanoprecipitation of HA in organic solvents was initially investigated by Fessi et al. [9]. This process requires two miscible solvents: generally, water and alcohol or water and acetone. The diffusion of solvent in water causes a reduction in the capacity of ion solvation, leading to polyelectrolytes as HA to instantaneously precipitate. Nanoprecipitation eliminates the use of oil-aqueous interfaces that may damage proteins or drugs and usually produces small particles (100 – 300 nm) with a narrow unimodal distribution. Furthermore, Hu et al. [10] patented a discontinuous nanoprecipitation process, free of surfactant and oil, for the production of HA nanoparticles with a uniform size of 200nm. The aqueous phase containing sodium hyaluronate was initially precipitated in acetone and then crosslinked with ADH in the presence of EDCl for over 44 h. In another relevant study, Bicudo et al. [11] compared the performance of ethanol, isopropyl alcohol, and acetone for HA nanoprecipitation and crosslinking with ADH and EDCI in a discontinuous process and in a continuous process in microchannels.

In addition, Sideris et al. [12] developed microgels by oil emulsification from an aqueous solution containing HA functionalized with acrylamide groups in a microfluidic system. The microgels were annealed to one another to form a bulk porous scaffold. Orthogonal chemistries based on an enzymatic reaction, light-based radical polymerization, and amine/carboxylic acid were used for crosslinking and annealing the microgels.

Shimojo et al. [13] prepared HA microparticles by shearing an HA dispersion previously crosslinked with 1,4-butanediol diglycidyl ether (BDDE) using the Ultra-Turrax equipment. The microparticles were associated with a fibrin gel from platelet-rich plasma. The association provided injectable formulations with better physicochemical and mechanical properties than those of bulk HA. Moreover, by

enabling *in vitro* proliferation of human adipose-derived mesenchymal cells (h-AdMSCs), the association can be promising for cartilage regeneration.

Overall, the fabrication of nano- and microparticles for tissue engineering and regenerative medicine includes top-down and bottom-up strategies that influence bioactivity and quality of the formed tissues [14-18]. While the conventional top-down scaffolds contain cells seeded in a preformed matrix, bottom-up approaches involve cell-laden modules assembled in repeating units that form a macrotissue [14]. In general, nano- and microparticles were reported to have many promising applications in cell-laden scaffolds for the production of modular tissues [17].

The partial oxidation of HA hydroxyl groups by sodium periodate introduces highly flexible links and causes structural and rheological changes. Furthermore, the partial oxidation enables crosslinking with small molecules, such as adipic acid dihydrazide (ADH), by the click reaction type [19, 20]. These properties are advantageous in terms of the process, eliminating the toxic effects of EDCI and allowing for facilitated synthesis without further purification requirements.

Owing to lower viscosity, improved injectability, biocompatibility, thermosensitivity, and in situ gelation, the oxi-HA/ADH hydrogels have been studied for medical applications in the last ten years Another important advantage of the oxi-HA and ADH is that they do not present cytotoxicity, and ADH is a small hydrazide metabolized in the human body [21].

Previous studies investigated the colloidal structural changes on oxi-HAs and the modulation of their physicochemical properties with the oxidation degree and ADH concentration [20]. While relevant clinical studies are still few, the oxi-HA/ADH bulk hydrogels carrying cells were found to be promising for nucleus pulposus regeneration [22], post epidural fibrosis surgery [23], and as drug carriers [24], as well as to have dual effects (drug delivery and regeneration) in tendinopathies [25]. The oxi-HA/ADH hydrogels were also found to be suitable for 3D bioprinting, offering a promising platform for developing new bioinks [26].

In this study, we focus on the synthesis and characterization of oxi-HA/ADH nano- and microparticles. To the best of our knowledge, our study is the first to evaluate the *in vitro* performance of oxi-HA/ADH nano- and microparticles as active carriers for the proliferation of human adipose-derived mesenchymal cells (h-AdMSC).

2. EXPERIMENTAL

2.1 Material and reagents

Hyaluronic acid (HA) with high molar mass (average $9.48x10^5$ Da) and low molar mass (average 15 kDa) was purchased from Shandong Topscience Biotech Co. (Rizhao, China) and Lifecore Biomedical (Chaska, Minnesota, USA), respectively. Sodium periodate ($NaIO_4$), ethylene glycol, adipic acid dihydrazide (ADH), dextrose, trehalose from *Saccharomyces cerevisiae* (D-(+)-Trehalose dihydrate), and phosphate-buffered saline (PBS) were obtained from Sigma-Aldrich Inc. (Saint Louis, Missouri, USA). Cetyltrimethylammonium bromide (CTAB), hydrochloric acid (HCl), and sodium hydroxide (NaOH) were purchased from LabSynth (Diadema, Brazil). Dialysis membranes with a nominal MWCO of 12,000 – 16,000 DA were sourced from Inlab (Diadema, Brazil).

2.2 Methods

2.2.1 Synthesis of partially oxidized hyaluronic acid

Partially oxidized hyaluronic acid (oxi-HA) was synthesized according to the previously reported protocol [1, 22], with modifications previously introduced by França et al. [20]. Briefly, HA (~ $9.48x10^5$ Da) at the concentration of 1% (*w/v*) was dispersed in double-distilled water at room temperature. Then, the aqueous sodium periodate ($NaIO_4$, 10.67%) solution was added and left to react at room temperature for 24 h in the dark. The $NaIO_4$: HA ratio was calculated as $NaIO_4$ mol per HA dimer mol, and the oxidation degree (OD) was 65% based on its properties. The reaction was stopped by adding ethylene glycol (1:6 ethylene glycol to $NaIO_4$) for 0.5 h. Oxi-HA was purified by dialysis using double-distilled water with changes twice per day for 3 days. Finally, the dialyzed solution was lyophilized in a freeze dryer (L101, Liobras, São Carlos, Brazil) to yield a white fluffy product.

2.2.2. Preparation and characterization of oxi-HA/ADH nanoparticles

The oxi-HA/ADH nanoparticles were produced by precipitation in ethanol. The process was conducted in a jacket glass reactor of 50 mL equipped with a mechanical stirrer (model TE-039/1, Technal, Piracicaba, Brazil). The temperature was controlled at 21 °C by a thermostat bath (model TE-184, Technal, Piracicaba, Brazil), and the system was maintained under stirring at 300 rpm for 24 h. Initially, the organic solvent with the flow rate of 0.8 mL/min was fed through a peristaltic pump (NE-300 Just Infusion™, New Era Pump System, Farmingdale, USA) and dripped into an aqueous solution composed of 10 mL of oxi-HA (0.097% (w/v)) and 250 µL of ADH (0.049% (w/v)).

Considering that concentration and viscosity influence water-solvent diffusion and precipitation [27, 28], diluted solutions of oxi-HA and ADH were used. For effective crosslinking, the system was maintained under stirring for 24 h. The particles were recovered by ultrafiltration through a 10 kDa Millipore membrane. All experiments were performed in triplicate.

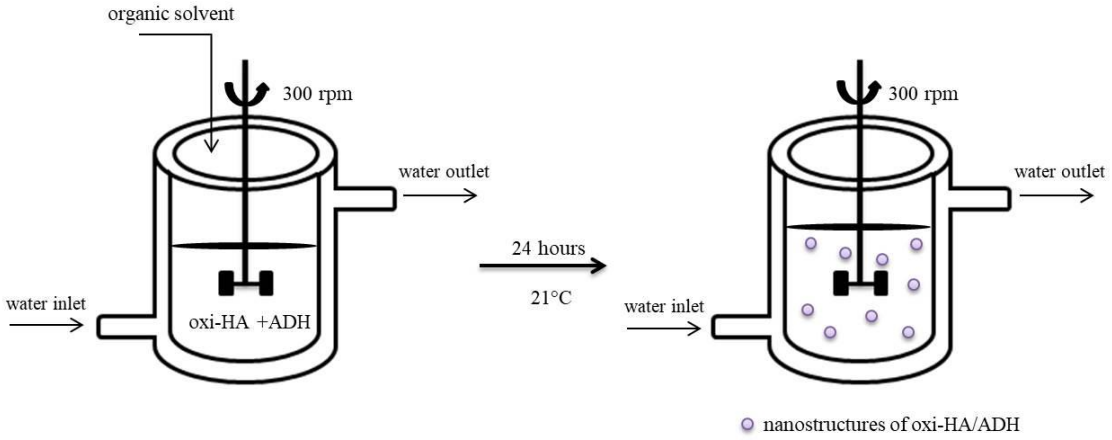

Fig. 1. The process of the synthesis of oxi-HA/ADH nanoparticles by precipitation in organic solvent.

The process was studied with ethanol using the volumes of 10.84 or 26.75 mL of the solvent to 10.25 mL of the oxi-HA/ADH aqueous solution. The pH values of 4.0 or 7.0 were maintained throughout the process. In order to examine the combined effects of dehydration by ethanol in the vicinity of oxi-HA on precipitation and ADH crosslinking, we considered ethanol volume and pH as independent variables. These effects were evaluated in terms of yield, mean diameter, and zeta potential of the nanoparticles. The system HA-water-ethanol has a surface tension of 28.64 mN/m and a dielectric constant of 30, both of which were previously reported to be favorable for HA nanoprecipitation [11].

The process yield was calculated based on HA quantification by the CTAB turbidimetric method [29]. Briefly, after ultrafiltration, 1 mL of the samples (filtered and retentate) was added to Eppendorf vials. The water was used as a blank, and 2 ml of the CTAB reagent was added to each Eppendorf. The solutions were gently shaken to ensure a full mixture. After 10 min of reaction, the absorbance of the nanostructures was measured using a Genesys 6 spectrophotometerTM (Thermo Fisher Scientific, Massachusetts, USA) at 400 nm.

The concentration of nanoparticles present in the filtrate and retentate was determined using a standard calibration curve constructed from the HA solutions in the range of 1 – 0.0078 g/L. The yield of the process was calculated using Eq. (1).

$$Yield(\%) = \left(\frac{m_t - m_f}{m_t}\right) \times 100 \quad (1)$$

where mt is the total mass (filtrate and retentate), and mf is the filtrate mass.

2.2.3. Preparation and characterization of o oxi-HA/ADH microparticles

The microparticles were prepared from the bulk oxi-HA/ADH hydrogel previously synthesized following França et al. [20]. Briefly, an oxi-HA 65% oxidation degree was dissolved in a PBS (pH of 7.4, at 4 °C) to obtain the final concentration of 6% (w/v). The 4% (w/v) ADH solution was also prepared in PBS at 4 °C. The oxi-HA and ADH solutions were mixed in the ratio of 4:1 in Eppendorf tubes, which were then submerged in a bath containing water and ice for crosslinking and bulk hydrogel formation. The crosslink reaction was performed at pHs 4.0 or 7.0. The microparticles were obtained by shearing according to Shimojo et al. [13, 30, 31]. Briefly, 1 g of the bulk oxi-HA/ADH hydrogels was swelled in 150 mL Milli-Q water and sheared in an Ultra-Turrax T25 homogenizer (IKA Labortechnik, Staufen, Germany) at 18000, 21000, and 24000 rpm in different times (10, 20, and 30 min) at 21 °C.

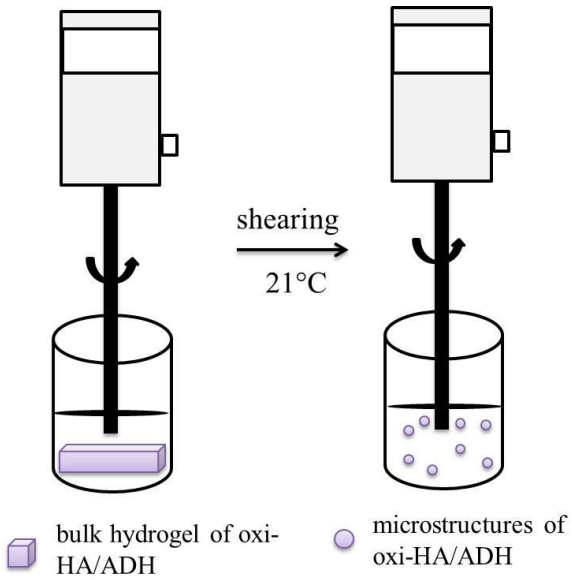

Fig. 1. The process of preparation of microparticles from bulk oxi-HA/ADH by shearing.

2.2.4. Mean diameter, polydispersity, potential zeta and surface area

The oxi-HA/ADH nano and microparticles were characterized by measuring the hydrodynamic mean diameter and polydispersity using dynamic light scattering and

zeta potential based on electrophoretic mobility. The measurements were performed in triplicate with a Zetasizer Nano Series ZS (Malvern Instruments, Malvern, United Kingdom) at the fixed angle of 173°.

2.2.5. Cryoprotection

The cryoprotectants dextrose, low molar mass HA (~ 15 kDa), and trehalose, in the concentrations 10 and 5 mg/mL, were used to investigate the stabilization and structure reconstitution after lyophilization. The microparticles used in the present study were produced by shearing under the following conditions: 1800 rpm, pH 7.0, and 10 min. Then, in order to eliminate the excess of water, the particles were centrifuged for 5 min at 2500 rpm.

The particles were frozen at -80°C and lyophilized for 24 h. The hydrodynamic mean diameter of the microparticles was analyzed before and after lyophilization. The measurements were performed in triplicate with the Mastersize S equipment (Malvern Instruments, Malvern, UK).

2.2.6. Rheology and injectability

The rheological behavior was investigated with the microparticles alone and mixed with the fluid phase of HA (~ 15 kDa). The assays were performed with microparticles produced at pH 7.0, 18000 rpm, and 10 min. The effects of the HA fluid phase were investigated by mixing the microparticles in the dispersion of 1% (*w/v*) HA in PBS, in proportions ranging from 0 to 100% (*w/w*).

The rheological measurements were performed using a rheometer (MCR-102, Anton Paar, Graz, Austria) with cone and plate geometry (CP-50-1) in the steady and oscillatory regimes at 25 °C. Oscillatory measurements were performed in the linear region, at the stress of 1.188 Pa and in the frequency range of 0.1–10 Hz. Steady shear measurements were obtained at shear rates in the range of 0.1 – 20 s^{-1}.

The injectability of the mixtures was determined by loading the hydrogels and their gel/fluid dispersions in 1-mL plastic syringes with 30-gauge needles. The measurements were performed with a Texture analyzer (TA.XT.plus, Stable Micro Systems, Vienna Court, United Kingdom) with a 50 kg load cell at 25 °C and the extrusion rate of 5.0 mm/min.

2.2.7. Morphology

The morphology of the structures was obtained by scanning electron microscopy (SEM) (LEO 440i, Cambridge, UK) at the current and voltage of 50 pA and 10 kV, respectively. The average size of the bulk hydrogel pores was determined by measuring 100 individual pores from three different images using the ImageJ software.

2.2.8. Cultivation of the human-adipose mesenchymal cells

Table 1 summarizes the operational parameters used for the synthesis, as well as the properties of the bulk hydrogel, nano- and microparticles used to cultivate the h-AdMSCs.

Table 1. Operational parameters and properties of the bulk oxi-HA/ADH hydrogel and its nano- and microparticles used for cultivation of h-AdMSCs.

Bulk hydrogel			
pH	Oxidation degree (%)	ADH crosslinking	Zeta potential (mV)
7.0	65	4%	-36 ±3
Nanoparticles			
pH	Ethanol rate (mL/min)	Volume of ethanol (mL)	Zeta potential (mV)
7.0	0.8	10.84	-17.8 ±1.9
Microparticles			
pH	Shear speed (rpm)	Time (min)	Zeta potential (mV)
7.0	18,000	10	-17.8 ±1.9

*Mean diameter and zeta potential measurements and surface area calculation were performed as described in Section 2.2.4.

The h-AdMSCs were isolated from the human subcutaneous adipose tissue of the patients who underwent lipo-aspiration at the university hospital and cultured according to a previously published protocol [14]. In brief, the cells were cultured in Dulbecco's modified eagle medium (DMEM), containing 15 mM HEPES buffer, L-glutamine, pyridoxine hydrochloride, 3.7 g $NaHCO_3$, and supplemented with 10% FBS (fetal bovine serum) and 1% P/S (penicillin/streptomycin). A volume of 100 µL of a cell suspension (5×10^4 cells/mL in passage 4th to 6th) was added to bulk hydrogel or 10 mg of nano/microparticles; along 2h for cell adhesion. Next, 700 µL of low-glucose DMEM

(Thermo Fisher Scientific, Waltham, MA, USA) were added, and the cells were cultured for 2 weeks in a humidified incubator at 37 °C and 5% CO2; the medium was changed every three days. The experiments were performed in triplicate (n = 3) for each group.

Cell proliferation was evaluated through its mitochondrial activity dosed by dimethyl-thia-zol-2-yl]-2,5-diphenyltetrazolium bromide (MTT) (Sigma-Aldrich, St Louis, MO, USA) assays. The samples were incubated with MTT for 4 h at 37 °C with predetermined for 14 days. Then, MTT was replaced with dimethyl sulfoxide (DMSO), the samples were left in an orbital shaker for 30 min, and the absorbance was measured at 570 nm [32]. The experiments were conducted in triplicate (n = 3) for each group.

2.2.8. Statistical analysis

The experiments were carried out in triplicate unless otherwise specified. All results are presented as the mean ± standard deviation (SD). The experimental data were analyzed using the analysis of variance (ANOVA). Statistical significance was set to p-value ≤ 0.05.

3. RESULTS AND DISCUSSION

3.1 Effects of operational variables on HA nanoparticles synthesis

The synthesis of HA nanoparticles by precipitation in organic solvents and ADH crosslink depends on pH, properties, and the proportion of the polymer, solvent, and non-solvent [11].

Table 2 summarizes the results of diameter, polydispersity, zeta potential and yield of the nanostructures obtained by discontinuous process as a function of ethanol volume and pH.

Table 2. Mean diameter, polydispersity and zeta potential of the nanostructures, and yield of the discontinuous process as a function of ethanol added volume and pH of a oxi-HA.

pH	Volume of organic solvent (mL)	Mean diameter (nm)	Polydispersity	Zeta potential (mV)	Yield (%)
4.0	10.84	310.0 ±7.4[a]	0.324 ±0.038[c]	-27.4 ±0.9[f]	98.00 ±0.87[i]
	26.75	220.4 ±7.0[b]	0.304 ±0.058[c]	-22.8 ±0.8[g]	97.61 ±0.77[i]
7.0	10.84	327.2 ±11.2[a]	0.149±0.024[d]	-17.8 ±1.9[h]	51.60 ±2.98[j]
	26.75	235.6 ±24.5[b]	0.151 ±0.035[d]	-15.8 ±2.3[h]	53.70 ±3.06[j]

*Mean±SD (n = 3). Mean values with the same letter indicate that there is no significant difference ($p < 0.05$).

The results show the yield was higher at pH 4 (≈ 98%), as this is the optimum pH for the crosslinking reaction. The mean diameters were higher and similar for the nanoparticles prepared with 26.75 mL, irrespective of pH, while significant differences with pH were obtained for the preparations with 10.84 mL. The highest diameters with the lowest ethanol volume were due to the lesser dehydration rate in the vicinity of oxi-HA, producing larger nanoparticles. The interplay between precipitation rate and ADH crosslinking justified the pH influence in diameter for the lowest ethanol volume. Reduction of size rearrangements by the highest reaction rate led to the highest polydispersity at pH 4.0.

The pH also influenced the zeta potential of the nanoparticles. At pH 7.0, the carboxylic groups of D-glucuronic acid in oxi-HA were ionized (pK 3-4) and, due to repulsion, they were distributed inside and on the external surface of the structure, generating a lower zeta potential. These repulsive forces also promote the polymer chains' expansion and difficult the diffusion of the organic solvent through the polymer [11, 33]. At pH 4.0, the higher zeta potential was due to the lower dissociation of the carboxyl groups on the external surface of the nanostructures, making them more stable. We also observed that the curvature of the nanoparticles decreased the zeta potential as compared to the bulk structure (zeta potential -36 ±3) (Table 1).

Fig. 3 shows the dynamic light spectra for the nanoparticles as a function of pH and ethanol volume used in nanoprecipitation.

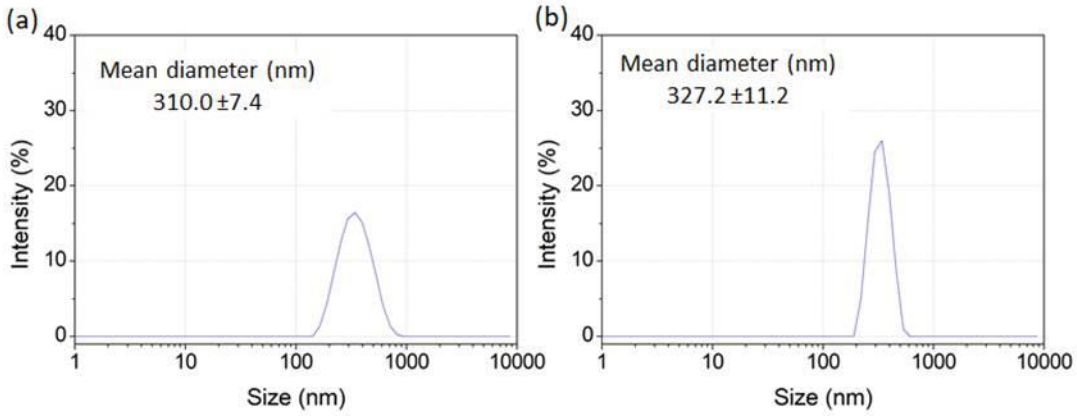

Fig 3. Dynamic light scattering spectra in terms of intensity distribution (I α (diameter)) and mean diameter of the nanoparticles prepared with 10.84 mL ethanol: (a) pH 4.0, (b) pH 7.0

The spectra showed unimodal distributions characteristic of nanoparticles prepared by precipitation in an organic solvent.

3.2. Effects of operational variables on HA microparticles synthesis

Fig. 4 shows the effects of shear speed, time, and pH on the mean diameter of the microparticles.

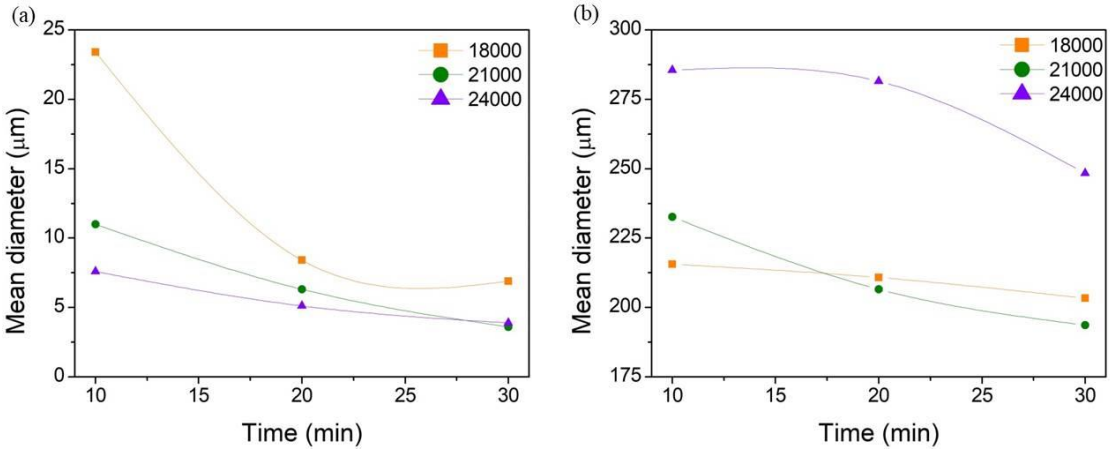

Fig. 4. Mean diameter of the microparticles obtained at different shear speed and pH: (a) pH = 4.0, and (b) pH = 7.0. The zeta potential was -17.8 ±1.9 mV and -27.4 ±0.9 mV for pH 4.0 and 7.0, respectively.

The results showed that pH affected the degree of crosslinking of oxi-HA/ADH and the structural conformation of the oxi-HA chains. Due to the partial deprotonation of the carboxylic acid and the presence of more hydrogen bonds [34], which promote break under shear forming the microparticles, the reaction between the aldehyde groups of oxi-HA and ADH resulted in a higher entanglement of oxi-HA chains in acid environments. At pH 4.0, the reduction of size was proportional to shear speed. The effects were more pronounced with time at 18,000 rpm. At a lower crosslinking (pH 7.0), aggregation occurred at the highest shear speed (24,000 rpm) due to the accumulation of energy in the system. The effects were similar at other speeds. In all cases, the preparation led to a low polydispersity. Zeta potential varied mainly with pH, with the lowest absolute values obtained at pH 7.0, which was due to the lower density of carboxyl groups on the surface resulting from the lowest crosslink.

The results reported above are consistent with those reported in several previous studies. Seong et al. [34] developed HA/BDDE microparticles by shearing and evaluated the influence of the shear speed on their size. The results showed that the

microparticles had a wide size distribution, and the mean diameters were 265, 222, and 74 μm for the rotational speeds of 2000, 5000, and 8000, respectively.

Furthermore, Shimojo et al. [35] investigated the influence of the degree of crosslinking on the mean diameter of microparticles of HA crosslinked with divinyl sulfone (DVS). The authors obtained HA/DVS microparticles with a diameter of 75 - 100 μm at the shear speed of 24000 rpm. In another relevant study, Shimojo et al. [30] obtained HA microparticles formed by auto-crosslinked at the same shear speed with an average diameter of 190 μm. Due to the opening of the D-glucuronic ring, the partial oxidation of HA introduces molecular modifications as flexible residues, causing decreases in the persistence length and the packing of the chains. Therefore, structural changes occur, which are controlled by the electrostatic repulsion of the carboxyl groups [36]. The sizes of particles depend on the structure and the crosslinking degree.

3.3. Cryoprotection

Fig. 5 shows the hydrodynamic mean diameter and distribution of the microparticles with and without cryoprotectant, before and after lyophilization.

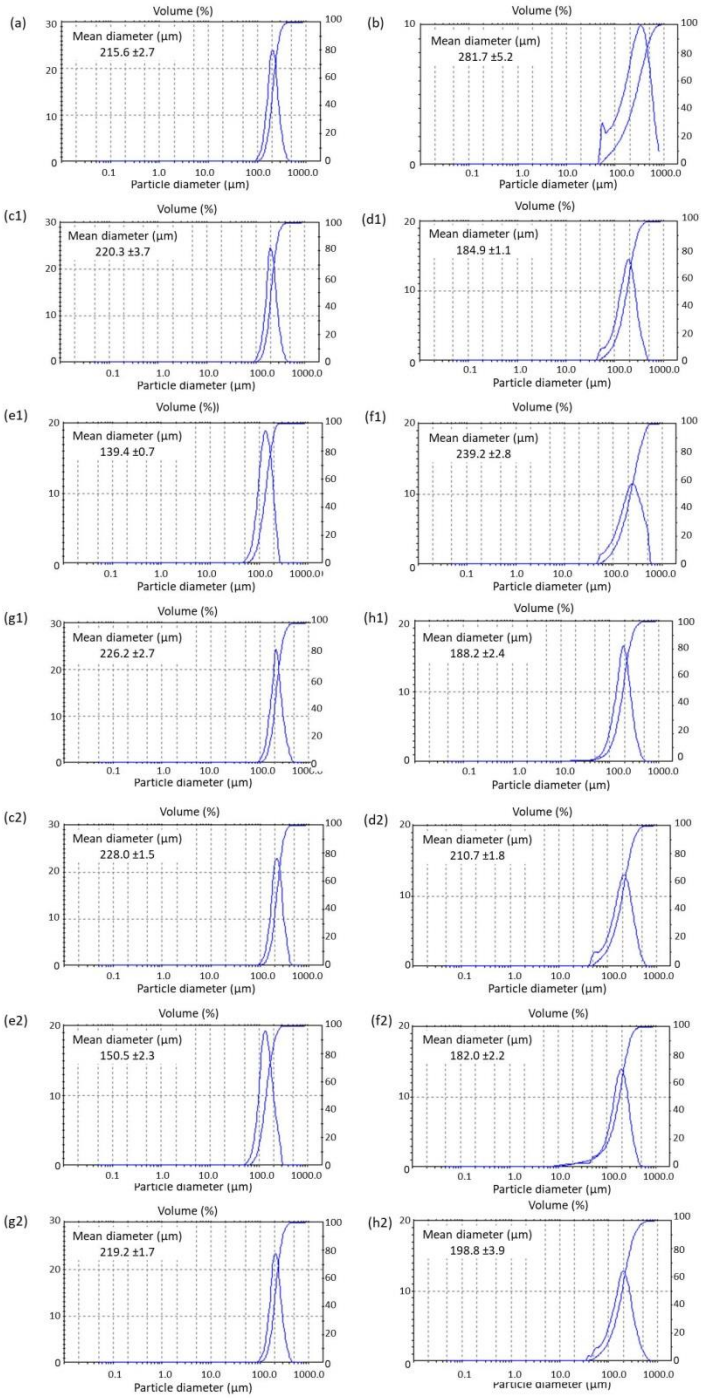

Fig. 5. Mean diameter and distribution of the microparticles without cryoprotectant (a) before and (b) after lyophilization, as well as the effects of the cryoprotectants (in left) before and (in right) after lyophilization. Cryoprotectant: (c, d) dextrose, (e,f) HA with molar mass 15 kDa, and (g, h) trehalose. Concentration: (1) 10 mg/mL and (2) 5 mg/mL.

As can be seen in Fig. 5b, the microparticles lyophilized without cryoprotectants aggregated according to the mean diameter and distribution. Lyophilization is essential for the preservation of the structures for long-term storage and commercialization.

Fig. 5c-h shows the effects of the cryoprotectants dextrose, HA of low molar mass (~ 15 kDa), and trehalose. As revealed by the results, cryoprotection was achieved by the cryoprotectants used. The best results were obtained with HA 15kDa at 5mg/mL (Fig. 5e2 and f2) and dextrose and trehalose at 10 mg/ml (Fig. 5g1 and h1). Therefore, low molar mass HA is advantageous by cryoprotect at a lower concentration.

3.4. Rheology and injectability

The rheological behavior, parameters, and injectability of the microparticles alone and in associated with different fractions of the non-oxidized fluid HA are shown in Fig. 6 and Table 3.

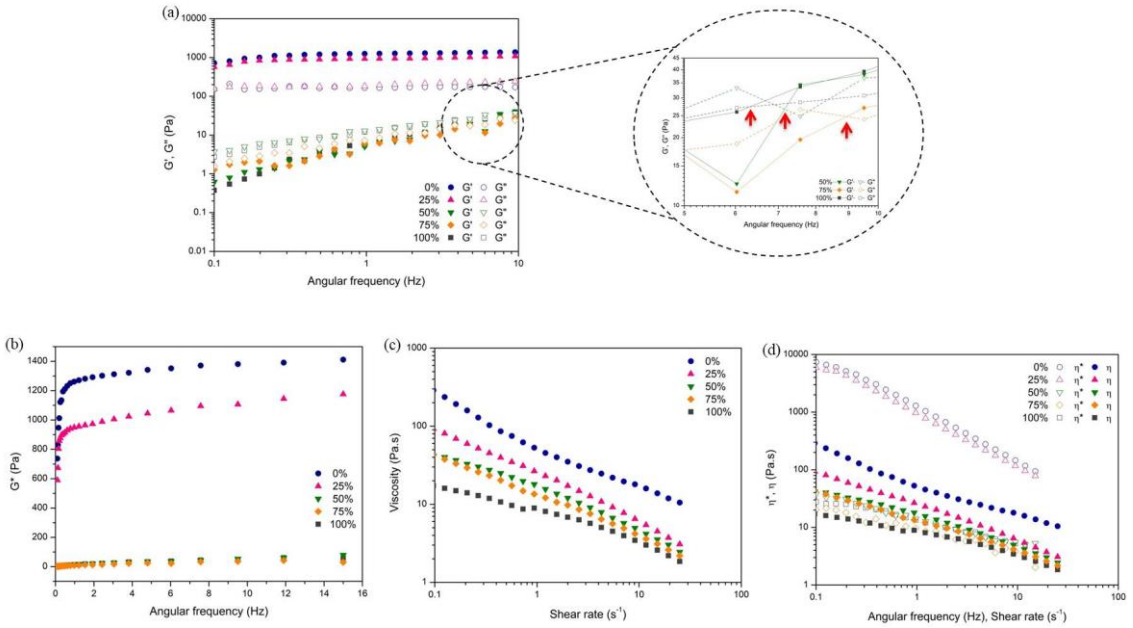

Fig. 6. (a) Storage G' (closed symbol) and loss G" (open symbol) moduli as a function of angular frequency. The red arrows indicate crossover points; (b) complex shear modulus (G*; $\boldsymbol{G^* = \sqrt{G'^2 + G"^2}}$) versus angular frequency; (c) flow curves of the microparticles with different percentages of the fluid phase; (d) complex viscosity (η*) versus angular frequency (open symbol) and apparent viscosity (η) versus shear rate (closed symbol).

Table 3. Calculated rheologic parameters for the microparticles and its associations with fractions of non-oxidized fluid HA.

Fluid phase (%)	B	Tan δ[1]	K	n	Injectability (N)*
0	0.0957	0.131	58.18	0.436	6.48[a]
25	0.0932	0.223	34.60	0.397	4.14[b]
50	0.8641	1.346	15.74	0.476	3.74[b]
75	0.6395	0.956	13.16	0.477	2.95
100	0.9419	1.026	8.01	0.613	2.65[c]

[1]Values were determined at 30 rad/s. $Tan\ \delta = {G'}/{G"}$.

[2]K values and the flow index (n) were determined by the following equation: $\eta = K \cdot \dot{\gamma}^{n-1}$ [37].
*Mean ± SD (n = 10) values with the same letter indicate that there is no significant difference ($p < 0.05$).

The results showed the microparticles and their association with 25% of the fluid phase exhibited a gel-like behavior, with curves parallel to the frequency axis and the predominance of elastic properties with G' higher than G" in all studied frequencies. At 50, and 75% of the fluid phase, the formulation lost its gel characteristics (G" > G'), demonstrating a typical fluid behavior with the crossover point (Fig. 6a).

As can be seen in Fig. 6b, the highest values of the complex modules G* were obtained for the microparticles (1.291 kPa) and their association with a 25% fluid phase (0.981 kPa), indicating higher resistance to deformation.

The flow curves (see Fig. 6c) demonstrated a shear-thinning behavior characteristic of pseudoplastic fluids for the microparticles and their associations with the fluid phase. In Fig. 6d, we also observed that, for the microparticles and their association with a 25% fluid phase, the curves tended to depart from the Cox-Merz rule [38], i.e. the steady shear viscosity significantly differed from the complex viscosity when the values of the shear rate were equal to angular frequency, confirming gelation. In contrast, at the higher fluid fractions, a transition to the gel state was observed [37].

The flow index (n) was not significantly affected for 0 to 75% of the fluid phase (Table 3). However, in line with our expectation, it was reduced for 100% fluid phase (n= 0.61), indicating a decrease in pseudoplastic behavior.

The B values define the mechanical strength of the hydrogels, where B = 0 is associated with covalent gels, while B > 0 with a physical gel [39, 40]. The higher are HA fluid fractions (50 to 100%), the greater is the B value (> 0.6), indicating the loss of gel-like behavior.

While hydrogels are predominantly elastic for tan δ < 0.1, for tan δ > 0.1, they are predominantly weak [41]. All compositions exhibited behavior typical of the so-called weak gels with a tan δ = (G”/G’) > 0.1 (Table 3).

In order to avoid side effects such as pain, discomfort, bruising, bleeding, and edema in the patients after injection, it is essential to determine the extrusion force. A suitable extrusion force was reported to be up to 20N [42, 43]. Although the microparticles and their association with 25% of the fluid phase showed G’ values close to 700 Pa in 1 Hz, which is the upper limit for the adequate range for injectable applications (100 – 700 Pa) [30], the results of injectability yielded low injection forces (max 6.48 N) for the microparticles alone (Table 3). The addition of the fluid phase reduced the extrusion force to 25% HA fluid phase. The same tendency with the addition of fluid phase but with higher extrusion forces (~60 N) was observed by Shimojo et al. for the microparticles crosslinked with divinylsulphove (DVS) (extrusion forces ~20N) [44], with 1,4-butanediol diglycidyl ether (BDDE) or auto-crosslinked [30,31]. Both microparticles were prepared by shearing. The discrepancy of extrusion forces reflects the structural changes from the oxidation with periodate and the substantial drop in oxi-HA viscosity even crosslinked with ADH [20]. In both cases, the extrusion forces were higher for the microparticles alone due to the packing into the syringe. The differences between the values of extrusion forces for fluid non-oxidized HA reported in the present study and our previous article [20] are due to the molar mass of the fluid phase mainly.

3.5 Morphology and cell proliferation

Fig. 7 shows the morphology and proliferation of h-AdMSCs cells during 14 days on microplate control (2D), bulk oxi-HA/ADH hydrogel, the nano-, and microparticles.

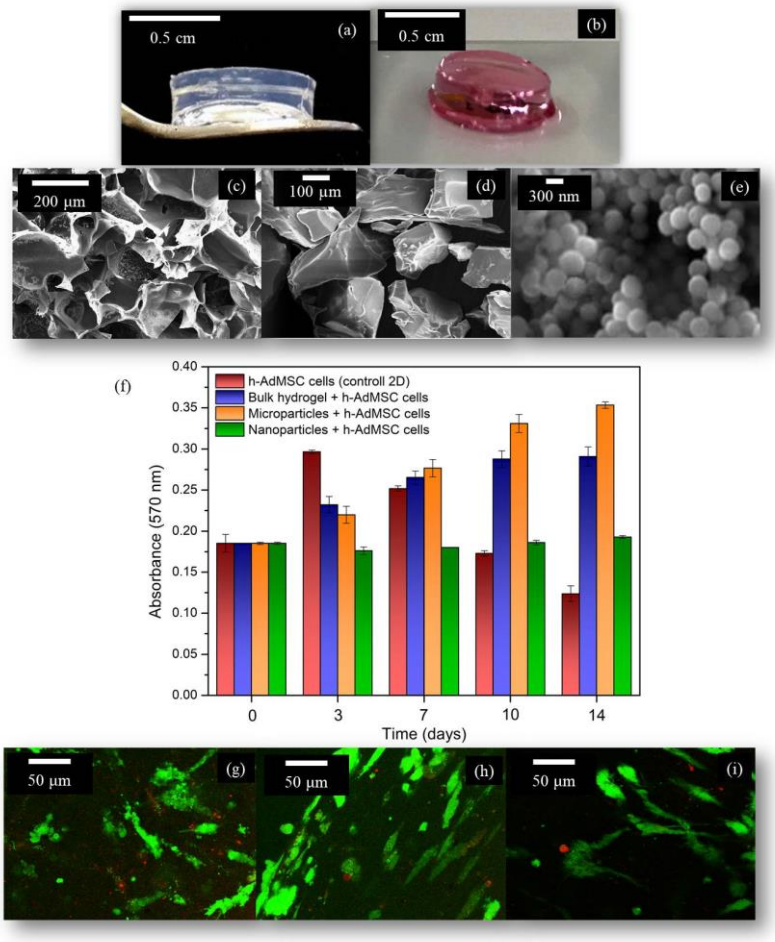

Fig. 7. Macroscopic images of the oxidized hyaluronic acid/adipic dihydrazide (oxi-HA/ADH) (a) bulk hydrogel and (b) the reddish shows the total absorption of the culturing medium into the bulk hydrogel. Scanning electron microscopy images of: (c) transversal section of the bulk hydrogel, (d) microparticles and (e) nanoparticles. (f) h-AdMSCs proliferation in the bulk hydrogel, nano- and microparticles during cultivation for 14 days in the supplemented DMEM medium evaluated by the MTT assay. The data are reported as means ±SD for experiments in triplicate. Live/dead images on day 7: (g) bulk hydrogel, (h) microparticles, and (i) nanostructures. The cells were seeded in the particles at $5x10^4$ cells per 10 mg sample.

The macroscopic images show a general view of the bulk oxi-HA/ADH hydrogel (Fig. 7a) and its capacity for absorption of the culture medium (Fig. 7b). The micrograph of the transversion section of the bulk hydrogel (Fig. 7c) shows three-dimensional structures with interconnected leaf-shape pores. The average pore size was approximately 105 ±24µm, and porosity was ca. 67%.

In the Ultra-Turrax shear process, the HA hydrogel was physically crushed to produce the microparticles. However, the process did not yield a uniform break, resulting in non-spherical particles with a high polydispersity [34, 43] (Fig. 7d). Despite

the non-regular sizes, the obtained microparticles maintained their size, with the mean diameter ranging from 3 to 280 μm, within limits for injectable application (< 700 μm) [43]. As expected, the nanoparticles (Figure 7e) presented spherical morphology.

As can be seen in Figure 7f-i, the bulk hydrogel and the microparticles were efficient for proliferation on h-AdMSCs over the 14 days of cultivation. However, at the same concentration, the nanoparticles-maintained cell survival only, which suggests that further optimization is needed. As compared to the bulk hydrogel, the microparticles demonstrated a better performance, which could be explained by their higher surface area and less negative zeta potential, which benefited the adhesion and proliferation of the cells (Table 1). The deficient proliferation with the nanoparticles can be due to various factors, including the large lag phase or higher curvature of the surface, which was not favorable for cell adhesion or aggregation.

While the experiments reported in the present study were performed on the microplate, the cultivations were 3D (except for the control 2D). Similar results of cell proliferation on microparticles of other polymers were reported by Declercq et al. [17] and Colle et al. [45].

Furthermore, Shimojo et al. [13] compared h-AdMSCs proliferation *in vitro* on HA microparticles crosslinked with BDDE (mHA -BDDE) with the same mass of fluid HA. Both structures were embedded in the fibrin gel from platelet-rich plasma. The results showed that, although cell proliferation was not intense on the microparticles, it was greater than that in fluid HA. In the present study, the oxi-HA/ADH microparticles showed better cell proliferation when compared to mHA-BDDE even without the stimulus of the growth factors of PRP. Among the factors that could have contributed to our results are the topology of the surface, zeta potential, and the weaker crosslinking provided by ADH. Along with acting individually as active cell carriers, the microparticles may be useful as building blocks of modular systems, with tunable properties depending on the size and crosslinking degree. Furthermore, cell proliferation can be improved by the association with empty nanoparticles or with those carrying bioactive compounds, such as antioxidants, amino acids, or proteins.

4. CONCLUSIONS

In this study, we produced nano- and microparticles from bulk partially oxidized hyaluronic acid cross-linked with adipic dihydrazide. The results showed that, as compared to the non-oxidized fluid HA crosslinked with other chemicals, the

microparticles offer promising advantages as cell-laden for the proliferation of h-AdMSCs, and in terms of injectability and cryoprotection. Individually, the nanoparticles yielded an amenable surface; however, cell adhesion and concentration should be adjusted. In conclusion, both types of particles can be meaningfully used in a wide range of applications in tissue engineering and regenerative medicine individually or as building blocks for modular systems.

ACKNOWLEDGMENTS The authors gratefully acknowledge Prof. Dr. Marcos Akira D'Ávila for the rheometer used in the experiments. This study was supported by the National Council for Scientific and Technological Development (CNPq, grant number 140924/2017-5) and São Paulo Research Foundation (FAPESP, grant numbers 2019/12665-3 and 2016/10132-0).

REFERENCES

[1] F.H. Lin, W.Y. Su, Y.C. Chen, K.H. Chen, Cross-linked oxidated hyaluronic acid for use as vitreous substitute, National Health Research Institutes, United States, 2011, US Patent Classification: 2011/0200676 A1.

[2] M.A. Nicholls, A. Fierlinger, F. Niazi, M. Bhandari, The disease-modifying effects of hyaluronan in the osteoarthritic disease state, Clinical Medicine Insights-Arthritis and Musculoskeletal Disorders. 10 (2017), https://doi.org/10.1177/1179544117723611.

[3] R.C. Gupta, R. Lall, A. Srivastava, A. Sinha, Hyaluronic Acid: Molecular Mechanisms and Therapeutic Trajectory, Frontiers in Veterinary Science. 6 (2019) 192, https://doi.org/10.3389/fvets.2019.00192.

[4] T. Ito, Y. Yeo, C.B. Highley, E. Bellas, C.A. Benitez, D.S. Kohane, The prevention of peritoneal adhesions by in situ cross-linking hydrogels of hyaluronic acid and cellulose derivatives, Biomaterials. 28(6) (2007) 975-983, https://doi.org/10.1016/j.biomaterials.2006.10.021.

[5] Y. Yeo, C.B. Highley, E. Bellas, T. Ito, R. Marini, R. Langer, D.S. Kohane, In situ cross-linkable hyaluronic acid hydrogels prevent post-operative abdominal adhesions in a rabbit model, Biomaterials. 27 (2006) 4698-4705, https://doi.org/10.1016/j.biomaterials.2006.04.043.

[6] B.V. Slaughter, S.S. Khurshid, O.Z. Fisher, A. Khademhosseini, N.A. Peppas, Hydrogels in Regenerative Medicine, Advanced Materials. 21 (2009) 3307-3329, https://doi.org/10.1002/adma.200802106.

[7] H.A. Wang, S.C.G. Leeuwenburgh, Y.B. Li, J.A. Jansen, The use of micro- and nanospheres as functional components for bone tissue regeneration, Tissue Engineering Part B-Reviews. 18 (2012) 24-39, https://doi.org/10.1089/ten.TEB.2011.0184.

[8] Y.H. Yun, D.J. Goetz, P. Yellen, W.L. Chen, Hyaluronan microspheres for sustained gene delivery and site-specific targeting, Biomaterials. 25 (2004) 147-157, https://doi.org/10.1016/S0142-9612(03)00467-8.

[9] H. Fessi, F. Puisieux, J.P. Devissaguet, N. Ammoury, S. Benita, Nanocapsule formation by interfacial polymer deposition following solvent displacement, International Journal of Pharmaceutics. 55 (1989) R1-R4, https://doi.org/10.1016/0378-5173(89)90281-0.

[10] Z. Hu, X. Xia, L. Tang, Process for synthesizing oil and surfactant-free hyaluronic acid nanoparticles and microparticles, United States, 2006, US Patent Classification: 2006/0040892 A1.

[11] R.C.S. Bicudo, M.H.A. Santana, Effects of organic solvents on hyaluronic acid nanoparticles obtained by precipitation and chemical crosslinking, Journal of Nanoscience and Nanotechnology. 12 (2012) 2849-2857, https://doi.org/10.1166/jnn.2012.5814.

[12] E. Sideris, D.R. Griffin, Y.C. Ding, S.R. Li, W.M. Weaver, D. Di Carlo, T. Hsiai, T. Segura, Particle hydrogels based on hyaluronic acid building blocks, Acs Biomaterials Science & Engineering. 2 (2016) 2034-2041, https://doi.org/10.1021/acsbiomaterials.6b00444

[13] A.A.M. Shimojo, S.E.M. Galdames, A.d.S.S. Duarte, L.M. Pina, A.A. Rodrigues, Â.C.M. Luzo, W.D. Belangero, M.H.A. Santana, The structuring of high molecular weight hyaluronic acid in microparticles or sponges improves its performance when associated with platelet-rich plasma, Trends in biomaterials and artificial organs. 29 (2014) 160-169.

[14] J.W. Nichol, A. Khademhosseini, Modular tissue engineering: engineering biological tissues from the bottom up, Soft Matter. 5 (2009) 1312-1319, https://doi.org/

[15] C.J. Connon, Approaches to corneal tissue engineering: top-down or bottom-up?, Procedia Engineering 110 (2015) 15-20, https://doi.org/ 10.1039/b814285h.

[16] J.G. Kang, T.H. Kim, S.H. Oh, J.H. Lee, Fabrication and evaluation of growth factor-immobilized injectable microspheres for the soft tissue augmentation, Tissue Engineering and Regenerative Medicine. 11 (2014) 8-15, https://doi.org/10.1007/s13770-013-1126-5.

[17] H. Declercq, T. De Caluwe, O. Krysko, C. Bachert, M. Cornelissen, Bone grafts engineered from human adipose-derived stem cells in dynamic 3d-environments: a top-down versus bottom-up approach, Journal of Tissue Engineering and Regenerative Medicine. 6 (2012) 23-24, https://doi.org/10.1016/j.biomaterials.2012.10.051.

[18] F. Urciuolo, G. Imparato, C. Palmiero, A. Trilli, P.A. Netti, Effect of process conditions on the growth of three-dimensional dermal-equivalent tissue obtained by microtissue precursor assembly, Tissue Engineering Part C-Methods. 17 (2011) 155-164, https://doi.org/10.1089/ten.TEC.2010.0355.

[19] S. Emoto, H. Yamaguchi, T. Kamei, H. Ishigami, T. Suhara, Y. Suzuki, T. Ito, J. Kitayama, T. Watanabe, Intraperitoneal administration of cisplatin via an in situ cross-linkable hyaluronic acid-based hydrogel for peritoneal dissemination of gastric cancer, Surgery Today. 44 (2014) 919-926, https://doi.org/10.1007/s00595-013-0674-6.

[20] C.G. França, D.P. Sacomani, D.G. Villalva, V.F. Nascimento, J.L. Dávila, M.H.A. Santana, Structural changes and crosslinking modulated functional properties of oxi-HA/ADH hydrogels useful for regenerative purposes, European Polymer Journal. 121 (2019) 109288, https://doi.org/10.1016/j.eurpolymj.2019.109288.

[21] X.Q. Jia, Y. Yeo, R.J. Clifton, T. Jiao, D.S. Kohane, J.B. Kobler, S.M. Zeitels, R. Langer, Hyaluronic acid-based microgels and microgel networks for vocal fold regeneration, Biomacromolecules. 7 (2006) 3336-3344, https://doi.org/10.1021/bm0604956.

[22] W.Y. Su, Y.C. Chen, F.H. Lin, Injectable oxidized hyaluronic acid/adipic acid dihydrazide hydrogel for nucleus pulposus regeneration, Acta Biomaterialia. 6 (2010) 3044-3055, https://doi.org/10.1016/j.actbio.2010.02.037

[23] M.H. Hu, K.C. Yang, Y.H. Sun, Y.C. Chen, S.H. Yang, F.H. Lin, In situ forming oxidised hyaluronic acid/adipic acid dihydrazide hydrogel for prevention of epidural fibrosis after laminectomy, European Cells & Materials. 34 (2017) 307-320, https://doi.org/10.22203/eCM.v034a19.

[24] B.D. Smith, D.A. Grande, The current state of scaffolds for musculoskeletal regenerative applications, Nature Reviews Rheumatology. 11 (2015) 213-222, https://doi.org/10.1038/nrrheum.2015.27.

[25] M.Y. Hsiao, A.C. Lin, W.H. Liao, T.G. Wang, C.H. Hsu, W.S. Chen, F.H. Lin, Drug-loaded hyaluronic acid hydrogel as a sustained-release regimen with dual effects in early intervention of tendinopathy, Scientific Reports. 9 (2019), https://doi.org/10.1038/s41598-019-41410-y.

[26] M. Weis, J.W. Shan, M. Kuhlmann, T. Jungst, J. Tessmar, J. Groll, Evaluation of hydrogels based on oxidized hyaluronic acid for bioprinting, Gels. 4 (2018), https://doi.org/10.3390/gels4040082.

[27] P. Legrand, S. Lesieur, A. Bochot, R. Gref, W. Raatjes, G. Barratt, C. Vauthier, Influence of polymer behaviour in organic solution on the production of polylactide nanoparticles by nanoprecipitation, International Journal of Pharmaceutics. 344 (2007) 33-43, https://doi.org/10.1016/j.ijpharm.2007.05.054.

[28] S.W. Choi, H.Y. Kwon, W.S. Kim, J.H. Kim, Thermodynamic parameters on poly(D,L-lactide-co-glycolide) particle size in emulsification-diffusion process, Colloids and Surfaces a-Physicochemical and Engineering Aspects. 201 (2002) 283-289, https://doi.org/10.1016/S0927-7757(01)01042-1.

[29] Y.H. Chen, Q. Wang, Establishment of CTAB Turbidimetric method to determine hyaluronic acid content in fermentation broth, Carbohydrate Polymers. 78 (2009) 178-181, https://doi.org/10.1016/j.carbpol.2009.04.037.

[30] A.A.M. Shimojo, A.D.S. Duarte, J. Lana, A.C.M. Luzo, A.R. Fernandes, E. Sanchez-Lopez, E.B. Souto, M.H.A. Santana, Association of platelet-rich plasma and auto-crosslinked hyaluronic acid microparticles: approach for orthopedic application, Polymers. 11 (2019) 1568, https://doi.org/10.3390/polym11101568.

[31] A.A.M. Shimojo, A.M.B. Pires, L.G. de la Torre, M.H.A. Santana, Influence of particle size and fluid fraction on rheological and extrusion properties of crosslinked hyaluronic acid hydrogel dispersions, Journal of Applied Polymer Science. 128 (2013) 2180-2185, https://doi.org/10.1002/app.38389.

[32] T. Mosmann, Rapid colorimetric assay for cellular growth and survival: application to proliferation and cytotoxicity assays, Journal of lmmunological Methods. 65 (1983) 55-63, https://doi.org/10.1016/0022-1759(83)90303-4.

[33] G.D. Prestwich, D.M. Marecak, J.F. Marecek, K.P. Vercruysse, M.R. Ziebell, Controlled chemical modification of hyaluronic acid: synthesis, applications, and biodegradation of hydrazide derivatives, Journal of Controlled Release. 53 (1998) 93-103, https://doi.org/10.1016/S0168-3659(97)00242-3.

[34] Y.J. Seong, G. Lin, B.J. Kim, H.E. Kim, S. Kim, S.H. Jeong, Hyaluronic acid-based hybrid hydrogel microspheres with enhanced structural stability and high injectability, Acs Omega; 4 (2019) 13834-13844, https://doi.org/10.1021/acsomega.9b01475.

[35] A.A.M. Shimojo, A.M.B. Pires, R. Lichy, A.A. Rodrigues, M.H.A. Santana, The crosslinking degree controls the mechanical, rheological, and swelling properties of hyaluronic acid microparticles, Journal of Biomedical Materials Research Part A. 103 (2015) 730-737, https://doi.org/10.1002/jbm.a.35225.

[36] S. Khunmanee, Y. Jeong, H. Park, Crosslinking method of hyaluronic-based hydrogel for biomedical applications, Journal of Tissue Engineering. 8 (2017), https://doi.org/10.1177/2041731417726464.

[37] F.A. Morrison, Understanding rheology, Oxford University Press. (2011).

[38] W.P. Cox, E.H. Merz, Correlation of dynamic and steady flow viscosities, Journal of Polymer Science. 28 (1958) 619-622, https://doi.org/10.1002/pol.1958.1202811812.

[39] D.H.S. Ramkumar, M. Bhattacharya, J.A. Menjivar, T.A. Huang, Relaxation behavior and the application of integral constitutive equations to wheat dough, Journal of Texture Studies. 27 (1996) 517-544, https://doi.org/10.1111/j.1745-4603.1996.tb00092.x.

[40] D. Khondar, R.F. Tester, N. Hudson, J. Karkalas, J. Morrow, Rheological behaviour of uncross-linked and cross-linked gelatinised waxy maize starch with pectin gels, Food Hydrocolloids. 21 (2007) 1296-1301, https://doi.org/10.1016/j.foodhyd.2006.10.008.

[41] S. Ikeda, K. Nishinari, "Weak gel"-type rheological properties of aqueous dispersions of nonaggregated kappa-carrageenan helices, Journal of Agricultural and Food Chemistry. 49 (2001) 4436-4441, https://doi.org/10.1021/jf0103065.

[42] A.A.M. Shimojo, S.E.M. Galdames, A.G.M. Perez, T.H. Ito, A.C.M. Luzo, M.H.A. Santana, In vitro performance of injectable chitosan-tripolyphosphate scaffolds combined with platelet-rich plasma, Tissue Engineering and Regenerative Medicine. 13 (2016) 21-30, https://doi.org/10.1007/s13770-015-9111-9.

[43] J. Kablik, G.D. Monheit, L.P. Yu, G. Chang, J. Gershkovich, Comparative physical properties of hyaluronic acid dermal fillers, Dermatologic Surgery. 35 (2009) 302-312, https://doi.org/10.1111/j.1524-4725.2008.01046.x.

[44] A.A.M. Shimojo, A.M.B. Pires, R. Lichy, M.H.A. Santana, The performance of crosslinking with divinyl sulfone as controlled by the interplay between the chemical modification and conformation of hyaluronic acid, Journal of the Brazilian Chemical Society. 26 (2015) 506-512, https://doi.org/10.5935/0103-5053.20150003.

[45] J. Colle, P. Blondeel, A. De Bruyne, S. Bochar, L. Tytgat, C. Vercruysse, S. Van Vlierberghe, P. Dubruel, H. Declercq, Bioprinting predifferentiated adipose-derived mesenchymal stem cell spheroids with methacrylated gelatin ink for adipose tissue engineering, Journal of Materials Science-Materials in Medicine. 31 (2020), https://doi.org/10.1007/s10856-020-06374-w.

3.3. The association of L-PRP and oxi-HA/ADH microparticles forms suitable structures for regenerative purposes

Artigo a ser publicado no periódico científico *Journal of Materials Science: Materials in Medicine.*

The association of fibrin from L-PRP and h-AdMSCs -oxi-HA/ADH microparticles forms effective matrices for regenerative medicine approaches

Carla Giometti França[1]; Juliana Magro Ribeiro[2]; Krissia Caroline Leme[3], Ângela Cristina Malheiros Luzo[3], Carolina Caliari Oliveira[2], José Fabio Lana[4] & Maria Helena Andrade Santana[,1]*

[1]Department of Materials and Bioprocess Engineering, School of Chemical Engineering, University of Campinas, 13083-852, Campinas, São Paulo, Brazil.

[2]*In situ* Cell Therapy, Supera Parque, 14056-680, Ribeirão Preto, São Paulo, Brazil.

[3]Haematology & Hemotherapy Center, Umbilical Cord Blood Bank, University of Campinas, 13083-878, Campinas, São Paulo, Brazil.

[4.]Bone and Cartilage Institute, Indaiatuba, SP 13334-170, Brazil

[*]Correspondence should be addressed to mariahelena.santana@gmail.com

Abstract

Hyaluronic acid (HA) is a glycosaminoglycan widely exploited as mimics of the extracellular matrix (ECM) due to its high hydration capacity and possibilities of chemical modifications. However, the recreation of the complex ECM environment from biomaterials still is a challenge. Oxi-HA/ADH is a hydrogel composed of HA chemically modified by partial oxidation (oxi-HA) with sodium periodate, crosslinked with adipic dihydrazide (ADH). L-PRP is an autologous product rich in leukocytes and platelets, dispersed in a small volume of plasma. L-PRP provides a fibrin network for cell proliferation, migration, and differentiation, growth factors from platelets, and cytokines from leukocytes, that together act in tissue regeneration. H-AdMSCs are mesenchymal cells, the most important stem cell class for regeneration, derived from the human adipose tissue. In the present study, we aimed to characterize the kinetic behavior for *in vitro* proliferation of h-AdMSCs previously adhered to the microparticles (h-AdMSC-oxi-HA/ADH) in a medium supplemented with L-PRP and also to optimize the microparticles concentration for cell proliferation. The results showed the data were adjusted to a Monod type kinetic, and the best maximum specific growth rates and doubling times were obtained with 2 and 5mg of microparticles. In these conditions, the microparticles did not suppress the fibrin network's expansion and improved cell proliferation, according to SEM and live and dead images. These results

contribute to the development of effective fibrin-based matrices for regenerative approaches.

Keywords: Platelet-rich plasma, oxidized hyaluronic acid, microparticles, mesenchymal cells, regenerative medicine

Graphical abstract. Fibrin network with oxi-HA/ADH microparticles and their properties for tissue engineering and regenerative medicine.

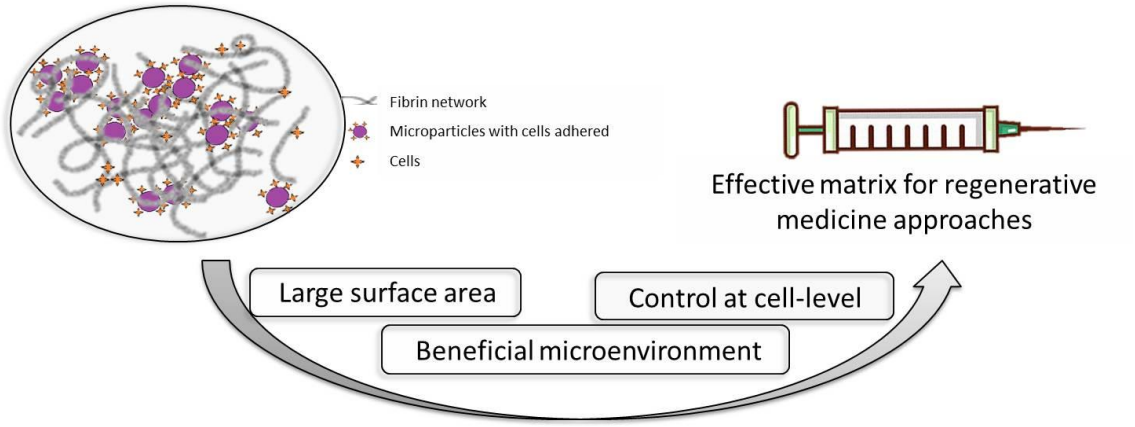

1. Introduction

Leukocyte and platelet-rich plasma (L-PRP) consist of a concentrate of platelets , leukocytes, cytokines, proteins, and other components dispersed in a small volume of plasma obtained by centrifugation of whole blood. Activation of L-PRP produces platelet degranulation and release of growth factors, with concomitant degradation of fibrinogen and formation of a fibrin network with gel consistency. L-PRP components stimulate stem cell proliferation and differentiation, acting in the inflammatory and remodeling phases of tissue regeneration. Due to its efficiency, L-PRP has been widely used in the treatments of musculoskeletal diseases [1].

Hyaluronic acid (HA) is a natural unbranched and non-sulfated glycosaminoglycan composed of repeated units of N-acetyl-D-glucosamine and D-glucuronic acid linked by β-1,4-glycosidic bonds [2]. HA is present in the extracellular matrix (ECM) of various tissues, including bone and cartilage. HA performs roles in joint lubrication and protection against shock, in addition to anti-inflammatory effects and pain relief [3]. *In vivo*, HA mediates interactions with receptors, thus regulating the signaling pathways associated with adhesion, proliferation, migration, and differentiation of cells, besides tuning the mechanical properties of ECM. Due to its

high capacity for hydration and possibilities of chemical modifications, HA is widely exploited as a scaffold for mimicking the ECM, thus offering a suitable niche for stem cells [4].

In general, the association of microparticles to bulk hydrogels adds features such as surface topography and a large surface for adhesion, enabling cell-scale control. Therefore, novel approaches are emerging to manufacture 3D constructs mimicking the cell microenvironment *in vivo* [5-7]. Cell-loaded microcarriers are promising for various applications, such as they can be injected directly in a lesion site [8], incorporated into a larger scaffold biomaterial [9], or assembled in bottom-up approaches for construction building blocks for the preparation of modular tissues [10].

A survey of the literature shows few studies on the association of hydrogels or microcarriers to the fibrin network from PRP or its derived components. A relevant study show an injectable HA associated with platelet lysate -derived in granular hydrogels [11].

In previous articles, we associated P-PRP (platelet-rich and leukocyte-poor plasma) to HA microparticles crosslinked with divinyl sulphone [12], 1,4-butanediol diglycidyl ether (BDDE) [13] or auto-crosslinked [14]. The results showed that the association provided injectable formulations with better physicochemical and mechanical properties than bulk HA. Moreover, both associations allowed for *in vitro* proliferation of h-AdMSCs. However, cell proliferation in P-PRP -BDDE microparticles was lower than in P-PRP, while it was similar for P-PRP when auto-croslinked microparticles were used.

Partial oxidation of HA hydroxyl groups (oxi-HA) is used to introduce highly flexible links into extended structures. Oxidized HA (oxi-HA) can be attached to small molecules such as adipic dihydrazide (ADH) to form injectable and biocompatible hydrogels (oxi-HA / ADH) [15]. Previously, we studied the structural changes in HA due to the partial oxidation and ADH concentration. The oxidation degree increased the zeta potential and decreased the hydrodynamic volume and viscosity, extrusion force, and injectability. The ADH concentration modulated the functional properties such as swelling, stability, gelation time, and thermosensitivity of the oxi-HA/ADH hydrogels. The structural changes also allowed ADH crosslink for click reaction, without a catalyst or further purification steps. Therefore, the oxi-HA/ADH hydrogels appear promising biomaterial for uses in regenerative approaches [15].

After previous studies on preparation and characterization of oxi-HA/ADH microparticles, in the present study, we aimed to characterize the kinetic behavior for *in vitro* proliferation of h-AdMSCs previously adhered to the microparticles (h-AdMSC-oxi-HA/ADH) in a medium supplemented with L-PRP, and to optimize the microparticle concentration for cell proliferation.

The rationale for using oxi-HA/ADH hydrogel is ADH metabolization in the human body, different from other crosslink agents, besides the beneficial properties and facilitated preparation, compared to non-oxidated HA hydrogels both in bulk or microparticles. Furthermore, the previous adhesion of h-AdMSCs to the oxi-HA/ADH microparticles aims for better control at the cell-level.

2. Materials and methods

2.1. Materials and reagents

Hyaluronic acid (HA) with an average molecular weight of $8.54x10^5$ Da was purchased from Tops Shandong Topscience Biotech Co. (Rizhao, CH). Sodium periodate ($NaIO_4$), ethylene glycol, adipic acid dihydrazide (ADH), and sodium bicarbonate ($NaHCO_3$) were purchased from Sigma-Aldrich Inc. (Saint Louis, Missouri, USA). Phosphate buffered saline (PBS) was supplied from Laborclin Ltda (Pinhais, Paraná, BR). Dialysis membranes with a nominal MWCO of 12,000 – 16,000 Da were sourced from Inlab (Diadema, São Paulo, BR). Dulbecco's modified eagle medium (DMEM), Fetal bovine serum (FBS), and Penicillin-Streptomycin (P/S) was purchased by Thermo Fisher Scientific (Waltham, Massachusetts, USA). Leukocyte and platelet-rich plasma (L-PRP), an autologous product, was obtained from whole blood of healthy donors, according to the approval of the Ethics Committee of the School of Medical Sciences of the University of Campinas-Brazil (Campinas; CAAE: 0972.0.146.000-11). Blood collection tubes (8.5 mL) containing 1 mL anticoagulant acid dextrose solution A (ACD-A) were sourced from Vacutainer, BD Bioscience, Allschwil, Switzerland). Calcium chloride used for activation of L-PRP was purchased from Sigma-Aldrich, St Louis, USA.

2.2. Methods

2.2.1. Preparation of oxi-HA

Oxi-HA was synthesized according to the reported procedure [16, 17] with modifications introduced by França et al. (2019) [15]. HA with a concentration of 1% (w/v) was dissolved in double-distilled water at room temperature, and then an aqueous

periodate ($NaIO_4$) solution (10.67%) was added at a molar ratio $NaIO_4$:HA 2:1, calculated as $NaIO_4$ mol per HA dimer mol. The reaction occurred in a dark environment for 24h, and it was stopped by the addition of ethylene glycol for a half hour (molar ratio 1:6 $C_2H_6O_2$:$NaIO_4$). The resulting solution was dialyzed with double-distilled water for three days using a semipermeable membrane (with an MWCO of 12,000–16,000 Da). Finally, the product was lyophilized, yielding a white fluffy product. The oxidation degree of the oxi-HA was 65%, measured by the number of aldehyde functional groups in oxi-HA using the reagents tert-butyl carbazate (t-BC) and trichloroacetic acid, picrysulfonic acid solution TNBS).

2.2.2. Preparation of oxi-HA/ADH bulk hydrogel

The oxi-HA/ADH bulk hydrogel was obtained, according to França *et al.* [15]. Briefly, oxi-HA with oxidation degree 65% was dissolved in PBS (pH of 7.4, at 4°C) to obtain a final concentration of 6% (w/v). Then, 8% (w/v) ADH solution was also prepared in PBS at 4°C. The oxi-HA and ADH solutions were mixed in an Eppendorf tube at a 4:1 oxi-HA/ADH volume ratio. The Eppendorf tubes were submerged in a bath containing water and ice (close to 0°C) to obtain the oxi-HA/ADH hydrogel. In the kinetic assays, the bulk hydrogels were cut in small cylinders (radius: 0,4 cm and height: 0,3 cm) for 3D cultivation of h-AdMSCs.

The oxi-HA and ADH solutions were sterilized separately through a 0.22 µm syringe filter. After sterilization, the entire gelation process was conducted within a laminar flow cabinet.

2.2.3. Preparation of oxi-HA/ADH microparticles

The oxi-HA/ADH microparticles (µP) were obtained from the oxi-HA/ADH bulk hydrogel swelled in ultrapure water and sheared in an Ultra-Turrax T25 homogenizer (IKA Labortechnik, Germany) at 18,000 rpm for 10 min. The particles'size was measured as a mean diameter by the dynamic light scattering technique in a Mastersizer-S (Malvern Instruments, UK). The standard deviation was calculated from ten measurements of the mean diameter.

The sterilization of the microparticles was performed by UV irradiation using a ultraviolet lamp (Germetec, Rio de Janeiro, RJ, Brazil) at a wavelength of 254 nm. The samples were irradiated during 1 h.

2.2.4. Blood collection and L-PRP preparation

L-PRP was prepared by centrifugation of whole blood of healthy donors as described by Melo et al. (2018) [18]. The use of whole blood in this study was approved

by the Ethics Committee of the Medical Sciences School of the University of Campinas, Campinas, SP, Brazil (UNICAMP) (CAAE: 0972.0.146.000-11).

Briefly, whole blood from a healthy donor was collected in a tube containing anticoagulant acid citrate dextrose solution A (ACD-A) before centrifugation. After collection, the 3.5 mL of the anticoagulated blood was transferred to empty 5-mL tubes and centrifuged at 100×g for 10 min at 25°C out in a ROTINA 380R centrifuge (Hettich Zentrifugen, Tuttlingen, Germany) with the tubes positioned at 45° relative to the rotor. L-PRP, composed of the top and middles layers of centrifuged blood, was collect using an automatic pipette and transfer to an empty tube for homogenization and quantification of components using an ABX Micros ES 60 hematologic analyzer (Horiba ABX Diagnostics, Montpellier, France). The experiment was performed in triplicate (n = 3), and three measurements were taken for each sample.

2.2.5. h-AdMSCs isolation and cultivation

The h-AdMSCs were isolated from the human subcutaneous adipose tissue of patients undergoing lipo-aspiration at the University Hospital and isolated and cultured according to a previous protocol [19]. The h-AdMSC cells were cultured in Dulbecco's modified eagle medium (DMEM), containing15 mM HEPES buffer, L-glutamine, pyridoxine hydrochloride, 3.7 g $NaHCO_3$, and supplemented with 10% FBS and 1% P/S. Cells from passage 4 to 6 were trypsinized and adhered to the surface of the microparticles or bulk hydrogel at a concentration of 2×10^4 cells/well.

2.2.6. Cell viability

The viability of h-AdMSCs in the presence of oxi-HA, ADH or oxi-HA/ADH hydrogel was evaluated by exposing the materials oxi-HA or ADH to the cell culture. Initially, the cells were distributed in 24-well plates, using a density of 5×104 cell/mL, and incubated at 37°C at 5% CO_2 for 24 hours. Later, the cells were treated with different concentrations (0 to 5 mg/mL) of oxi-HA dispersion or ADH solution, or oxi-HA/ADH hydrogel for 72 hours. After incubation, the medium was removed, the wells were washed with PBS, and 200 µL of 3-(4,5-dimethylthiazol-2-yl)-2,5-diphenyltetrazolium bromide (MTT) solution (1 mg/mL) was added to each well. The plate was incubated for 3 h at 37°C, MTT solution was removed and the formazan crystal was solubilized in 1 mL of dimethyl sulfoxide (DMSO). Thus, the plate was shaken for 5 min, and the absorbance of each well was read using an Infinity M200Pro spectrophotometer (Tecan, Männedorf, Switzerland). The measured absorbance at λ =

570 nm was normalized to the value obtained for the control (Cell 2D - the cells are adhered to the plate) [20].

2.2.7. Kinetics of cell adhesion

The kinetic behavior for h-AdMSCs adhesion to the surface of the microparticles was evaluated by incubation of a previously prepared cell suspension with 2.5 - 10 mg de microparticles in the liquid culture medium described in item 2.2.7. Each well was added 100 μL contain $5x10^4$ cells. The incubation was carried out in 48-well plate for 2 hours. At time intervals, samples were taken from the culture medium, and cell counts were made using a Newbauer camera. The adhered cells were calculated by subtracting its initial concentration from the remaining concentration in the culture medium. The counts were done in triplicate (n=3) for each plate.

2.2.8. Association of L-PRP and h-AdMSCs-oxi-HA/ADH microparticles

After adhesion (2 hours), the microparticles containing h-AdMSCs were mixed with 160 μL of L-PRP and transferred to a 48-well plate. After, L-PRP was activated with serum-containing thrombin and $CaCl_2$ solution (10% *m/v*) as agonists in volumetric proportion 9:1. The volumetric proportion of agonist/L-PRP was 40:160 (*v/v*). Activation of L-PRP leads to the decomposition of fibrinogen and formation of a fibrin network gel. These used proportion provided a fibrin network architecture with fibers of 160 nm average radius, which favors the proliferation of h-AdMSCs due to its paracrine nature [21, 22].

Once the fibrin gels were formed, 700 μL of low-glucose DMEM (Thermo Fisher Scientific, Waltham, MA, USA) was added to the wells, and cells were cultured for two weeks in a humidified incubator at 37 °C, and 5% CO_2 with the medium changed every three days. The experiment was performed in triplicate (n = 3) for each group.

2.2.9. Behavior of h-AdMSCs proliferation

The proliferation of h-AdMSCs in 3D culture, previously adhered on the bulk cylinder or on the microparticles was conducted in 48-well plates, as described in item 2.2.7.

2.2.10. Maximum specific growth rate

The cell proliferation data were treated to calculate the maximum specific rate of cell growth ($\mu_{máx}$) and cell doubling time (t_d). Initially a polynomial curve was adjusted to the kinetic data express in terms of absorbance. A second-degree polynomial curve

adjusted the experimental data with a correlation coefficient of 1. From the polynomial equations, we estimated values at small intervals within the studied range and delineated the cell exponential phase. The $\mu_{máx}$ was calculated using Eq. 1, considering the Monod-type kinetic for h-AdMSCs [23], and t_d was calculated by Eq. 2.

$$ln\left({Abs}/{Abs_0}\right) = \mu_{máx} \cdot t \quad \text{(Eq. 1)}$$

$$t_d = {\ln 2}/{\mu_{máx}} \quad \text{(Eq. 2)}$$

2.2.11. Assessment of h-AdMSC viability images

Images of the cultured cells were determined by Live & Dead assay over seven days using the LIVE/DEAD cell imaging kit (Thermo Fisher Scientific, Waltham, MA, USA). At predetermined days, the medium was removed from the wells and the hydrogels were washed with PBS. Then, 200 µL of LIVE/DEAD reagent was added and incubated for 30 min. After this period, images of the samples were taken with a confocal microscope (Leica Microscope TCS SP5 II, Wetzlar, Germany). The number of living and dead cells was calculated by counting cells from three different images using ImageJ software.

2.2.12. Morphology of the hydrogels

After polymerization and the formation of the fibrin nanofibers, the networks were fixed in a 4% paraformaldehyde and 2.5% glutaraldehyde solution prepared in phosphate buffer (PBS), pH 7.4, for 2 h at 4 °C. Dehydration of fixed hydrogels was carried out by dipping them in ethanol of different concentrations (50%, 70%, 95%, and 100%) at 15 min intervals. Then, the samples were dried at the critical point in a BALTEC critical point dryer (CPD) 030 dryer (Schalksmühle, Germany).

The morphology of the oxi-HA/ADH hydrogels were obtained by scanning electron microscopy (SEM) (LEO 440i, Cambridge, England) using a current and voltage of 50 pA and 10 kV, respectively. The average fiber sizes were determined by measuring 100 individual pores from three different images using ImageJ software.

2.3. Statistical analysis

Each experiment was carried out in triplicate unless otherwise specified. All the results are presented as the mean ± standard deviation (SD). The experimental data from all the studies were analyzed using analysis of variance (ANOVA). The statistical significance was set to p-value ≤ 0.05.

3. Results

3.1. Cell viability

The cell viability assays, were performed in the presence of a range of concentrations of oxi-HA dispersions, ADH solutions and in the presence of oxi-HA/ADH bulk hydrogel. The results are shown in Figure 1.

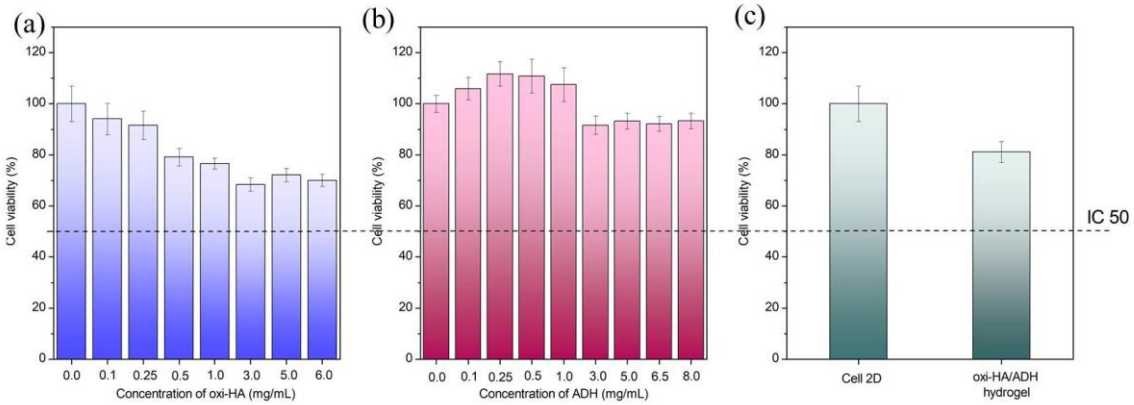

Figure 1. Evaluation of cell viability at different concentrations of (a) oxi-HA dispersion, (b) ADH solution, and (c) oxi-HA/ADH bulk hydrogel Hydrogel properties: pore size 105 ±24 μm.

The viability of the cells was preserved after exposition to the various materials and concentrations Therefore, the results revealed no potential cytotoxicity over 3 days according to the standard values (IC 50). However, there was a decrease in cell viability for oxi-HA dispersion at concentrations above 0.5 mg/mL (Figure 2a). Aldehyde-modified polymers, such as oxi-HA, also showed a dose-dependent effect on cell viability in macrophages and mesothelial cells [24-26]. The lower bar for oxi-HA/ADH (Figure 1c) is due to nutrient diffusion or cell migration limitations in the internal porous structure.

3.2. Physicochemical characterization of the oxi-HA/ADH bulk hydrogel and microparticles

Table 1 shows the physicochemical properties of the bulk hydrogel and the microparticles both used in h-AdMSCs cultivations. The pore size and porosity of the microparticles were not determined.

Table 1. Physicochemical properties of the bulk hydrogel and the microparticles.

Property	**Bulk Hydrogel**	**Microparticles**
Pore size (μm)	105 ±24	-
Porosity (%)	67	-
Cell seeding (cell/mL)	$2x10^4$	$2x10^4$
Zeta potential (mV)	-36 ±3	-17.8 ±1.9
Mean diameter (μm)	8000	215

It could be observed in Table 1 the ADH crosslink produced a porous bulk hydrogel with 67% porosity and large pores (105 ±24 μm)**.** Although the porosity of the microparticles could not be determined, they are also porous structures, as indirectly observed from the results of Figure 1c. Microparticles with 215 μm mean diameter were produced shearing the bulk hydrogel in controlled conditions. The absolute value of zeta potential was reduced from the bulk hydrogel to the microparticles. This reduction is due to surface modifications in consequence of the shearing process for size reduction.

3.3. Blood and L-PRP compositions

Table 2 shows the concentration of the components in whole blood and L-PRP after one step centrifugation.

Table 2. Concentrations of blood components in the whole blood and L-PRP.

	Whole blood	**L-PRP**
Platelets $x10^3$/mm	268 ±4	485 ±8
Leukocytes $x10^3$/mm	5.43 ±0.00	1.85 ±0.07
Lymphocytes $x10^3$/mm	2.25 ±0.07	1.55 ±0.07
Monocytes $x10^3$/mm	0.30 ±0.00	0.10 ±0.00
Granulocytes $x10^3$/mm	2.40 ±0.14	0.25 ±0.07
Erythrocytes $x10^3$/mm	3.52 ±0.03	0.03 ±0.01

One step centrifugation concentered platelets twice approximately, in respect to whole blood. Platelet and leukocyte concentration levels in the L-PRP were 485 $\pm 8x10^3/mm^3$ and 1.85 $\pm 0.007x10^3/mm^3$, respectively, with a platelet/leukocyte ratio of 262 ±0.1. The centrifugation conditions enabled the recovery of a relatively high concentration of lymphocytes compared to that of granulocytes with a ratio of 6.2 ±0.6.

This spectrum of concentrations in L-PRP is favorable to cell stimulation for proliferation because of the release of much more growth factors, proportional to platelet and lymphocyte concentrations, than inflammatory cytokines from granulocytes.

3.4. Images of the fibrin network from L-PRP, oxi-HA/ADH microparticles and their associations

For microstructural perspective, the effects of L-PRP with microparticles were observed by scanning electron microscopy (Figure 2). After activation of L-PRP, fibrin networks were formed.

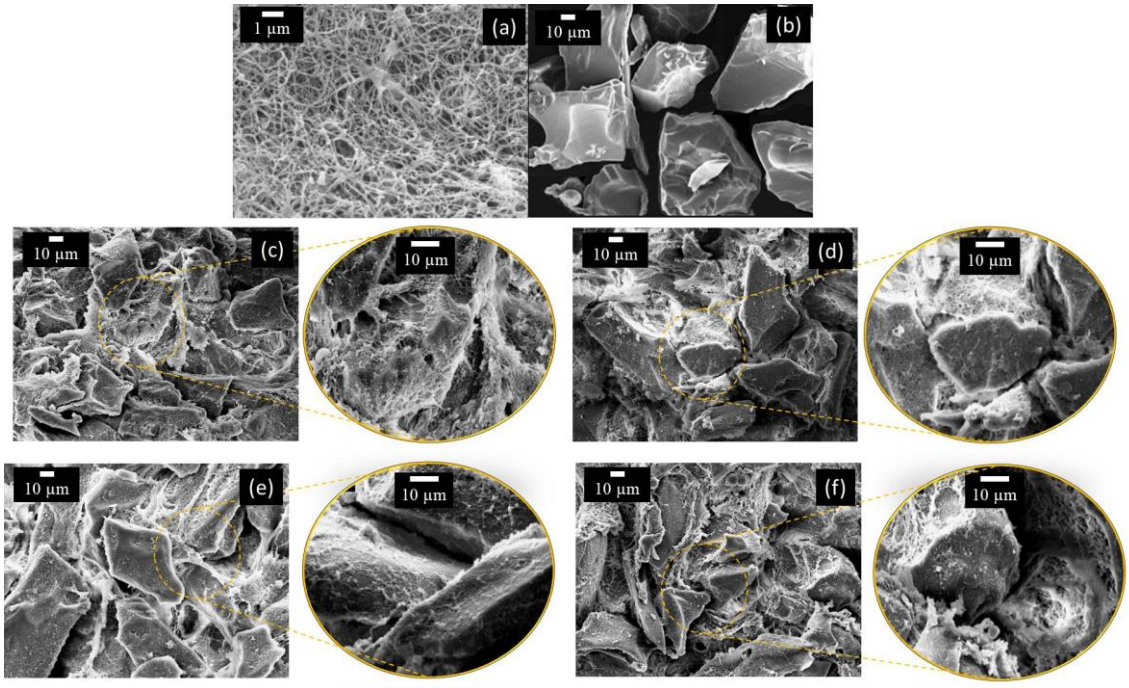

Figure 2. Scanning electron microscopy (SEM) images: (a) Fibrin network from L-PRP (b) oxi-HA/ADH microparticles (µP) (c) µP (2.5 mg) with L-PRP, (d) µP (5 mg) with L-PRP, (e) µP (7.5 mg) with L-PRP, and (f) µP (10 mg) with L-PRP.

The SEM image for L-PRP (Figure 2a) shows the interconnected fibers organization in a highly porous network. However, the presence of microparticles (Figure 2c-f) disturbs the fibrin network, which seems to entangle as the particle concentration increased, suppressing the elongation of the fibers. It is possible to observe a denser and less porous network with high concentration of microparticles (Figure 2e-f).

3.5. h-AdMSCs adhesion and proliferation

We investigate the adhesion time and proliferation of h-AdMSCs on the bulk hydrogel and on oxi-HA/ADH microparticles in 3D culture.

The h-AdMSCs were previously characterized, being adherent to the culture flask, and positive for cell markers CD90 (99.7%), CD73 (52.0%), CD105 (70.8%), and negative CD34 (5.62%), CD45 (6.49%). The adhesion of h-AdMSCs to the materials investigated was determined in terms of the gradual reduction in the number of cells in suspension with time, as shown in Figure 3a. The adhesion profiles show that more than 50% of the total initial population had already adhered to the materials 2 h after h-AdMSCs inoculation. The adhesion was faster to the surface of the control culture plate as expected. Four hours after the inoculation, the number of cells in the supernatant was minimum and more than 98% of the cells inoculated adhered to the materials. It could be observed, after 6 hours of innoculation, there is a tendency for cell detachment from the bulk hydrogel and the microparticles.

Figure 3b shows the kinetic proliferation of the adhered h-AdMSCs on the surface of the bulk hydrogel and oxi-HA/ADH microparticles at different concentrations in terms of absorbance (570 nm) versus time. Figure 3c shows the same results in semi-logarithmic scale of the relative absorbance, for the estimation of the times for cell adaptation and exponential phases. Thus, the maximum specific growth rate (μmáx) and double time (td) were determined for each situation (Table 3).

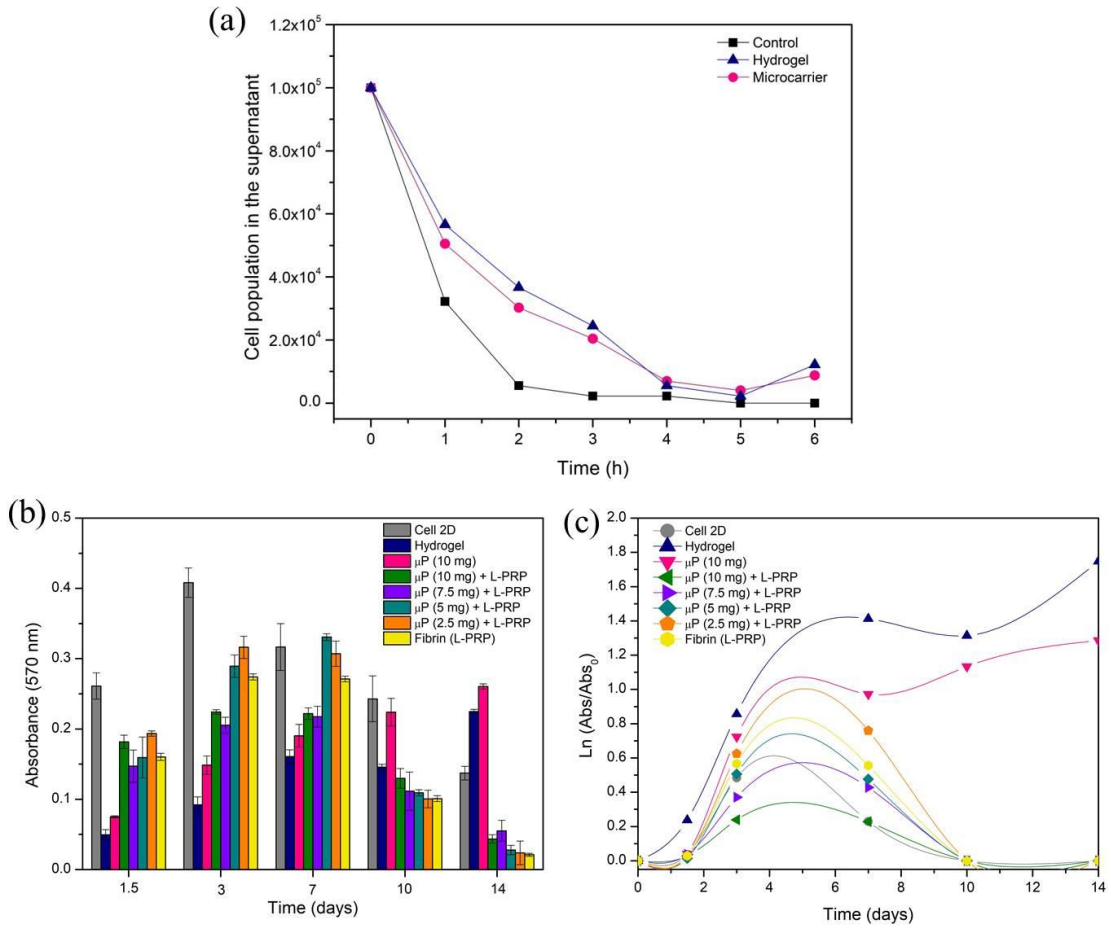

Figure 3. (a) Adhesion kinetic of h-AdMSCs on the bulk hydrogel and 10 mg of microparticles (b) Proliferation kinetic of h-AdMSCs cultured in L-PRP and in different concentration of the microparticles for two weeks (c) Proliferation kinetics for h-AdMSCs in L-PRP and in semi-logarithmic scale.

Table 3. Maximum specific growth rate and doubling time, for the various cultivation conditions.

Condition	**Max specific growth rate** μ_{max} **(h^{-1})**	**Doubling time** t_d **(h)**
Cell 2D	0.012	57.8
Hydrogel	0.016	43.3
μP (10 mg)	0.019	36.5
μP (10 mg) + L-PRP	0.007	99.0
μP (7.5 mg) + L-PRP	0.011	63.0
μP (5 mg) + L-PRP	0.015	46.2
μP (2.5 mg) + L-PRP	0.017	40.8
Fibrin (L-PRP)	0.016	43.3

μ_{max} was calculated by Eq. 1; and t_d was calculated by Eq. 2.

The profiles of Figure 3c show that in the absence of L-PRP, cell proliferation on oxi-HA/ADH bulk hydrogel and microparticles (10 mg) continued to rise although at a slower rate, until 14 days in culture. This is due to the distribution of the cells between the plate and the microparticles or bulk hydrogel. Although this interference, these results are important to show the favorable surface of the microparticles and the bulk hydrogel for the proliferation of h-AdMSCs. In contrast, the presence of the fibrin gel limited cell proliferation, with decreasing curves after 7 days, in consequence of the collapse of the fibrin gel.

In the presence of L-PRP, the profiles show that the concentration of microparticles influenced cell proliferation. The best situation was at 2.5 and 5 mg microparticle concentrations, in which the microparticles improved cell proliferation compared to those in L-PRP. At higher microparticle concentrations cell proliferation decreased due to the disturbances of the fibrin network we observed in the images of Figure 2. Further experiments may characterize better these effects.

The observed effects are in agreement with the determined parameter maximum specific growth rate and double time (Table 3). The doubling times are noticeably longer than those calculated for the same AdMSCs in T-flask culture which is typically 45 – 60 h depending on the medium exchange strategy used [27, 28].

L-PRP is widely used in clinical practice and recent researchers show the benefits of association with fluid HA [29, 30]. According to Chen et al. the HA and L-

PRP mixture induced chondrogenesis via regenerative signaling associated with an inhibition of the inflammatory pathways. These effects were synergistic compared to either HA or L-PRP alone [31].

Live/Dead images (Figure 4) were captured in a fluorescence confocal microscope using live/dead reagents after seven days of culture.

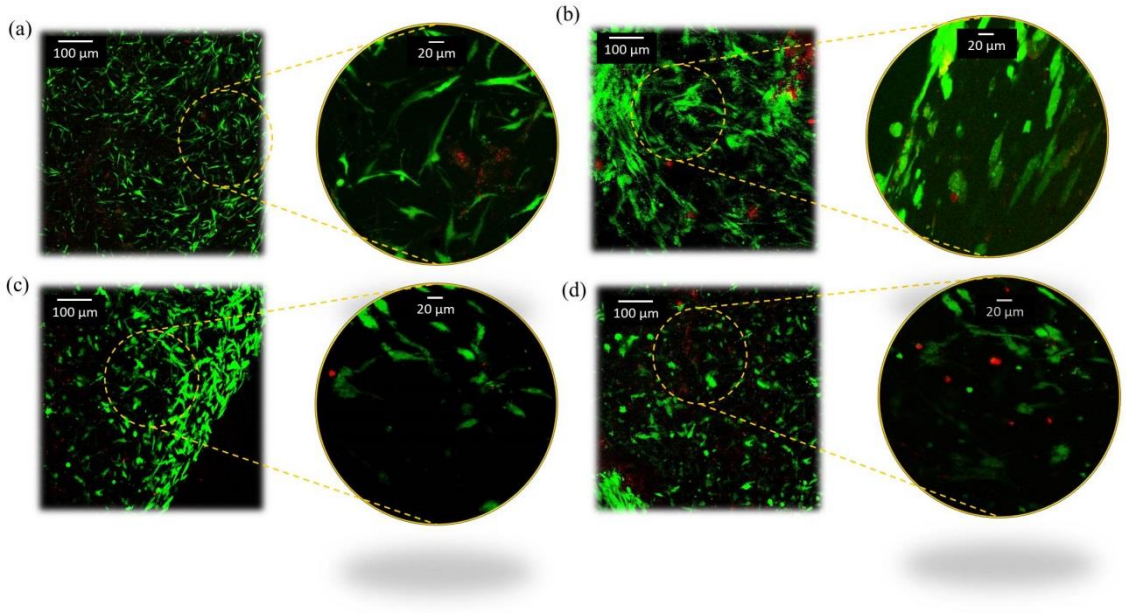

Figure4. Live/Dead images taken on day 7 of the h-AdMSCs cells with (a) L-PRP, (b) µP, (c) µP (2.5 mg) with L-PRP, and (d) µP (10 mg) with L-PRP.

The images show that h-AdMSCs proliferation in the presence of L-PRP with 2.5 mg of microparticles was significantly greater compared to fibrin cells. The cells were more abundant at the microparticles interface, with elongated morphology, characteristic of a beneficial microenvironment for proliferation. The morphology of h-AdMSCs was elongated and seemed to spread across the network in fibrin, while in L-PRP with 10 mg of microparticles, round-shaped cells predominant. These images confirm the kinetic profiles from cell cultivation (Figure 3) and the calculated kinetic parameters (Table 3).

Overall, the results show the studied association is promising for regenerative approaches. Further studies may investigate the capability of the cells for differentiation and formation of the microtissues.

4. Conclusion

The association of fibrin from L-PRP and h-AdMSCs-oxi-HA/ADH microparticles provided an effective matrix for cell proliferation and therefore it represent a promising strategy for clinical uses in regenerative medicine.

Acknowledgments

The authors acknowledge *In Situ* Cell Therapy for providing the laboratory.

Funding

This study was supported by the CNPq (Conselho Nacional de Desenvolvimento Científico e Tecnológico Brazil) (process 140924/2017-5), CAPES (Coordenação de Aperfeiçoamento de Pessoal de Nível Superior) (process 88882.435123/2019-01), andFAPESP (Fundação de Amparo à Pesquisa do Estado de São Paulo) (process 2016/10132-0).

Conflicts of Interest

The authors declare no conflicts of interest.

References

1. Lana JFSD, Santana MHA, Belangero WD, Luzo ACM. Platelet-rich plasma - Regenerative medicine: sports Medicine, orthopedic, and recovery of musculoskeletal injuries. Springer; 2014.

2. Hascall VC, Laurent TC: Hyaluronan: structure and physical properties. https://www.glycoforum.gr.jp/article/01A2.html (1997). Accessed 2020.

3. Samadi P, Sheykhhasan M, Khoshinani HM. The Use of Platelet-Rich Plasma in Aesthetic and Regenerative Medicine: A Comprehensive Review. Aesthetic Plastic Surgery. 2019;43(3):803-14. doi: 10.1007/s00266-018-1293-9.

4. Zhu Z, Wang Y-M, Yang J, Luo X-S. Hyaluronic acid: a versatile biomaterial in tissue engineering. Plastic and Aesthetic Research. 2017;4:219-27. doi: 10.20517/2347-9264.2017.71.

5. Wu KC, Tseng CL, Wu CC, Kao FC, Tu YK, So EC, et al. Nanotechnology in the regulation of stem cell behavior. Science and Technology of Advanced Materials. 2013;14(5). doi: 10.1088/1468-6996/14/5/054401.

6. Gauvin R, Parenteau-Bareil R, Dokmeci MR, Merryman WD, Khademhosseini A. Hydrogels and microtechnologies for engineering the cellular microenvironment. Wiley

Interdisciplinary Reviews-Nanomedicine and Nanobiotechnology. 2012;4(3):235-46. doi: 10.1002/wnan.171.

7. Guan XF, Avci-Adali M, Alarcin E, Cheng H, Kashaf SS, Li YX, et al. Development of hydrogels for regenerative engineering. Biotechnology Journal. 2017;12(5). doi: 10.1002/biot.201600394.

8. Chung HJ, Park TG. Injectable Cellular Aggregates Prepared from Biodegradable Porous Microspheres for Adipose Tissue Engineering. Tissue Engineering Part A. 2009;15(6):1391-400. doi: 10.1089/ten.tea.2008.0344.

9. Declercq HA, Gorski TL, Tielens SP, Schacht EH, Cornelissen MJ. Encapsulation of osteoblast seeded microcarriers into injectable, photopolymerizable three-dimensional scaffolds based on D,L-lactide and epsilon-caprolactone. Biomacromolecules. 2005;6(3):1608-14. doi: 10.1021/bm050031s.

10. Declercq H, De Caluwe T, Krysko O, Bachert C, Cornelissen M. Bone grafts engineered from human adipose-derived stem cells in dynamic 3d-environments: a top-down versus bottom-up approach. Journal of Tissue Engineering and Regenerative Medicine. 2012;6:23-4.

11. Mendes BB, Daly AC, Reis RL, Domingues RMA, Gomes ME, Burdick JA. Injectable hyaluronic acid and platelet lysate-derived granular hydrogels for biomedical applications. Acta Biomaterialia. 2020. doi: 10.1016/j.actbio.2020.10.040.

12. Shimojo AAM, Pires AMB, Lichy R, Santana MHA. The Performance of Crosslinking with Divinyl Sulfone as Controlled by the Interplay Between the Chemical Modification and Conformation of Hyaluronic Acid. Journal of the Brazilian Chemical Society. 2015;26(3):506-12. doi: 10.5935/0103-5053.20150003.

13. Shimojo AAM, Pires AMB, Lichy R, Rodrigues AA, Santana MHA. The crosslinking degree controls the mechanical, rheological, and swelling properties of hyaluronic acid microparticles. Journal of Biomedical Materials Research Part A. 2015;103(2):730-7. doi: 10.1002/jbm.a.35225.

14. Shimojo AAM, Duarte ADS, Lana J, Luzo ACM, Fernandes AR, Sanchez-Lopez E, et al. Association of Platelet-Rich Plasma and Auto-Crosslinked Hyaluronic Acid Microparticles: Approach for Orthopedic Application. Polymers. 2019;11(10). doi: 10.3390/polym11101568.

15. França CG, Sacomani DP, Villalva DG, Nascimento VF, Dávila JL, Santana MHA. Structural changes and crosslinking modulated functional properties of oxi-HA/ADH

hydrogels useful for regenerative purposes. European Polymer Journal. 2019;121(109288). doi: 10.1016/j.eurpolymj.2019.109288.

16. Lin FH, Su WY, Chen YC, Chen KH. Cross-linked oxidated hyaluronic acid for use as vitreous substitute. United States: National Health Research Institutes; 2011. p. 19.

17. Ma XB, Xu TT, Chen W, Wang R, Xu Z, Ye ZW, et al. Improvement of Toughness for the Hyaluronic Acid and Adipic Acid Dihydrazide Hydrogel by PEG. Fibers and Polymers. 2017;18(5):817-24. doi: 10.1007/s12221-017-6986-1.

18. de Melo BAG, Shimojo AAM, Perez AGM, Lana J, Santana MHA. Distribution, recovery and concentration of platelets and leukocytes in L-PRP prepared by centrifugation. Colloids and Surfaces B-Biointerfaces. 2018;161:288-95. doi: 10.1016/j.colsurfb.2017.10.046.

19. Manzini BM, Duarte ADS, Sankaramanivel S, Ramos AL, Latuf P, Escanhoela C, et al. Useful properties of undifferentiated mesenchymal stromal cells and adipose tissue as the source in liver-regenerative therapy studied in an animal model of severe acute fulminant hepatitis. Cytotherapy. 2015;17(8):1052-65. doi: 10.1016/j.jcyt.2015.04.010.

20. Mosmann T. Rapid colorimetric assay for cellular growth and s urvival: application to proliferation and c ytotoxicity assays. Journal of lmmunological Methods. 1983(65):55-63.

21. Perez AGM, Lichy R, Lana JFSD, Rodrigues AA, Luzo ACM, Belangero WD, et al. Prediction and modulation of platelet recovery by discontinuous centrifugation of whole blood for the preparation of pure Platelet-Rich Plasma. Bioresearch Open Access. 2013;2(4):307-14. doi: 10.1089/biores.2013.0015.

22. Perez AGM, Lana JFSD, Rodrigues AA, Luzo ACM, Belangero WD, Santana MHA. Relevant aspects of centrifugation step in the preparation of platelet-rich plasma. ISRN Hematology. 2014;2014:8. doi: 10.1155/2014/176060.

23. Higuera G, Schop D, Janssen F, van Dijkhuizen-Radersma R, van Boxtel T, van Blitterswijk CA. Quantifying In Vitro Growth and Metabolism Kinetics of Human Mesenchymal Stem Cells Using a Mathematical Model. Tissue Engineering Part A. 2009;15(9):2653-63. doi: 10.1089/ten.tea.2008.0328.

24. Ito T, Yeo Y, Highley CB, Bellas E, Benitez CA, Kohane DS. The prevention of peritoneal adhesions by in situ cross-linking hydrogels of hyaluronic acid and cellulose derivatives. Biomaterials. 2007;28(6):975-83. doi: 10.1016/j.biomaterials.2006.10.021.

25. Yeo Y, Highley CB, Bellas E, Ito T, Marini R, Langer R, et al. In situ cross-linkable hyaluronic acid hydrogels prevent post-operative abdominal adhesions in a rabbit model. Biomaterials. 2006;27(27):4698-705. doi: 10.1016/j.biomaterials.2006.04.043.

26. Emoto S, Yamaguchi H, Kamei T, Ishigami H, Suhara T, Suzuki Y, et al. Intraperitoneal administration of cisplatin via an in situ cross-linkable hyaluronic acid-based hydrogel for peritoneal dissemination of gastric cancer. Surgery Today. 2014;44(5):919-26. doi: 10.1007/s00595-013-0674-6.

27. Schop D, Janssen FW, van Rijn LDS, Fernandes H, Bloem RM, de Bruijn JD, et al. Growth, Metabolism, and Growth Inhibitors of Mesenchymal Stem Cells. Tissue Engineering Part A. 2009;15(8):1877-86. doi: 10.1089/ten.tea.2008.0345.

28. Rafiq QA, Coopman K, Nienow AW, Hewitt CJ. A quantitative approach for understanding small-scale human mesenchymal stem cell culture implications for large-scale bioprocess development. Biotechnology Journal. 2013;8(4):459-+. doi: 10.1002/biot.201200197.

29. de Melo BAG, Franca CG, Davila JL, Batista NA, Caliari-Oliveira C, d'Avila MA, et al. Hyaluronic acid and fibrin from L-PRP form semi-IPNs with tunable properties suitable for use in regenerative medicine. Materials Science & Engineering C-Materials for Biological Applications. 2020;109. doi: 10.1016/j.msec.2019.110547.

30. Lana J, Weglein A, Sampson S, Vicente EF, Huber SC, Souza CV, et al. Randomized controlled trial comparing hyaluronic acid, platelet-rich plasma and the combination of both in the treatment of mild and moderate osteoarthritis of the knee. Journal of Stem Cells & Regenerative Medicine. 2016;12(2):P69-P78.

31. Chen WH, Liu HY, Lo WC, Wu SC, Chi CH, Chang HY, et al. Intervertebral disc regeneration in an ex vivo culture system using mesenchymal stem cells and platelet-rich plasma. Biomaterials. 2009;30(29):5523-33. doi: 10.1016/j.biomaterials.2009.07.019.

CAPÍTULO 4:
CONCLUSÕES

4. CONCLUSÃO GERAL

Os resultados obtidos nesse trabalho mostraram que o grau de oxidação e de reticulação do hidrogel oxi-HA/ADH afetam as características físico-químicas, modulando as propriedades estruturais e funcionais do hidrogel. A estruturação do oxi-HA/ADH em micropartículas demostrou ser promissora como carreadores celulares para a proliferação de h-AdMSCs e representam vantagens em termos de injetabilidade em comparação com o HA reticulado com outros compostos. Além disso, as micropartículas associadas com o L-PRP proporcionou uma matriz eficaz para a proliferação celular e, portanto, representa uma estratégia promissora para usos clínicos em medicina regenerativa.

As conclusões específicas desse trabalho foram:

- As modificações moleculares ocorrem apenas nos resíduos de D-glucuronato, enquanto os grupos N-acetil glucosamina permanecem intactos e protegem contra a oxidação total e a cisão das cadeias;
- O alto grau de oxidação, devido aos obstáculos estéricos, induzem limitações de difusão e reticulação incompleta, apesar do alto número de grupos aldeído disponível no oxi-HA;
- O grau de oxidação aumentou o potencial zeta e diminuiu o volume hidrodinâmico e a viscosidade, a força de extrusão e a injetabilidade;
- A concentração de ADH modulou as propriedades funcionais, como intumescimento, estabilidade, tempo de gelificação e termossensibilidade;
- Nano e micropartículas de oxi-HA/ADH foram obtidas por processos de nanoprecipitação e cisalhamento, respectivamente, e nenhum dos processos necessitou de uma purificação adicional;
- É possível controlar o rendimento, diâmetro médio e potencial zeta, através de parâmetros operacionais como pH, vazão e taxa de cisalhamento;
- As micropartículas, particularmente, demostraram mais eficientes para a proliferação de AdMSCs; enquanto que, na mesma concentração, as nanopartículas permitiam apenas a sobrevivência celular;
- As taxas de crescimento específico das AdMSCs e os tempos de duplicação justadas pela cinética Monod foram melhores nas micropartículas com 2 e 5 mg, o que nessas condições, as micropartículas não suprimiram a expansão da rede de fibrina do L-PRP e melhoraram a proliferação celular.

CAPÍTULO 5:
SUGESTÕES PARA TRABALHOS FUTUROS

5. SUGESTÕES PARA TRABALHOS FUTURO

Os resultados obtidos nessa tese de doutorado abrem espaço para uma série de trabalhos futuros de oxi-HA/ADH. Dentre eles, algumas sugestões são citadas abaixo:

- Avaliação da capacidade de diferenciação condrogênica das h-AdMSCs nas microcarregadores de oxi-HA/ADH pelas análises de imunofluorescência e RT-PCR;
- Estudos da produção de microcarregadores por microcanais;
- Associação dos microcarregadores de oxi-HA/ADH com tempol, avaliando a liberação e os benefícios;
- Estudos pré-clínicos e clínicos dos microcarregadores de oxi-HA/ADH para validação *in vivo* dos resultados obtidos *in vitro*;
- Estudos de bioimpressão tridimensional de oxi-HA/ADH com h-AdMSCs para o desenvolvimento de tecidos e órgãos;
- Estudos de biorreatores para crescimento de células mesenquimais.

CAPÍTULO 6:
REFERÊNCIAS

6. REFERÊNCIAS

ALTMAN, R. D.; MANJOO, A.; FIERLINGER, A.; NIAZI, F. *et al.* The mechanism of action for hyaluronic acid treatment in the osteoarthritic knee: a systematic review. **Bmc Musculoskeletal Disorders**, 16, Oct 2015.

BADLEY, E. M.; WILFONG, J. M.; YIP, C.; MILLSTONE, D. B. *et al.* The contribution of age and obesity to the number of painful joint sites in individuals reporting osteoarthritis: a population-based study. **Rheumatology**, 0, p. 1 - 8, 2020.

BHOSALE, A. M.; RICHARDSON, J. B. Articular cartilage: structure, injuries and review of management. **British Medical Bulletin**, 87, n. 1, p. 77-95, Sep 2008.

BICUDO, R. C. S.; SANTANA, M. H. A. Effects of Organic Solvents on Hyaluronic Acid Nanoparticles Obtained by Precipitation and Chemical Crosslinking. **Journal of Nanoscience and Nanotechnology**, 12, n. 3, p. 2849-2857, Mar 2012a.

BICUDO, R. C. S.; SANTANA, M. H. A. Production of hyaluronic acid (HA) nanoparticles by a continuous process inside microchannels: Effects of non-solvents, organic phase flow rate, and HA concentration. **Chemical Engineering Science**, 84, p. 134-141, Dec 2012b.

BICUDO, R. C. S.; SANTANA, M. H. A. The influence of pH on the synthesis of hyaluronic acid nanoparticles by precipitation. **International Review of Biophysical Chemistry**, 5, n. 4, 2014.

BOAS, N. F. ISOLATION OF HYALURONIC ACID FROM THE COCKS COMB. **Journal of Biological Chemistry**, 181, n. 2, p. 573-575, 1949.

BRASIL, P. H. **A artrose em números**. https://portalhospitaisbrasil.com.br/a-artrose-em-numeros/, 2017.

BURDICK, J. A.; PRESTWICH, G. D. Hyaluronic Acid Hydrogels for Biomedical Applications. **Advanced Materials**, 23, n. 12, p. H41-H56, Mar 2011.

CAVALCANTI, A. D. D.; MELO, B. A. G.; OLIVEIRA, R. C.; SANTANA, M. H. A. Recovery and Purity of High Molar Mass Bio-hyaluronic Acid Via Precipitation Strategies Modulated by pH and Sodium Chloride. **Applied Biochemistry and Biotechnology**, 188, n. 2, p. 527-539, Jun 2019.

CAVALCANTI, A. D. D.; SANTANA, M. H. A. Structural and surface properties control the recovery and purity of bio-hyaluronic acid upon precipitation with isopropyl alcohol. **Colloids and Surfaces a-Physicochemical and Engineering Aspects**, 573, p. 112-118, Jul 2019.

CHENG, O. T.; SOUZDALNITSKI, D.; VROOMAN, B.; CHENG, J. G. Evidence-Based Knee Injections for the Management of Arthritis. **Pain Medicine**, 13, n. 6, p. 740-753, Jun 2012.

CHONG, B. F.; BLANK, L. M.; MCLAUGHLIN, R.; NIELSEN, L. K. Microbial hyaluronic acid production. **Applied Microbiology and Biotechnology**, 66, n. 4, p. 341-351, Jan 2005.

COWMAN, M. K.; SCHMIDT, T. A.; RAGHAVAN, P.; STECCO, A. Viscoelastic properties of Hyaluronan in physiological conditions. **F1000Research 4**, 4, n. 622, 2015.

DE MELO, B. A. G.; FRANCA, C. G.; DAVILA, J. L.; BATISTA, N. A. *et al.* Hyaluronic acid and fibrin from L-PRP form semi-IPNs with tunable properties suitable for use in regenerative medicine. **Materials Science & Engineering C-Materials for Biological Applications**, 109, Apr 2020.

DE MELO, B. A. G.; SHIMOJO, A. A. M.; PEREZ, A. G. M.; LANA, J. *et al.* Distribution, recovery and concentration of platelets and leukocytes in L-PRP prepared by centrifugation. **Colloids and Surfaces B-Biointerfaces**, 161, p. 288-295, Jan 2018.

DECLERCQ, H. A.; DE CALUWE, T.; KRYSKO, O.; BACHERT, C. *et al.* Bone grafts engineered from human adipose-derived stem cells in dynamic 3D-environments. **Biomaterials**, 34, n. 4, p. 1004-1017, Jan 2013.

FALLACARA, A.; BALDINI, E.; MANFREDINI, S.; VERTUANI, S. Hyaluronic Acid in the Third Millennium. **Polymers**, 10, n. 7, Jul 2018.

FRANÇA, C. G.; SACOMANI, D. P.; VILLALVA, D. G.; NASCIMENTO, V. F. *et al.* Structural changes and crosslinking modulated functional properties of oxi-HA/ADH hydrogels useful for regenerative purposes. **European Polymer Journal**, 121, n. 109288, 2019.

FRASER, J. R. E.; LAURENT, T. C.; LAURENT, U. B. G. Hyaluronan: Its nature, distribution, functions and turnover. **Journal of Internal Medicine**, 242, n. 1, p. 27-33, Jul 1997.

GOMEZ-GALAN, M.; PEREZ-ALONSO, J.; CALLEJON-FERRE, A. J.; LOPEZ-MARTINEZ, J. Musculoskeletal disorders: OWAS review. **Industrial Health**, 55, n. 4, p. 314-337, Jul 2017.

GRASSEL, S.; MUSCHTER, D. Recent advances in the treatment od osteoarthritis. **F1000 Reaearch**, 9, 2020.

HASCALL, V. C.; LAURENT, T. C. **Hyaluronan: structure and physical properties**. 1997. Disponível em: https://www.glycoforum.gr.jp/article/01A2.html.

HE, Y. C.; LI, Z.; ALEXANDER, P. G.; OCASIO-NIEVES, B. D. *et al.* Pathogenesis of Osteoarthritis: Risk Factors, Regulatory Pathways in Chondrocytes, and Experimental Models. **Biology-Basel**, 9, n. 8, Aug 2020.

IBGE. **Projeção da população brasileira**. 2008. Disponível em: http://www.ibge.gov.br/apps/populacao/projecao/. Acesso em: 01 de abril de 2016.

JIA, X. Q.; COLOMBO, G.; PADERA, R.; LANGER, R. *et al.* Prolongation of sciatic nerve blockade by in situ cross-linked hyaluronic acid. **Biomaterials**, 25, n. 19, p. 4797-4804, Aug 2004.

KAUX, J. F.; SAMSON, A.; CRIELAARD, J. M. Hyaluronic acid and tendon lesions. **Mltj-Muscles Ligaments and Tendons Journal**, 5, n. 4, p. 264-269, Oct-Dec 2015.

KEENEY, M.; LAI, J. H.; YANG, F. Recent progress in cartilage tissue engineering. **Current Opinion in Biotechnology**, 22, n. 5, p. 734-740, Oct 2011.

KHAN, I. U.; AWAN, A. S.; KHAN, A. S.; MARWAT, I. *et al.* Efficacy of a single-injection sodium hyaluronate treatment in lateral epicondylitis. **Journal of Ayub Medical College**, 30, n. 1, p. 85-89, 2018.

KNUDSON, W.; KNUDSON, C. B. **The hyaluronan receptor, CD44**. 1999. Disponível em: https://www.glycoforum.gr.jp/article/03A2.html.

LANA, J.; WEGLEIN, A.; SAMPSON, S.; VICENTE, E. F. *et al.* Randomized controlled trial comparing hyaluronic acid, platelet-rich plasma and the combination of both in the treatment of mild and moderate osteoarthritis of the knee. **Journal of Stem Cells & Regenerative Medicine**, 12, n. 2, p. P69-P78, 2016.

LANA, J. F. S. D.; SANTANA, M. H. A.; BELANGERO, W. D.; LUZO, A. C. M. **Platelet-rich plasma - Regenerative medicine: sports Medicine, orthopedic, and recovery of musculoskeletal injuries**. Springer, 2014.

LOESER, R. F. The role of aging in the development of osteoarthritis. **Transactions of the American Clinical and Climatological Association**, 128, p. 44 - 54, 2017.

MALDA, J.; FRONDOZA, C. G. Microcarriers in the engineering of cartilage and bone. **Trends in Biotechnology**, 24, n. 7, p. 299-304, Jul 2006.

MEYER, K.; PALMER, J. W. The polysaccharide of the vitreous humor. **Journal of Biological Chemistry**, 107, n. 3, p. 629-634, Dec 1934.

NICHOLLS, M. A.; FIERLINGER, A.; NIAZI, F.; BHANDARI, M. The Disease-Modifying Effects of Hyaluronan in the Osteoarthritic Disease State. **Clinical Medicine Insights-Arthritis and Musculoskeletal Disorders**, 10, Aug 2017.

PRESTWICH, G. D. **Biomaterials from chemically-modified hyaluronan**. 2001. Disponível em: http://www.glycoforum.gr.jp/science/hyaluronan/HA18/HA18E.html.

SCOTT, J. E. **Secondary and tertiary structures of hyaluronan in aqueous solution. Some biological consequences.** Glycoforum, 1998. Disponível em: http://glycoforum.gr.jp/science/hyaluronan/HA02/HA02E.html.

SHIMOJO, A. A. M.; BRISSAC, I.; PINA, L. M.; LAMBERT, C. S. *et al.* Sterilization of auto-crosslinked hyaluronic acid scaffolds structured in microparticles and sponges. **Bio-Medical Materials and Engineering**, 26, n. 3-4, p. 183-191, 2015.

SHIMOJO, A. A. M.; DUARTE, A. D. S.; LANA, J.; LUZO, A. C. M. *et al.* Association of Platelet-Rich Plasma and Auto-Crosslinked Hyaluronic Acid Microparticles: Approach for Orthopedic Application. **Polymers**, 11, n. 10, Oct 2019.

SHIMOJO, A. A. M.; GALDAMES, S. E. M.; DUARTE, A. D. S. S.; PINA, L. M. *et al.* The structuring of high molecular weight hyaluronic acid in microparticles or sponges improves its performance when associated with platelet-rich plasma. **Trends in biomaterials and artificial organs** 29, n. 2, p. 160-169, 2014.

SHIMOJO, A. A. M.; GALDAMES, S. E. M.; PEREZ, A. G. M.; ITO, T. H. *et al.* In vitro performance of injectable chitosan-tripolyphosphate scaffolds combined with platelet-rich plasma. **Tissue Engineering and Regenerative Medicine**, 13, n. 1, p. 21-30, Feb 2016.

SHIMOJO, A. A. M.; PEREZ, A. G. M.; GALDAMES, S. E. M.; BRISSAC, I. C. S. *et al.* Stabilization of porous chitosan improves the performance of its association with platelet-rich plasma as a composite scaffold. **Materials Science & Engineering C-Materials for Biological Applications**, 60, p. 538-546, Mar 2016.

SHIMOJO, A. A. M.; PIRES, A. M. B.; DE LA TORRE, L. G.; SANTANA, M. H. A. Influence of particle size and fluid fraction on rheological and extrusion properties of crosslinked hyaluronic acid hydrogel dispersions. **Journal of Applied Polymer Science**, 128, n. 3, p. 2180-2185, May 2013.

SHIMOJO, A. A. M.; PIRES, A. M. B.; LICHY, R.; RODRIGUES, A. A. *et al.* The crosslinking degree controls the mechanical, rheological, and swelling properties of

hyaluronic acid microparticles. **Journal of Biomedical Materials Research Part A**, 103, n. 2, p. 730-737, Feb 2015.

SHIMOJO, A. A. M.; PIRES, A. M. B.; LICHY, R.; SANTANA, M. H. A. The Performance of Crosslinking with Divinyl Sulfone as Controlled by the Interplay Between the Chemical Modification and Conformation of Hyaluronic Acid. **Journal of the Brazilian Chemical Society**, 26, n. 3, p. 506-512, Mar 2015.

SU, W. Y.; CHEN, K. H.; CHEN, Y. C.; LEE, Y. H. *et al.* An Injectable Oxidated Hyaluronic Acid/Adipic Acid Dihydrazide Hydrogel as a Vitreous Substitute. **Journal of Biomaterials Science-Polymer Edition**, 22, n. 13, p. 1777-1797, 2011.

SU, W. Y.; CHEN, Y. C.; LIN, F. H. Injectable oxidized hyaluronic acid/adipic acid dihydrazide hydrogel for nucleus pulposus regeneration. **Acta Biomaterialia**, 6, n. 8, p. 3044-3055, Aug 2010.

SUS, R. H. **80% da população mundial com mais de 65 anos sofre de artrose, segundo a OMS**. http://redehumanizasus.net/89575-80-da-populacao-mundial-com-mais-de-65-anos-sofre-de-artrose-segundo-a-oms/, 2015.

SWANN, D. A.; CAULFIELD, J. B. Studies on hyaluronic acid V. Relationship between the protein content and viscosity of rooster comb dermis hyaluronic acid. **Connective Tissue Research**, 4, n. 1, p. 31 - 39, 1975.

TEMPLE-WONG, M. M.; REN, S. W.; QUACH, P.; HANSEN, B. C. *et al.* Hyaluronan concentration and size distribution in human knee synovial fluid: variations with age and cartilage degeneration. **Arthritis Research & Therapy**, 18, Jan 2016.

TIRUVANNAMALAI-ANNAMALAI, R.; ARMANT, D. R.; MATTHEW, H. W. T. A Glycosaminoglycan Based, Modular Tissue Scaffold System for Rapid Assembly of Perfusable, High Cell Density, Engineered Tissues. **Plos One**, 9, n. 1, Jan 2014.

TURLEY, E. A.; NOBLE, P. W.; BOURGUIGNON, L. Y. W. Signaling properties of hyaluronan receptors. **Journal of Biological Chemistry**, 277, n. 7, p. 4589-4592, Feb 2002.

VALERO, E.; SIVANATHAN, A.; BOSCHE, F.; ABDEL-WAHAB, M. Musculoskeletal disorders in construction: A review and a novel system for activity tracking with body area network. **Applied Ergonomics**, 54, p. 120-130, May 2016.

VEGA, S. L.; KWON, M. Y.; BURDICK, J. A. Recent advances in hydrogels for cartilage tissue engineering. **European Cells & Materials**, 33, p. 59-75, Jan-Jun 2017.

WEIS, M.; SHAN, J. W.; KUHLMANN, M.; JUNGST, T. *et al.* Evaluation of Hydrogels Based on Oxidized Hyaluronic Acid for Bioprinting. **Gels**, 4, n. 4, Dec 2018.

YEO, Y.; HIGHLEY, C. B.; BELLAS, E.; ITO, T. *et al.* In situ cross-linkable hyaluronic acid hydrogels prevent post-operative abdominal adhesions in a rabbit model. **Biomaterials**, 27, n. 27, p. 4698-4705, Sep 2006.

CAPÍTULO 7:

ANEXOS

7. ANEXOS

7.1. Hyaluronic acid and fibrin from L-PRP form semi-IPNs with tunable properties suitable for use in regenerative medicine

Artigo publicado no periódico científico *Materials Science and Engineering C* (doi:10.1016/j.msec.2019.110547).

7.2. Nanoporous silicon microparticles embedded into oxidized hyaluronic acid/adipic acid dihydrazide hydrogel for enhanced controlled drug delivery

Artigo publicado no periódico científico *Microporous and Mesoporous Materials* em setembro de 2020 (doi: 10.1016/j.micromeso.2020.110634).